Acta
Technica
Jaurinensis

Vol. 14, No. 3, pp. 228-243, 2021
DOI: 10.14513/actatechjaur.00573

Speckle pattern optimization for DIC technologies

Sz. Szalai[1,*], G. Dogossy[2]

[1]Széchenyi István University, Department of Vehicle Manufacturing, Egyetem tér 1, 9026 Győr, Hungary
[2]Széchenyi István University, Department of Materials Science and Engineering, Egyetem tér 1, 9026 Győr, Hungary
***e-mail: szalaisz@sze.hu**

Submitted: 11/11/2020; Accepted: 08/04/2021; Published online: 26/04/2021

Abstract: This paper contains the relation between speckle pattern and Digital Image Correlation (DIC). The most important advance in experimental mechanics has been DIC since the strain gage. The deformation (strain) of an object can be visualized by DIC. Among all scientific fields, the DIC Technologies have seen a dynamic increase. The relationship between the paint and the sample - as the patterns mediate the deformation to the cameras - has been the most important technological issue. In this article the method developed for the detection of isolated particles in alloys is used to characterize the spots, which help the best speckle pattern has determined.

Keywords: speckle pattern; digital image correlation (DIC); paint; airbrush

1. Introduction

Several methods are known from the literature for measuring deformations, displacements and stresses. Traditional measurement methods include, but are not limited to, strain gauges and inductive transmitters. These measurement methods require a lot of preparation and the use of expensive tools and instruments. The Digital Image Correlation (DIC) method used in my research, on the other hand, is a non-contact method that can be used to examine a complete displacement and elongation field in the parts of the specimen visible to the camera using ordinary tools. It is not necessary to know the location of the failure in advance for these measurements, as the measurement results apply to the entire specimen and are processed afterwards. Digital image correlation as a test procedure was first developed by a research team at the University of South Carolina in the 1980s and then developed continuously, but the dynamic leap began in the 2000s in parallel with the technological advancement of cameras, as shown in Fig. 1. The technology is not only emerging in the field of testing metallic materials, but is now also being used in the testing of polymeric, composite or even biological materials. In addition to conventional specimens, it has gained ground in complex components, machines, or even building components, or in biomechanics and medicine [1, 2, 3, 4].

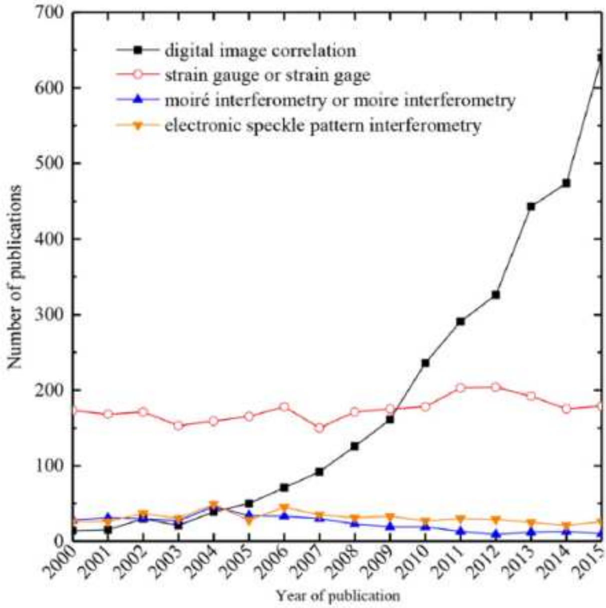

Figure 1. DIC growth in scientific articles [3]

According to the literature, the measurement of shape, displacement or deformation by the DIC technique requires the following:

- making a pattern – This pattern is placed on the surface of the examined objects and mediates the deformation of the object, in fact it has a kind of information-carrying role.

- taking pictures (photos) – The pattern and thus the specimen are recorded in different states, if we record with one camera we are talking about 2D DIC, in case of two cameras we can talk about stereo DIC or 3D DIC.

- image analysis – After capture, the distorted images are compared to a reference or initial image using a special cross-correlation algorithm that will extract the displacement and stress fields [3].

It follows from the above and several other researches that one of the essential conditions for DIC measurements is the appropriate pattern (preferably random), which conveys the deformation information and greatly influences the fit of the images and the accuracy of the measurements.

When characterizing the patterns, the literature provides more aspects than an important research aspect. The speckle size should be determined from the relationship between the camera resolution used during image digitization and the measured area. From these two quantities, the pixel size in mm can be calculated, from which the literature indicates the optimal speckle size between 3-5 pixels [6, 7, 8]. Determining contrast is also an important factor in mapping (Fig. 2/a). A good contrast can be achieved with white spots on a black background or black spots on a white background to aid identification. For any patterned image, increase the contrast and reduce the noise. The best way to do this is a good paint and proper lighting [9, 10, 11]. Aliasing is also an important feature of the image (Fig. 2/b). Overlapping speckle points should be avoided at all costs. Any overlapping point increases the noise of the pattern, which compromises the accuracy of the measurement [12, 13, 14].

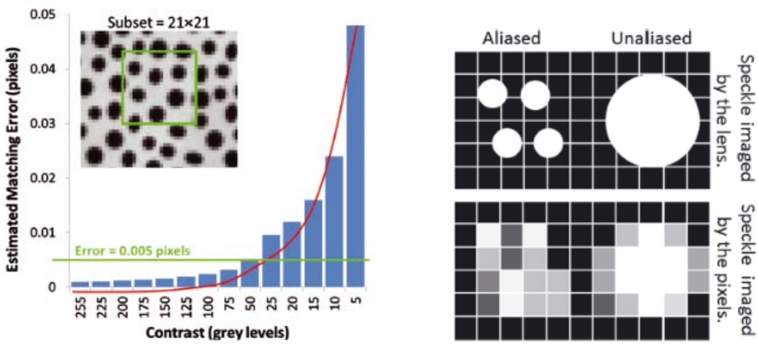

a) b)

Figure 2. Effect of contrast (a) and aliasing (b) [8, 15]

In terms of determining contrast gradient, practice shows that it is always better to optimize the contrast, the size of the spots, and the degree of distribution at the cost of the sharpness of the edge of the spots. This is because traditional patterning methods often have sharp boundaries at the edges of the patterns, but this is difficult to accomplish with spray technologies. The traditional pattering methods include the raster technique, laser marking, dot painting, stenciling and dot stamping, which results a well-defined contour with good contrast. However, these techniques do not provide adequate randomness and richness of detail. The spot density is also basic requirement. The different traditional and spraying patterns can be seen in Fig. 3. Although it is difficult to make such a uniform pattern that would cause an erroneous hit, it is worthwhile to make the pattern as random as possible [15, 16, 17].

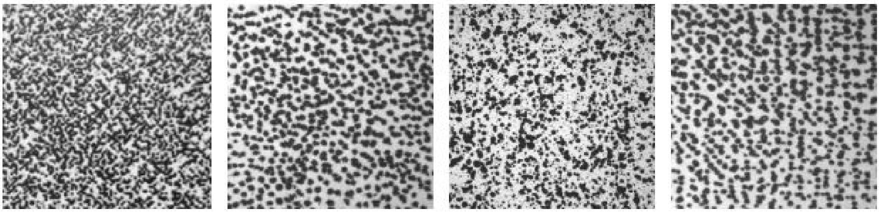

a) *b)* *c)* *d)*

Figure 3. Patterns of different densities and layouts [7]

The pattern of DIC techniques can be prepared by several methods as can be seen in the literature. The easiest and most accessible method of making patterns is spraying. In this case, a white base coat must be blown onto the specimen, on which the matte black diffused mottled pattern is applied (whether it is white on a black background or, conversely, it does not matter from the DIC point of view, the point is contrast). There are also several methods for applying stains. The following technique has proven to be useful for larger specimens and can be used quickly during most experiments: the specimen is sprayed by barely pressing the sprayer button. The propellant gas escaping slowly from the bottle will then not be able to completely disperse the dye, so droplets of ideal size will fall on the specimen. Another common procedure is to create a pattern with an airbrush gun, where you can better control the nozzle diameter and pressure, resulting in a much finer pattern and more reproducible results with the settings you set [3, 5, 19, 20].

For large specimens, stenciling can result in a similarly good pattern as in the case of a spray gun. However, electrolytic stenciling requires more expertise and cannot be applied to all materials. It is recommended to prepare medium or large products by printing. The pattern can also be applied to the surface with a laser or inkjet printer. Patterning with ink felt is also a possible solution. With this technique, quite large deformations can be measured, but it is very time consuming to apply. They can also be used directly on the surface, but it is also worth applying a white base coat here to increase the contrast. The grid pattern can be used among some certain restrictions, according to the literature it is a necessary rather than an optimal solution. Unlike the grid pattern, it is not a random pattern that allows for comparison, but in a raster design, the points are predetermined (intersection points). In the images, the points are not followed by searching for individual patterns, but by identifying each intersection point of the grid. This also results in an error in the method, as the raster may be so perfectly designed that one intersection point can be confused with another intersection point. However, due to the unevenness of the felt and the inhomogeneity of the surface to be examined, the areas are typically unique enough for continuous tracking. Some materials, such as wood veneer, have their own pattern, which, if the pattern parameters are appropriate, can be used for DIC measurements. If the material to be examined has a characteristic texture, it can still be used, but illumination can cause different shading on the textures, which makes two-camera measurements significantly more difficult and therefore not common [3, 5, 19, 20].

In addition to describing the various technologies and construction methods, it is important to clarify a few basic things about paints. The main components of paints are pigments, which give the color of the paint, binders, thinners and special materials. The paint can be water-based or oil-based. Water-based paints generally take less time to dry and cure than oil-based paints. Acrylic is also a popular type of paint. Acrylic paint is a paint emulsion consisting of pigments and plastic particles. The binder for the particles is a modified acrylic resin. The advantage of these paints is that they can be applied to almost any surface. They cure extremely quickly, usually in 2-3 hours, and today acrylic paints are water-based and thus water-soluble when wet. In the DIC technique, based on literature data and own experience, the following properties of paint should be used [3, 19]:

- matt gloss - should not flicker during the measurement,
- flexible - must follow the deformation of the specimen,
- only harden completely after more than 24 hours, because of the persistence of flexibility,
- easy to spray - preferably do not dilute as it also degrades the spectrum,
- deep black color - contains good quality pigment,
- water-based - this is more favorable for indoor applications [18].

It is clear from the list that these are often contradictory aspects, so it is difficult to find the right paint for the right job, and the composition of the paints can vary from country to country due to different regulations.

The literature classifies the parameters of a painting experiment according to several aspects, it is important that these parameters can only be set properly for airbrush (Fig. 4):

- dilution ratio,
- airflow or nozzle opening/size,

- spreading distance,
- operating pressure [3, 6, 18].

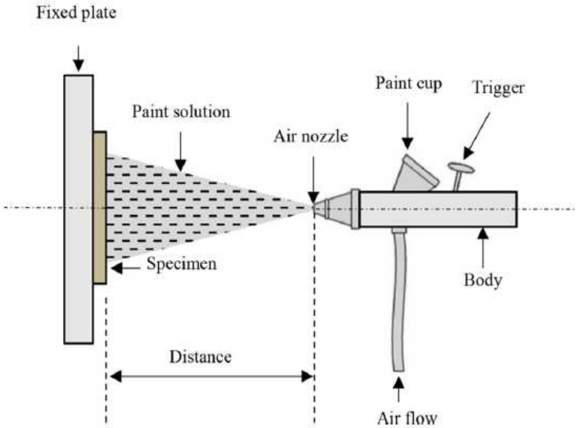

Figure 4. Airbrush set-up [3]

It is clear from the literature review that the difficulty of the characterization of the patterns stem from the technological production of the patterns on the one hand and the preparatory phase of DIC studies on the other hand. This article intends to place more emphasis on the appropriate pattern making technology, the pattern qualification process is discussed only in detail [21, 22, 23].

2. Applied materials and methods

There is no established method for characterizing the patterns, so a new, more comprehensive evaluation was developed than before. As a basic technique (Réti's window technique [24]), the method developed for the detection of isolated particles in alloys to characterize the spots was used. The patterns made with different technologies with the patterns issued and accepted by GOM was compared with the help of the method developed by the implementation of Réti's window technique [24]. Réti’s window technique is used in metallography application to determine particulate rates. In the comparison, it was examined which painting technology can be used to achieve a nearly similar pattern.

During the research different types of black color paints were used:

1. water-based high quality lacquer spray, matte finish,
2. graphite-based graphite spray, matte finish,
3. acryl lacquer acryl spray, matte finish,
4. enamel paint, silky finish,

5. elastic rubber paint, silky finish,
6. water-based enamel paint, matte finish.

The images were taken with Zeiss Axio Imager M1 optical stereo microscope with AxioVision 4.8 software and 2.5x optics. The tensile tests were carried out by Instron 5582 universal testing machine with 10 kN and 100 kN load cells, and Bluehill 2 software according to EN ISO 6892-1:2016 standard. The GOM ARAMIS 5M was used as DIC camera system with 800 mm adjustable base and GOM ARAMIS software. The Zeiss optical length measuring microscope with 1 µm accuracy was used in validation. The Iwata HP-SP Plus adjustable nozzle airbrush pistol with oil-free compressor was used as airbrush system. The GOM ATOS Triple Scan II, with ATOS 2019 software was used as optical surface digitalization system. The Mahr PMC 800 coordinate measuring machine with MarSoft Vision 3D 4.1 software was used in validation. During the experiment Mitutoyo Absolute Digimatic ID-SX 543-781B was used as dial indicator and Testo 174H calibrated digital temperature and humidity meter as thermometer. The used equipment can be seen in Fig. 5.

Figure 5. Zeiss Optical Stereo Microscope (a) and ARAMIS 5M test setup with tensile testing machine (b) and Iwata AirBrush pistol (c)

The specimen was made from AlMg3 alloy (thickness of 1.5 mm) and was produced with water cutting machine and complied with the dimensions specified in the standard (MSZ EN ISO 6892-1:2020). The specimen width was 20 mm, measuring length was 120 mm and the total length was 250 mm.

3. Experiment and Results

The validation of the ARAMIS measurements process and the evaluation of the different types of paints will be presented in this chapter. In addition to the results the patterns - which produced with different paints - will be described.

3.1. Validation of the measuring system

In the first step the measuring result of the ARAMIS system was verified. During this study the result of ARAMIS thickness reduction was compared with the result of ATOS, Mahr PCM 800 coordinate measuring machine and Mitutoyo dial indicator. Two of the three traditional measurements are tactile, while the ATOS and ARAMIS measures optically. Each system was calibrated and certified. The following figure (Fig. 6) shows the measurement results of ATOS and ARAMIS systems. The specimen was a 200x200x2.5 mm AlMg3 sheet for Nakazima test, it has been formed by a 100 mm diameter sphere until the crack.

During the validation process, the thickness of the formed plate was measured along the longitudinal axis of the specimen. The thickness was also measured with a dial indicator, a coordinate measuring machine and the ATOS system. These results were compared with the results of the ARAMIS system. The ATOS is also a coordinate measurement procedure, so it was interesting to compare it with traditional thickness measurement methods. The ARAMIS 5M system measures the major and minor strain on the surface (with the help of the painted pattern) and from this calculates the thickness reduction. The accuracy of the measurements is largely determined by the painted pattern, therefore the GOM calibration pattern was used for validation. It can be seen from the measurement results that next to 1.5 mm sheet thickness the measured results remained below 3% difference (Table 1). A comparison of the ATOS and ARAMIS systems shows that the thickness reduction curves are also similar (Table 1 and Fig. 6). This test was verified by the thickness reduction measured with ARAMIS system.

Table 1. Thickness measuring results

Measuring method	Thickness next to the crack [mm]	Thickness on the top of the specimen [mm]
Dial indicator	1.37	1.63
Coordinate measuring machine	1.381	1.632
ATOS system	1.39	1.65
ARAMIS system	1.41	1.64

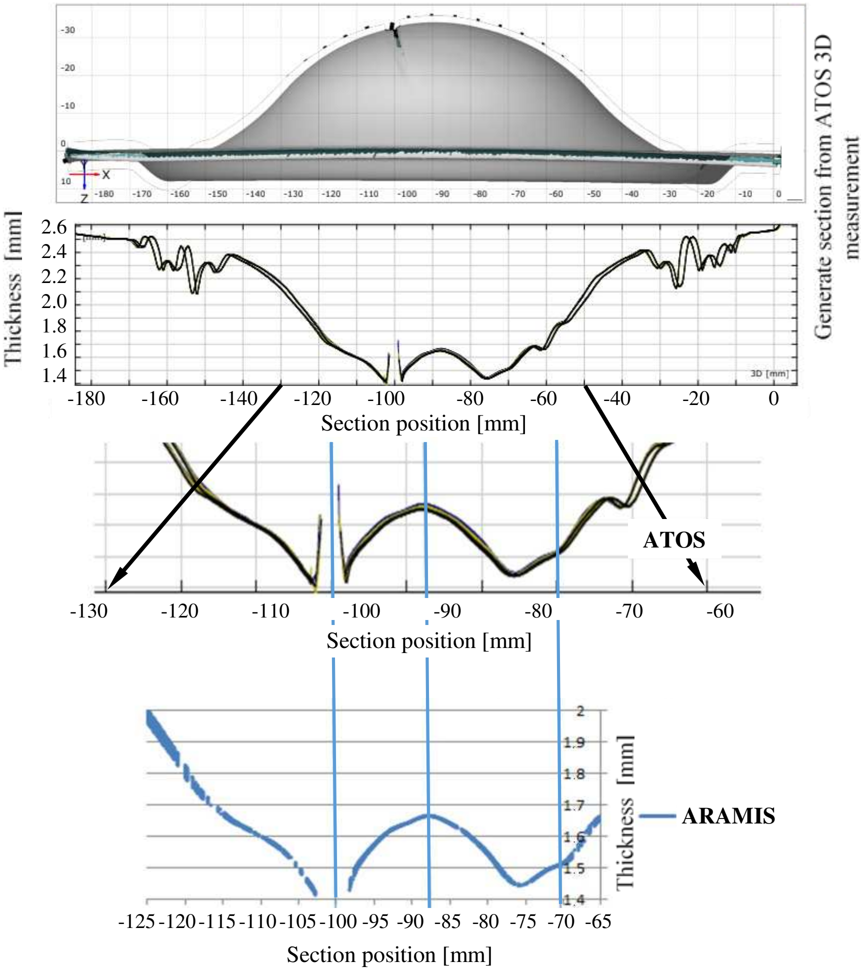

Figure 6. Validation of ARAMIS 5M system with thickness reduction

The aim of the research is to determine the appropriate patterns and staining parameters for ARAMIS systems. Whereas the ARAMIS system is a real-time 2D or 3D deformation measurement system, it is more important to verify the "online" elongation results when measuring the "static" thickness reduction. The tensile test is a 2D (from a metrological aspects) measurement process with good approximation, so validation is easier to perform with this test. Another major aspect is that the elongation measurement is important to determine the formability properties of the sheet. The next step was to validate this.

The AlMg3 validation specimens was 20 mm width and 1.5 mm thickness, the signal distance was 80 mm, the total test section was 120 mm and the clamp width was 30 mm. On the back of the specimens was made a Vickers imprint with load of 98.1 N at distance of 50 mm. This distance was measured in an unformed state with an optical length measuring microscope with 0.001 mm accuracy. The specimens were formed in an Instron 5582 tensile testing machine with 5 mm crosshead displacement at speed of 5 mm/min. The DIC analysis of the specimens was performed with an ARAMIS 5M measuring system.

The tensile testing machine was stopped after 5 mm displacement, then the force was decreased to 0, after then the samples were removed. The unloaded specimen was also recorded, so the whole process of the deformation history was recorded. In every 5 mm displacement from 5 to 25 mm the measure was stopped, this method 5 related DIC measurement and normal elongation measurement were recorded from each specimen. The results can be seen on Fig. 7.

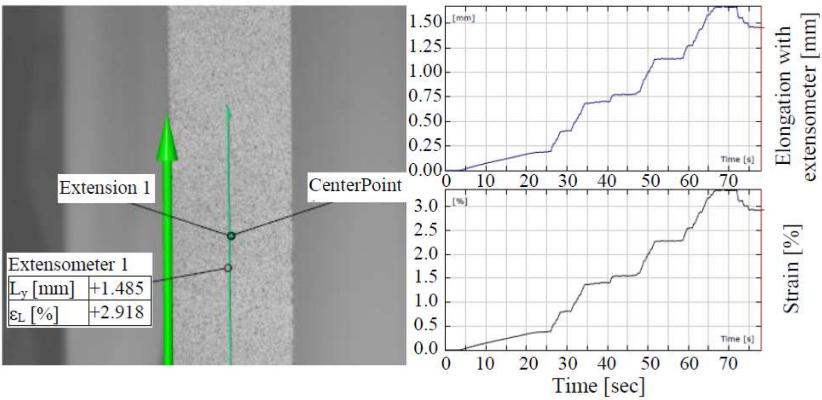

Figure 7. Virtual extensometer and extensometer results in ARAMIS software

After each increment the GOM sets the virtual extensometer to 50 mm and compares the ΔL_i increment in mm and the engineering strain in %. The optical measuring microscope added the next increase to the raised deformation, so the elongation can be calculated from these data. The cumulative value of the increments was calculated during the evaluation, so the engineering strain were given in logarithmic strain as they can be summed.

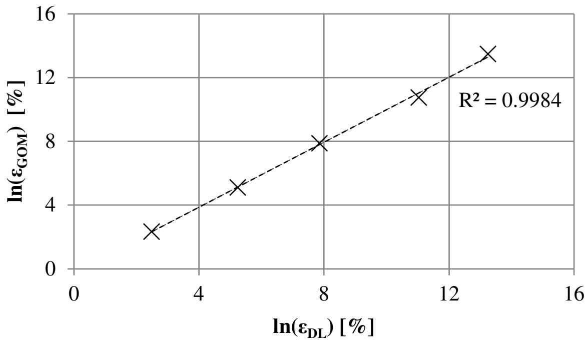

Figure 8. ARAMIS system validation with extensometer

The slope correlation coefficient diagram for all specimens is shown in Fig. 8. It can be seen that the coefficient of determination of the linear regression line of the measuring points is 0.9984. With the uncertainty of this measuring system this is a very good result.

3.2. Presentation of speckle painting experiments

After the validation process different paints and painting technologies were tested. Spraying had to be done in such a way that the finished speckle pattern was as close as possible to the GOM calibrated pattern image. This is important so that the pattern error has the least effect on the measurement results, so only the effect of different painting methods and paints was measured. The different painting specimens were also compared to this. The adhesion of the primer layer was also critical. This layer transmits the deformation of the specimen to the cameras. If the adhesion of this layer is not good, then not the sheet deformation will be measured [7-15]. Surface preparation is also critical, so the specimen surface was cleaned with isopropanol alcohol. The primer layer testing process is not described in this article, but each specimen was dried 12 hours long at 22 °C and 40 RH% humidity. Measurements were made within 24 hours in all cases to avoid overdrying of the primer layer.

The painting was done with all 6 paints using (described in Section 2) airbrush and spray technology. The prepared patterns were checked and analyzed on an optical microscope. The corresponding patterns were compared with the GOM calibration image by visual inspection, with the AxioVision 4.8 software particle analysis and with the modified window technique (described in Section 2). In this measurement the particle size, contrast, distribution, pattern density, and particle dimension was measured. The patterns were also tested with the validation measurement process (elongation validation) to determine the acceptable patterns.

The measurements showed that paint types 3 and 4 are not suitable for the test as they were extremely shiny. That is very important because the excessive reflection cannot be measured with the ARAMIS system. The glare is difficult to measure and it also distorts the measurement results. Their contrast is not adequate either, they were grey rather than black. Due to the properties of the type 5 elastic rubber paint, it cannot be applied with airbrush technology and it was also extremely shiny. These paints could not be used for further tests or measurements. The result can be seen on the Fig. 9.

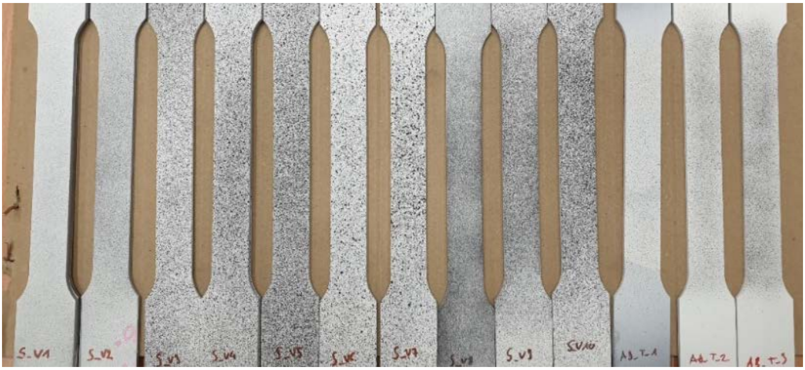

Figure 9. Specimens made with different paints and different techniques

The type 1, 2 and 6 paints were well suited and had good reflection. These results are the outcome of visual inspection. Further tests were made with these materials. In the next phase of the research the speckle patterns were analyzed. The coverage, the speckle area, average diameter, speckle number were measured for each specimen (Fig. 10). The results of the specimens were also compared with the results of the elongation measurements. Specimens where the error of the elongation measurement dropped below 1.5% were selected as acceptable patterns (Table 2). The 1.5% limit is derived from literature data.

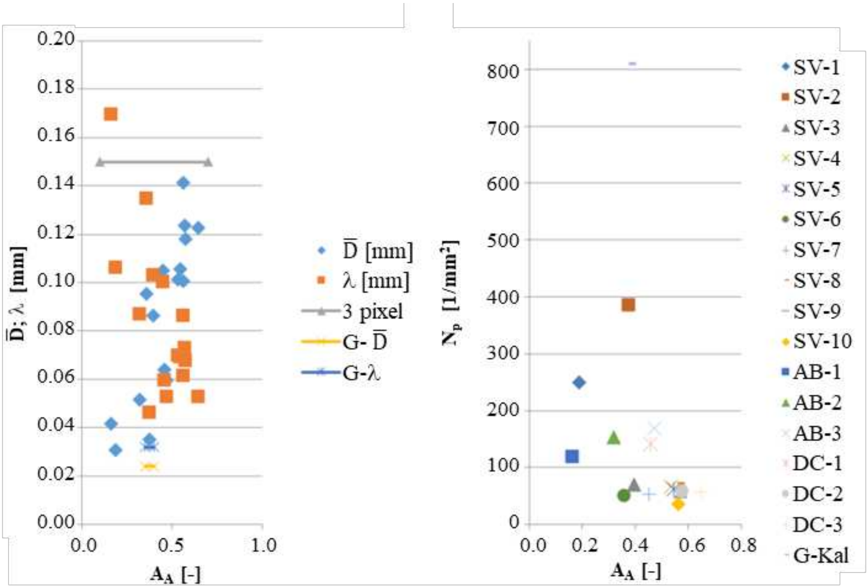

Figure 10. Comparison of patterns

Table 2. Samples with an error of less than 1.5% as a function of parameters (SV and AB was the name of the specimen on Fig. 9)

ABS(H%)<1.5	SV-1	SV-2	SV-3	SV-5	AB-1	AB-2	AB-3
N_p 50-250	SV-1		SV-3	SV-5	AB-1	AB-2	AB-3
A_A 0.2-0.5	SV-1	SV-2	SV-3			AB-2	AB-3

An increase in the pattern aliasing and the average diameter of the speckles increases the error, while the number of speckle per 1 mm^2 and the number of incisions in 1 mm decreases the failure. Based on the analysis of the approximate functions, it can be stated that in the middle of the ranges shown, the error is reduced to an acceptable level of about 1%. Based on these, the parameters of the most favorable pattern can be determined which were also achieved with type 1, 2, 6 water based and graphite paints. Since these paints can be used with both spray and airbrush techniques, good results can be obtained by setting the painting parameters correctly. The usage of spray technique is faster but requires experience and better dexterity, while the usage of airbrush technology is slower, but when set up well does not require much professional knowledge.

4. Conclusion

It was found in the analysis of the literature that the speckle patterns play critical role in DIC measurements. In the first phase of research the ARAMIS 5M DIC system was validated in two ways. In the second phase of research the different paints and paint spraying technologies were examined. It was determined that the best speckle pattern for DIC elongation tests has the following parameters: 0.3…0.4 coverage, 100…200 1/mm^2 speckle number and 0.06…0.10 mm average diameter. As a consequence, these above-mentioned parameters can be achieved by the water-based high-quality matte finish lacquer spray, or the graphite-based matte finish spray, at 22 °C and 40 RH% environment conditions. This research will be continued with various spraying techniques under different environmental conditions.

References

[1] M. A. Sutton, J. J. Orteu et al., Introduction to digital image correlation: Best practices and applications, Experimental Techniques 36 (1) (2012) pp. 3–4.
doi: `https://doi.org/10.1111/j.1747-1567.2011.00798.x`

[2] Y. L. Dong, B. Pan, A Review of Speckle Pattern Fabrication and Assessment for Digital Image Correlation, Experimental Mechanics 57 (8) (2017) pp. 1161–1181.
doi: `https://doi.org/10.1007/s11340-017-0283-1`

[3] S. Gualtieri, Novel technique for DIC speckle pattern optimization and generation, Thesis, Polotecnico di Milano (2012).

[4] D. Lecompte, A. Smits et al., Quality assessment of speckle patterns for digital image correlation, Optics and Lasers in Engineering 44 (11) (2006) pp. 1132–1145.
doi: `https://doi.org/10.1016/j.optlaseng.2005.10.004`

[5] A. Freddi, G. Olmi, L. Cristofolini, Experimental Stress Analysis for Materials and Structures - Stress Analysis Models for Developing Design Methodologies, Springer, New York City, 2015.
doi: `https://doi.org/10.1007/978-3-319-06086-6`

[6] Application Note AN-1701 – Speckle Pattern Fundamentals, Correlated Solutions, 2018.

[7] P. Reu, All about speckles: Aliasing, Experimental Techniques 38 (5) (2014) pp. 1–3.
doi: *https://doi.org/10.1111/ext.12111*

[8] P. Reu, All about speckles: Speckle density, Experimental Techniques 39 (3) (2015) pp. 1–2.
doi: *https://doi.org/10.1111/ext.12161*

[9] P. Reu, All about speckles: Edge sharpness, Experimental Techniques 39 (2) (2015) pp. 1–2.
doi: *https://doi.org/10.1111/ext.12139*

[10] P. Reu, Calibration: A good calibration image, Experimental Techniques 37 (6) (2013) pp. 1–3.
doi: *https://doi.org/10.1111/ext.12059*

[11] P. Reu, Points on Paint, Experimental Techniques 39 (4) (2015) pp. 1–2.
doi: *https://doi.org/10.1111/ext.12147*

[12] P. Reu, Speckles and their relationship to the digital camera, Experimental Techniques 38 (4) (2014) pp. 1–2.
doi: *https://doi.org/10.1111/ext.12105*

[13] P. Reu, Virtual Strain Gage Size Study, Experimental Techniques 39 (5) (2015) pp. 1–3.
doi: *https://doi.org/10.1111/ext.12172*

[14] P. Reu, All about speckles: Contrast, Experimental Techniques 39 (1) (2015) pp. 1–2.
doi: *https://doi.org/10.1111/ext.12126*

[15] P. Reu, All about speckles: Speckle Size Measurement, Experimental Techniques 38 (6) (2014) pp. 1–2.
doi: *https://doi.org/10.1111/ext.12110*

[16] G. Crammond, S. W. Boyd, J. M. Dulieu-Barton, Speckle pattern characterisation for high resolution digital image correlation, Applied Mechanics and Materials 70 (2011) pp. 261–266.
doi: *https://doi.org/10.4028/www.scientific.net/AMM.70.261*

[17] W. S. LePage, J. A. Shaw, J. A., S. H. Daly, Optimum Paint Sequence for Speckle Patterns in Digital Image Correlation, Experimental Techniques, 41(5) (2017) pp. 557–563.
doi: https://doi.org/10.1007/s40799-017-0192-3

[18] CSI Application Note AN-525 – Speckle Pattern Fundamentals, Correlated Solutions, 2014.

[19] G. Lionello, L. Cristofolini, A practical approach to optimizing the preparation of speckle patterns for digital-image correlation, Measurement Science and Technology 25 (10) (2014) (107001).

[20] J. L. W. Carter, M. D. Uchic, M. J. Mills, Impact of Speckle Pattern Parameters on DIC Strain Resolution Calculated from In-situ SEM Experiments. In: J. Carroll, S. Daly (eds) Fracture, Fatigue, Failure, and Damage Evolution, Volume 5. Conference Proceedings of the Society for Experimental Mechanics Series. Springer, Cham, 2015, pp. 119-126.
doi: https://doi.org/10.1007/978-3-319-06977-7_16

[21] G. F. Bomarito, J. D. Hochhalter et al., Increasing accuracy and precision of digital image correlation through pattern optimization, Optics and Lasers in Engineering 91 (2017) pp. 73–85.
doi: https://doi.org/10.1016/j.optlaseng.2016.11.005

[22] B. Pan, Z. Lu, H. Xie, Mean intensity gradient: An effective global parameter for quality assessment of the speckle patterns used in digital image correlation, Optics and Lasers in Engineering 48 (4) (2010) pp. 469–477.
doi: https://doi.org/10.1016/j.optlaseng.2009.08.010

[23] P. Reu, The Art and Application of DIC; DIC: A Revolution in Experimental Mechanics, Experimental Techniques 39 (6) (2015) pp. 1–2.
doi: https://doi.org/10.1111/ext.12173

[24] T. Réti, Qualification of morphological similarity of microscopic tissue images by image analysis procedure, BKL – Kohászat 116 (1) (1983) pp. 17-25, in Hungarian.

Acta
Technica
Jaurinensis

Vol. 14, No. 3, pp. 244-258, 2021
DOI: 10.14513/actatechjaur.00602

Calculating the equivalent temperature for mechanistic pavement design according to the French method for Hungarian climatic conditions

C. Tóth[1,*], L. Pethő[2]

[1]Budapest University of Technology and Economics, Department of Highway and Railway Engineering, Műegyetem rakpart 3, 1111 Budapest, Hungary
[2]Fulton Hogan Infrastructure Services, 180 Burnside Road, Ormeau, QLD, Australia
[*]e-mail: toth.csaba@emk.bme.hu

Submitted: 12/03/2021; Accepted: 10/05/2021; Published online: 20/05/2021

Abstract: The French pavement design method provides a very comprehensive, probability-based design approach. It also provides a fairly sophisticated method for establishing the equivalent pavement temperature, which has been used worldwide for different applications. The objective was to analyse the applicability of the French method for calculating the equivalent pavement temperature for Hungarian climatic conditions. It considers the thickness of the pavement structure and facilitate pavement temperature distribution. It was found that the French method provides a comprehensive approach and can facilitate variable climatic conditions and pavement temperature distribution while considering the thickness of the pavement structure. This provides fit for purpose solutions and eliminates the overly simplified approach to use a single equivalent pavement temperature for variable climatic and pavement conditions. Real pavement temperature data provided crucial input into the accuracy of the methodology. Asphalt modulus values and asphalt fatigue properties at different temperatures were estimated using an internationally well accepted method. The next focus item of this research work will be to refine the calculations based on asphalt modulus master-curves and fatigue data collected from laboratory testing at different temperatures.

Keywords: pavement design; climatic conditions; equivalent temperature

1. Introduction

Strains and deformations of any asphalt pavement is influenced by the distribution of the pavement temperature. Pavement engineers and researchers have been trying to describe the temperature dependency of a given pavement structure by an easily manageable index which provides an equivalent pavement temperature.

For both full depth asphalt pavements and concrete pavements, the environmental impact should be considered at the design phase, which has been proven as a very complex task. The international practice usually simplifies the complex environmental impact to two items, namely the temperature and precipitation [1] [2].

The temperature influences the properties and performance of the materials mixed with bituminous binders, while the precipitation and moisture have an impact on the unbound granular pavement layers. This impact should be considered at the time of the pavement design [3]; also, the impact on the mix design of hot mix asphalt [4]. and on the mix design of base layers treated with bitumen [5] should be carefully considered.

Due to limited access to real temperatures in the pavement structure in the past, it was also important to derive the in-depth temperature from air temperature readings. Capturing air temperature is relatively simple by established and widely used weather stations; measuring pavement temperatures is becoming less expensive, therefore access to such a dataset is becoming more common [6]. However, establishing such a weather station for pavement in-depth temperatures still remains difficult especially when the probes have to be placed under traffic into a road pavement in service.

In order to overcome the difficulties and minimise computing volumes, various methods have been developed since the early 1960s to use equivalent pavement temperatures [7]. This approach uses the core of the Miner's hypothesis [8]; accordingly, the effective stress generated in a given pavement structure characterised by a single pavement temperature is equivalent to the cumulative stress generated in the same pavement structure under variable temperature conditions. The calculation can be performed according to Equation (1).

$$N_{eff} = \frac{1}{\frac{1}{n}\sum_{i=1}^{n}\left(\frac{1}{N_i}\right)} \tag{1}$$

where

N_{eff} = the effective loading cycles at the effective single temperature applied for the design according to Miner's hypothesis,

N_i = the actual allowed loading cycles calculated on the basis of various temperatures,

n = the number of temperature brackets.

The French pavement design method provides a very comprehensive, probability-based design approach. It also provides a fairly sophisticated method for establishing the equivalent pavement temperature, which has been used worldwide for different applications [6] [9].

The objective of this paper is analysing the applicability of the French method for calculating the equivalent pavement temperature for Hungarian climatic conditions. The input data is the measured pavement temperature distribution for the region of Budapest. It is expected that this methodology would provide more accurate pavement design outcomes for different climatic conditions within Hungary. This way using the overly simplified average pavement temperature models would be discontinued and the new method would provide an optimised pavement structure for a given climatic condition.

2. The Equivalent (Design) Temperature in the French Pavement Design Method

Detailed calculation for the equivalent temperature is provided in Laboratoire Central des Ponts et Chausees [10]. The equivalent temperature is defined according to Equation (2), which is based on the Miner hypothesis.

$$\sum_{i=1}^{n} n_i \cdot d_i = 1 \tag{2}$$

where

n_i = the number of equivalent axle passages undergone by the pavement,

d_i = the elementary damage.

The elementary damage is expressed in Equation (3).

$$d_i = \frac{1}{N_i} \tag{3}$$

where

d_i = the elementary damage,

N_i = the number of loadings causing fatigue failure at a strain level $\varepsilon(\theta_i)$.

By combining Equations (2) and (3), Equation (4) follows:

$$\sum_{i=1}^{n} \frac{n_i}{N_i} = 1 \tag{4}$$

Pavement structural design is performed at a constant temperature, referred to as the equivalent temperature θ_{eq}. This temperature is such that the cumulative damage undergone by the pavement over a year, for a given temperature distribution, is equal to the damage that the pavement would undergo with the same traffic but for a constant temperature θ_{eq} [10]. The equivalent temperature is determined by Equation (5), which is the Miner hypothesis written in a different format (Equation (2)).

$$\sum_i \frac{n_i(\theta_i)}{N_i(\theta_i)} = \frac{\sum_i n_i(\theta_i)}{N(\theta_{eq})} \tag{5}$$

where

$N_i(\theta_i)$ = is the number of loadings causing failure due to fatigue for the strain level $\varepsilon(\theta_j)$,

$n_i(\theta_i)$ = is the number of equivalent axle passes undergone by the pavement at a temperature (θ_i),

$N(\theta_{eq})$ = is the number of loadings causing failure due to fatigue for the strain level $\varepsilon(\theta_{eq})$,

θ_{eq} is the equivalent temperature.

Equation (6) is derived from Equation (5) after re-organising the parameters.

$$\frac{1}{N(\theta_{eq})} = \frac{1}{\sum_i n_i(\theta_i)} \left[\sum_i n_i(\theta_i) \left\{\frac{1}{N_i(\theta_i)}\right\}\right] \tag{6}$$

Loading cycles $N_i(\theta_i)$ which cause failure can be deduced from the pavement response at a temperature $\varepsilon(\theta_i)$ and the laboratory test results $\varepsilon_6(\theta_i)$ according to Equation (7).

$$N_i(\theta_i) = \left\{\frac{\varepsilon(\theta_i)}{\varepsilon_6(\theta_i)}\right\}^{1/b} \cdot 10^6 \tag{7}$$

where

$\varepsilon(\theta_i)$ = pavement response at a given temperature,

$\varepsilon_6(\theta_i)$ = fatigue properties from laboratory test results.

The reciprocate of $N_i(\theta_i)$ as defined in Equation (7) equals, by definition, the elementary damage $d(\theta_i)$ at the strain level $\varepsilon(\theta_i)$ (Equation (8)).

$$\frac{1}{N_i(\theta_i)} = d(\theta_i) = \left\{\frac{\varepsilon_6(\theta_i)}{\varepsilon(\theta_i)}\right\}^{1/b} \cdot 10^{-6} \quad (8)$$

Equation (9) be derived by the combination of Equations (6) and (8).

$$\frac{1}{N(\theta_{eq})} = \frac{1}{\sum_i n_i(\theta_i)}\left[\sum_i n_i(\theta_i)\left\{\frac{\varepsilon_6(\theta_i)}{\varepsilon(\theta_i)}\right\}^{1/b} \cdot 10^{-6}\right] \quad (9)$$

The total elementary damage at different temperatures (right side of Equation (9)) is calculated; the equivalent temperature (design temperature) θ_{eq} is the temperature where the elementary damage for $\frac{1}{N(\theta_{eq})}$ equals to the total elementary damage at different temperatures [10] [11].

The value of $\varepsilon_6(\theta)$ can be obtained from laboratory testing or by using the correlation Equation (10) at 10^6 loading cycles (EN 12697-24–2012) [12].

$$\lg(N) = a + \left(\frac{1}{b}\right) \cdot \lg(\varepsilon) \quad (10)$$

where

N = number of load cycles,

a = constant,

b = slope of fatigue line,

ε = strain (microstrain).

Table 1 illustrates an example used for the calculation according to Laboratoire Central des Ponts et Chausées (1997) [10]. The temperature distribution, expressed in 5 °C intervals, and with the relative duration of the designated temperature is shown in the table.

Table 1. Example calculation of the equivalent temperature
Source: Laboratoire Central des Ponts et Chausees (1997) [10]

θ_i (°C)	–5	0	5	10	15	20	25	30
Duration (%)	10	12	18	14	18	18	8	2
ε_t ($\times 10^6$) – pavement response (microstrain)	24	27	32	40	51	68	98	149
$\varepsilon_6(\theta_i)$ ($\times 10^6$) – fatigue performance (microstrain)	95	95	94	92	96	100	110	121

The sum of the weighted elementary damage $d(\theta_i)$ is 0.15 in this example. The equivalent temperature is determined by interpolation, where the single elementary damage is equal to this value; this results in an equivalent pavement temperature of 18.7 °C in this example.

The above calculation for the equivalent pavement temperature is based on fundamental mechanics and considers real pavement structure responses and asphalt fatigue properties. The calculation requires detailed input on the pavement temperature distribution. When real and accurate data can be obtained for the pavement structure for a certain climatic environment, it could provide reliable input into the mechanistic pavement design as described in the rest of this paper.

3. Calculating the Equivalent Temperature for Hungary using the French Method

3.1. Data collection

The vertical temperature distribution of the pavement structure depends on weather conditions and the properties of the subgrade, subbase and upper pavement layers [13]. In order to capture the full extent of the variation, a weather station was established on a private road in Budapest. Sensors were established in a full depth asphalt pavement following completion of the roadworks. The device measured the temperature of the pavement at 0, 2, 7, 14, 29 and 49 cm at a frequency of every 10 minutes. The internal resolution of the temperature sensors were 0.0625 °C and the accuracy of the output was 0.1 °C. Over a period of one year this provided 52,560 data point for each depth, which is considered fairly detailed characterisation of a pavement structure [14].

3.2. Data input

The calculation of the equivalent temperature using the French method was carried out on for two full depth asphalt pavement structures with different thicknesses. One pavement structure was complying with the Hungarian pavement design catalogue [15] for loading class R (extremely heavy traffic) and the other one for loading class D (medium volume traffic). The individual layer thickness, the asphalt moduli and the total pavement thickness is summarised in Table 2. In these calculations it was considered that the subgrade has a consistent support of 50 MPa (surface modulus).

Table 2. Layer moduli for different pavement temperatures – input into the models

Asphalt layer type	***Thickness (mm)***		***Relative temperature distribution in the pavement structure (%)***							
	Traffic category		–5	0	5	10	15	20	25	30
	R	D	Modulus at the pavement temperature bracket (MPa)							
AC11 wearing (50/70) (heavy duty)	40	40	21,900	17,700	13,800	10,400	6,640	3,980	2,320	1,200
AC22 intermediate (35/50) (heavy duty)	80	80	24,000	19,700	15,900	12,500	9,160	5,790	3,520	2,070
AC22 base (50/70) (heavy duty)	190	90	22,700	18,500	14,600	11,000	7,230	4,460	2,670	1,440
Subgrade	N/A	N/A	50	50	50	50	50	50	50	50
Total pavement thickness (mm)	310	210								

The asphalt fatigue properties ($\varepsilon_{(6)}$) for the Hungarian asphalt pavement catalogue were established using the BANDS software. In these calculations the asphalt base layer fatigue performance was predicted at the equivalent temperatures of 10 °C and 10 Hz. It should be noted that since the catalogue was developed a number of modifications were suggested to these parameters; however, these modifications have not been implemented. Also, type testing of asphalt is carried out at significantly different test conditions. In order to remain consistent with the catalogue, for these calculations. The fatigue properties were established using the BANDS software (Shell) and this value returned 100 microstrain (10 °C, 10 Hz). This value was also converted to the various temperature brackets as outlined in Table 2. The BANDS software (Shell) was also used for establishing the various asphalt layer moduli; the properties in Table 3 were used for calculating the properties in Table 2.

Table 3. Layer moduli for different pavement temperatures – input into the models

Asphalt layer	***Bitumen volume of the asphalt mix (%)***	***Poisson's ratio***
AC11 wearing (50/70) (heavy duty)	12.8	0.35
AC22 intermediate (35/50) (heavy duty)	11.4	0.35
AC22 base (50/70) (heavy duty)	11.0	0.35

3.3. Asphalt Fatigue Properties at a Given Equivalent Temperature

Although in metropolitan France the equivalent temperature of 15 °C is used, Laboratoire Central des Ponts et Chausees [10] provides a general approach which can be utilised at any selected temperatures. This methodology can be used over a fairly broad range of positive temperatures, based on the calculation that the approximate value for the dependency of the modulus E and the strain ε_6 can be obtained from Equation (11).

$$\varepsilon_6(\theta) \times E(\theta)^n = constant \tag{11}$$

where

$\varepsilon_6(\theta)$ = fatigue resistance of the asphalt mix, determined at 10^6 loading cycles at the equivalent temperature θ,

$E(\theta)$ = stiffness of the asphalt material at the equivalent temperature θ,

n = material constant.

In the absence of results of fatigue tests for a given material at different temperatures, a mean value of 0.5 can be selected for n and the equation can be re-organised as in Equation (12).

$$\varepsilon_6(\theta_i) = \varepsilon_6(10°C; 10Hz) \times \sqrt{\frac{E(10°C;10Hz)}{E(\theta_i;10Hz)}} \tag{12}$$

Equation (12) provides a model and estimation of the fatigue properties at different temperatures. By using Equation (12), the fatigue properties at any given equivalent temperatures could be readily calculated, given that the standardised fatigue test and a temperature-frequency sweep for stiffness has been completed.

Bodin et al. [16] presented a series of fatigue tests at different temperatures, using two different asphalt materials, which provides validation of the above model. For another validation of the model, flexural fatigue tests were carried out on an Australian EME2 mix at 10, 20 and 30 °C and 10 Hz using four-point bending test. It was found that the fatigue properties at different temperatures can be reliably estimated for Australian test conditions by using Equation (11) with n=0.5. By using a value of n=0.5, Equation (11) can be reorganized as shown in Equation (12) [9].

For the analysis in this paper, it is assumed that the value of n=0.5 is valid for the Hungarian test conditions and Equation (12) is used. In this equation $E(\theta_i)$ is the modulus of the asphalt layer at the given temperature. This is summarised in Table 2; for a more accurate analysis these values need to be established in the laboratory through testing; however, for this paper, the estimated moduli values were used.

The method of calculation is summarised in Tables 4 and 5; the methodology is visualised in Figs. 1 and 2, respectively.

Table 4. Input into calculations for pavement model in the traffic loading category R

θ(°C)	–5	0	5	10	15	20	25	30
Temperature distribution (%)	1.3	12.5	16.2	11.3	9.1	18.7	16.2	14.7
E (θi; 10 Hz) (AC22 base)	22,700	18,500	14,600	11,000	7,230	4,460	2,670	1,440
ε(6), θ(i), n=0.5	70	77	87	100	12	157	203	276
ε(t) (×10⁻⁶) - pavement response	56.0	66.0	81.0	101.0	142.0	210.0	314.0	501.0
ε(6), θ(i) (×10⁻⁶) - fatigue performance	70	77	87	100	123	157	203	276
d (θ,i) (×10⁶) - elementary damage	0.337	0.459	0.708	1.051	2.022	4.275	8.860	19.571
d (θ,i) (×10⁶) - weighted elementary damage	0.004	0.057	0.115	0.119	0.184	0.800	1.433	2.885
d (θ,i) (×10⁶) – total	5.60							
d (θ,i) (×10⁶) – weighted elementary damage (cumulative)	0.004	0.062	0.176	0.295	0.479	1.280	2.712	5.597

Table 5. Input into calculations for pavement model in the traffic loading category D

θ(°C)	–5	0	5	10	15	20	25	30
Temperature distribution (%)	1.3	12.5	16.2	11.3	9.1	18.7	16.2	14.7
E (θi; 10 Hz) (AC22 base)	22,700	18,500	14,600	11,000	7,230	4,460	2,670	1,440
ε(6), θ(i), n=0.5	70	77	87	100	12	157	203	276
ε(t) (×10⁻⁶) - pavement response	56.0	66.0	81.0	101.0	142.0	210.0	314.0	501.0
d (θ,i) (×10⁶) - elementary damage	0.337	0.459	0.708	1.051	2.022	4.275	8.860	19.571
d (θ,i) (×10⁶) – weighted elementary damage	0.004	0.057	0.115	0.119	0.184	0.800	1.433	2.885
d (θ,i) (×10⁶) – total	5.60							
d (θ,i) (×10⁶) – weighted elementary damage (cumulative)	0.004	0.062	0.176	0.295	0.479	1.280	2.712	5.597

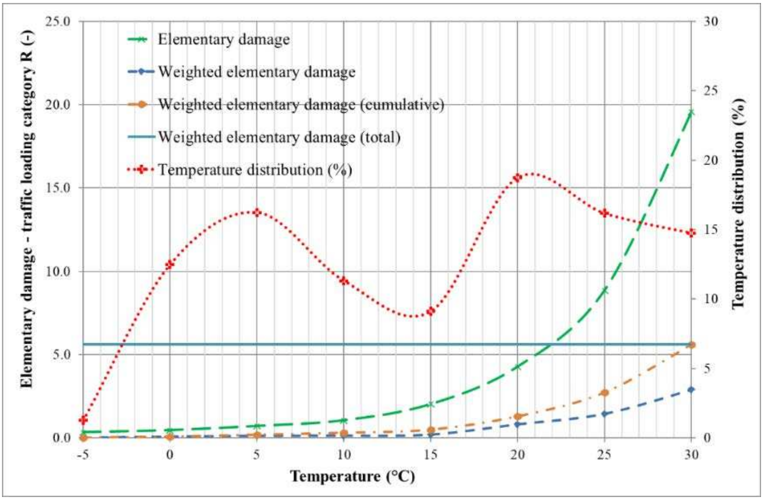

Figure 1. Establishing the equivalent temperature based on the calculation of elementary damage – traffic loading category R

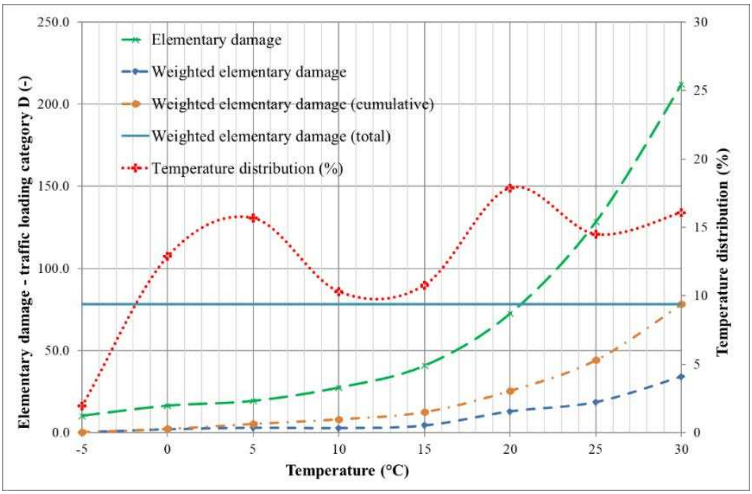

Figure 2. Establishing the equivalent temperature based on the calculation of elementary damage – traffic loading category D

The equivalent temperature (design temperature) θ_{eq} is the temperature where the elementary damage equals to the total elementary damage at different temperatures; this is calculated by interpolating the data set. For the pavement structure for traffic loading category R this value was calculated as 22 °C and for traffic loading category D this was 20.5 °C. By using the average monthly air temperature values the weighted mean annual pavement temperature (wMAPT) was calculated with the SPDM 3.0. software [17] as 17.7 °C.

4. Summary of the Calculations and Practical Application of the Methodology

The current Hungarian pavement design catalogue [15] was developed by Nemesdy et al. in 1992 [18]. Nemesdy et al. utilised the BANDS nomographs for the asphalt types used in the 1990s; the methodology described in this paper utilised the same approach, i.e. using the BANDS nomographs; however, supported by a computer software. Since the asphalt compositions significantly changed since the 1990s, in this work the asphalt moduli were determined based on the combined aggregate grading, bitumen content and air voids contents as outlined in the current Hungarian asphalt specification [19].

The calculations were conducted at 5°C intervals between –5 and +30 °C; the calculated bitumen and the asphalt moduli values are summarised in Table 6. Unmodified binders were selected for this analysis that the BANDS nomographs can be used. While 35/50 binder is not commonly used in Hungary, this was selected in line with best practice that intermediate layers should have a higher rutting resistance.

Table 6. Bitumen and asphalt moduli of the various asphalt types as a function of temperature

Temperature (°C)	***AC11 wearing (heavy duty)***		***AC22 intermediate (heavy duty)***		***AC22 base (heavy duty)***	
Binder type	50/70		35/50		50/70	
	S_{binder} (MPa)	$E_{asphalt}$ (MPa)	S_{binder} (MPa)	$E_{asphalt}$ (MPa)	S_{binder} (MPa)	$E_{asphalt}$ (MPa)
–5	604	21,900	700	24,000	604	22,700
0	387	17,700	455	19,700	387	18,500
5	229	13,800	286	15,900	229	14,600
10	124	10,400	169	12,500	124	11,000
15	60.7	6,640	90.1	9,160	60.7	7,230
20	28.8	3,980	44.9	5,790	28.8	4,460
25	13.1	2,320	21.1	3,520	13.1	2,670
30	5.05	1,200	9.37	2,070	5.05	1,440

Based on the above calculations the results were different for the two different traffic loading categories of R and D, resulting in equivalent temperature values of 22 °C and 20.5 °C respectively; for practical considerations it is recommended using 20 °C as a starting point for the new Hungarian pavement design methodology. At this temperature the asphalt moduli and parameters are summarised in Table 7, where the values are rounded to the nearest 100 MPa for practical reasons.

Table 7. Suggested asphalt moduli and parameters for pavement structural design

Asphalt layer	***Asphalt moduli at equivalent temperature of 20°C (MPa)***	***Bitumen volume of the asphalt mix (%)***	***Poisson's ration***
AC11 wearing (50/70) (heavy duty)	4,000	12.8	0.35
AC22 intermediate (35/50) (heavy duty)	5,800	11.4	0.35
AC22 base (50/70) (heavy duty)	4,500	11.0	0.35

The above described methodology can be refined and updated based on long-term temperature measurement in different Hungarian regions. Considering the differences in different climatic regions within the country, the pavement structure may be further optimised and refined. This way the pavement structures in the different climatic regions would be designed based on real data and not on average values established for the entire country.

The above methodology provided the basis for a fundamental research work. As a result, a new mechanistic pavement design approach was developed for Hungary, which also considers the realistic bearing capacity of the locally available subgrade and base layers. This provided an avenue to further optimise pavement structures in a holistic way, with considering the local climatic conditions and local material availability. It also provides pathways for new and innovative technologies by incorporating the mechanistic properties of newly developed potential materials and technologies. The research work, methodology and outcomes are described in details by Primusz and Toth [20], where the material parameters described in Table 7 were applied for the calculations.

5. Summary and conclusions

The French pavement design method provides a very comprehensive, probability-based design approach. It also provides a fairly sophisticated method for establishing the equivalent pavement temperature, which has been used worldwide for different applications. The objective of this paper was analysing the applicability of the French method for calculating the equivalent pavement temperature for Hungarian climatic conditions. It was found that the French method provides a comprehensive approach and can facilitate variable climatic conditions and pavement temperature distribution while considering the thickness of the pavement structure. This provides fit for purpose solutions and eliminates the overly simplified approach to use a single equivalent pavement temperature for variable climatic and pavement conditions.

Real pavement temperature data provided crucial input into the accuracy of the methodology. Asphalt modulus values and asphalt fatigue properties at different temperatures were estimated using an internationally well accepted method. The next focus item of this research work will be to refine the calculations based on asphalt modulus master-curves and fatigue data collected from laboratory testing at different temperatures.

References

[1] P. Pereira, J. Pais, Main flexible pavement and mix design methods in Europe and challenges for the development of an European method. *Journal of Traffic and Transportation Engineering (English Edition)* 4 (4) (2017) pp. 316–346.
doi: `https://doi.org/10.1016/j.jtte.2017.06.001`

[2] X. Gao, Y. Wei, W. Huang, Strain-based equivalent temperature gradient in concrete pavement and comparison with other quantification methods, *Road Materials and Pavement Design* 18 (6) (2017) pp. 1460–1472.
doi: `10.1080/14680629.2016.1218788`

[3] R. Ktari, F. Hammoum et al., Consideration of Seasonal Temperature Changes in the French Pavement Design Method. In P. Kotronis (Ed.), Risk Evaluation and Climate Change Adaptation of Civil Engineering Infrastructures and Buildings, *ISTE Ltd and John Wiley & Sons, Inc.*, London, 2019, pp. 1–55.
doi: `https://doi.org/10.1002/9781119671428.ch1`

[4] A. Saleh, L. Gáspár: Advantages and limitations of using foamed bitumen. *Acta Technica Jaurinensis* (2021).
doi: `https://doi.org/10.14513/actatechjaur.00587`

[5] A. Saleh, L. Gáspár: Functional and environmental impacts of the use of reclaimed asphalt pavement materials and of foamed asphalt. *Acta Technica Jaurinensis* (2021).
doi: `https://doi.org/10.14513/actatechjaur.00590`

[6] M. Pszczola, J. Judycki, Equivalent temperature for design of airport pavements using mechanistic-empirical methods, May 2014.

[7] L. Petho, Influence of temperature distribution on the design of pavement structures. *Periodica Polytechnica Civil Engineering* 52 (1) (2008) pp 45–53. doi: `https://doi.org/10.3311/pp.ci.2008-1.07`

[8] M.A. Miner, Cummulative Damage in Fatigue. *The American Society of Mechanical Engineers* 67 (1945) pp. 159–164.

[9] L. Petho, P. Bryant, P, EME2 fatigue properties and pavement design in a sub-tropical climate. *8th RILEM international conference on mechanisms of cracking and debonding in pavements*, Springer, Nantes, 2016, pp. 431-436.

[10] Laboratoire Central des Ponts et Chaussées (LCPC) 1997, French design manual for pavement structures, LCPC, Paris, France.

[11] Road pavement structural design – Application to new pavements, NF P 98-086–2011 (2011) (in French).

[12] Bituminous mixtures: test methods for hot mix asphalt: part 24: resistance to fatigue, EN 12697-24:2012 (2012).

[13] W. Arand, H. Lorenzl, influence of bitumen hardness on the emergency behavior of asphalt paving of different thickness depending on the capacity of the surface, the traffic load and the temperature; part 2 (original title: Einfluß der Bitumenhärte auf das Ermüdungsverhalten von Asphaltbefestigungen unterschiedlicher Dicke in Abhängigkeit von der Tragfähigkeit der Unterlage der Verkehrsbelastung und der Temperatur). *Forschung Straßenbau und Straßenverkehrstechnik* 696 (1995) pp. 1–40 (in German). URL `https://trid.trb.org/view/996178`

[14] I. Fi, L. Petho, Calculation of the equivalent temperature of pavement structures, *Periodica Polytechnica Civil Engineering*, 52 (2) (2008) pp. 91–96.
doi: `https://doi.org/10.3311/pp.ci.2008-2.05`

[15] Designing and strengthening of asphalt pavements, e-UT e-UT06.03.13 (ÚT 2-1.202:2005 (2005) (in Hungarian).

[16] D. Bodin, J. Terrier et al., Effect of temperature on fatigue performances of asphalt mixes. *11th International conference on asphalt pavements*, ISAP, USA, Nagoya, 2010.

[17] C.P. Valkering, The Shell Pavement Design Method on a Personal Computer, *Proceedings of the 7th International Conference on the Structural Design of Asphalt Pavements* (1992) pp. 351–374.

[18] E. Nemesdy, Background of the mechanistic approach of new Hungarian pavement design catalogue (original title: Az új magyar tipus pályaszerkezetek mechanikai méretezésének háttere). *Mélyépitési Szemle* 42 (8) (1992) pp. 293–306 (in Hungarian).

[19] Requirements for Asphalt Pavement Mixtures of Road Structures, ÚT 2-3.301-1-2010 (2010) (in Hungarian).

[20] C. Toth, P. Primusz, New Hungarian Mechanistic-Empirical Design Procedure for Asphalt Pavements. *Baltic Journal of Road and Bridge Engineering* 15 (1) (2020) pp. 161–186.
doi: https://doi.org/10.7250/bjrbe.2020-15.466

Acta
Technica
Jaurinensis

Vol. 14, No. 3, pp. 259-269, 2021
DOI: 10.14513/actatechjaur.00603

Vibration levels of stacked parcel packages in laboratory test environment. Over-tested or under-tested?

Zs. Németh[1], B. Molnár[1], Cs. Pánczél[1], P. Böröcz[1,*]

[1]Széchenyi István University, Department of Logistics and Forwarding
Egyetem sq. 1, 9026, Hungary
[*]e-mail: boroczp@sze.hu

Submitted: 12/03/2021; Accepted: 19/04/2021; Published online: 26/04/2021

Abstract: Courier express parcel (CEP) shipments become one of the most important delivery methods in the Business-to-Consumer sales model. This paper observed and analyzed the vertical vibration levels that occur in stacked and unsecured parcels during express delivery versus the simulation in the laboratory. At the end, a detailed comparison is reported between the field and laboratory vibration levels (based on standard PSD test profile) in the frequency range of 1 – 200 Hz. For the measurement a three-layer stacked unit was used building from corrugated box samples. The result shows and analyzes the vibration levels in the stacked layers in comparison to the ISTA (International Safe Transport Association) vibration protocol where only a single parcel is required to be tested without any stacking configuration.

Keywords: Random vibration; packaging; PSD; stacked unit, parcel delivery

1. Introduction

The global parcel delivery service has grown significantly over the past decade [1]. In this service, the first and last step is practically a normal road transportation with small vehicles like vans, when the operators (Fedex, TNT, DPD, etc.) collect or deliver the parcels.

Of course, this mode of delivery brought some new physical circumstances that former was not analyzed by packaging engineers. This way the worldwide used standards has not focused on some aspect of the transportation environment yet. Here a very interesting circumstances should be highlighted, namely the unsecured and not unitized load of parcels. This can be seen in Fig. 1. The reasons of this later phenomenon are the very intensive flow and wide range of packages at the same time, in the same vehicle. This often means that the operators try to use the most of the vehicle capacity; thereby many identical or different kinds of parcels are stacked on top of each other [2]. This situation is more complex due to the fact that practically any fixation accessories are used in this transportation mode.

Figure 1. Stacked parcels in CEP service

As it can be seen the parcels practically can move in the vertical with unrestrained stacked configuration. This physical condition is very important to analyze in order for packaging engineers to design suitable protective packaging systems.

Many of former studies dealt with the vibration level during transportation and investigated the effect of payloads, suspension system and road condition to vibration levels [3-8]. The response vibration levels that can be observed on the vehicle can be grouped on factors such as vehicle body structure, type of vehicle suspension and tires, road roughness, vehicle speed and actual payload, respectively [9]. However, these studies measured and analyzed the vibration levels on the floor of the vehicle.

Another aspect is why the result of this study is important for the packaging engineers is that the generally widely used laboratory test standards for parcel shipment simulation deal with single package testing, not with stacked units.

The main goal of this paper was to measure the vibration levels in layers of stacked packages during laboratory test for stacked parcel delivery shipments and to compare the layers' vibration levels to the most popular standard test level. The new results can be useful for packaging engineers to make better and precise pre-shipment testing. Furthermore, the results help the use of the vibration test technique in the simulation of parcel delivery goods in a stacked way.

For the investigation a three-layer stacked unit was built to observe the vibration levels on vibration table at the laboratory using ISTA 3A pick-up-and-delivery vibration spectrum (International Safe Transport Association). The results showed that the vibration level increases in the stacked load upwards and how over-run or under-test can be experienced in the top most layer in comparison to the lower one. These findings are limited to single axis vibration simulation and unsecured loads.

2. Methods

2.1. Samples and laboratory circumstances

For this study three identical small, corrugated box parcels were set up for the measurements of the stacked unit. Each sample packaging contained a Lansmont SAVER 3x90 field data recorder (Lansmont Corp., CA, USA), which was fixed to an aluminum frame (Fig. 2). Inside the package this ITEM aluminum profile frame (©item Industrietechnik GmbH) ensured the rigid fixation of SAVERs and the best fitting to the boxes' geometrical sizes. Thereby, a total of four SAVERs were used for the measurements, three of the SAVERs were in the sample boxes and one of the SAVERs was mounted to the vibration table directly. Table 1 describes the sample specifications and SAVER settings for this study.

Table 1. Specifications for samples used and accelerometer sensors

Samples		***Sensors' setup***	
Corrugated board	35BC	Timer triggered data	1 s
Weight of board	742 g/m^2	Wake-up interval	1 s
ECT	9.0 kN/m	Recording time	1.000 s
BST	1 685 kPa	Sample / sec	500 Hz
Weight of box	190 g	Sample size	500
Size of box (w x d x h)	180x180x195 mm	Frequency resolution (PSD)	0.50 Hz
Weight of ALU frame	1 440 g	Anti-Aliasing frequency	200 Hz
Entire weight	2 630 g		

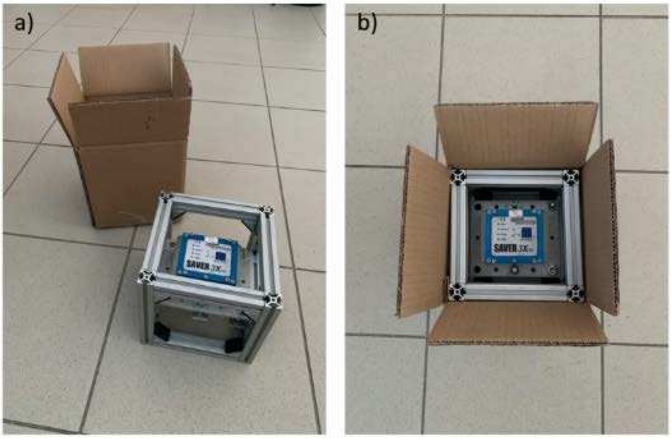

Figure 2. Samples used with the built-in accelerometer sensor

A measurement system was built for the laboratory standard test in order to obtain and compare vibration levels between the layers. This can be seen in Fig. 3. The stacked unit was located above the center of hydraulic vibration table and an aluminum fence was used to prevent the stacked unit from moving in lateral and longitudinal directions. This way, the stacked layers' motion in the vertical direction was not restricted at all.

Figure 3. Stacked parcels in CEP service

The laboratory measurement was performed at Packaging Laboratory, Hungary (University of Győr). The ISTA 3A Pick-up and delivery random vibration profile (Fig. 4) was programmed for the vibration system. This testing procedure is the one generally used for packed-products for parcel delivery shipment, but it uses only single parcel during the laboratory testing without stacking requirements or circumstances. The Power Spectral Density (PSD) spectrum of this vibration profile produces time-compressed random signal for small vehicle vibration during the test procedure. The frequency range and overall G_{rms} of this profile between 1 – 200 Hz is 0.46.

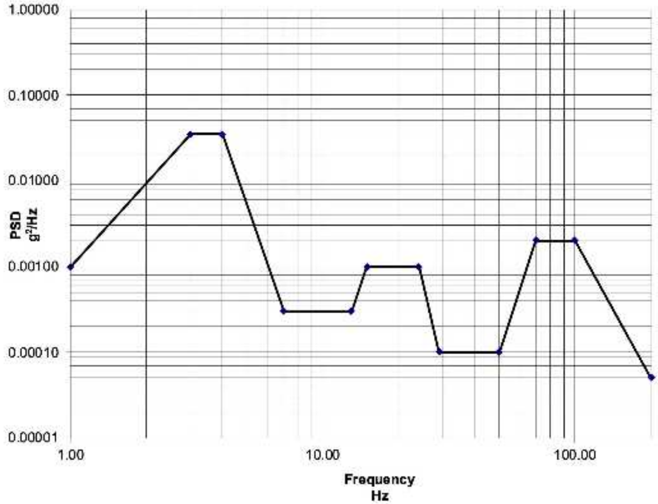

Figure 4. ASTM D7386 - Standard Practice for Performance Testing of Packages for Single Parcel Delivery Systems PSD spectrum.

The average power density (Eq. 1.) within a narrow band of frequencies (BW) of a given spectrum can be determined by G_{rms} values based on the number of samples of a given bandwidth. In this way G_{rms} is determined by the root mean square value of the acceleration in G's in the given bandwidth of frequency, based on the number of (n) samples. Table 2 contains the frequency breakpoints and vibration intensity for this ISTA spectrum.

$$PD = \frac{1}{BW} \sum_{i=1}^{n} (RMS\ G_i^2)/n \qquad (1)$$

Table 2. Frequency breakpoints and PD levels for ISTA 3A spectrum

Frequency (Hz)	PSD level, g^2/Hz
1	0.001
3	0.035
4	0.035
7	0.0003
13	0.0003
15	0.001
24	0.001
29	0.0001
50	0.0001
70	0.002
100	0.002
200	0.00005

2.2. Data analyst

PSDs were calculated from the measured vibration data using Fast Fourier Transformation (FFT) of Xware software and MATLAB R2014a (MathWorks Inc, Massachusetts, USA). The values of power density (PD) levels are presented between 1 – 200 Hz. This frequency range represents those vibration events, which have enough intensity to influence the integrity of product-package system used in general industry. Fig. 5 shows an example of a PSD lot for normal truck vibration during transportation with lead spring suspension.

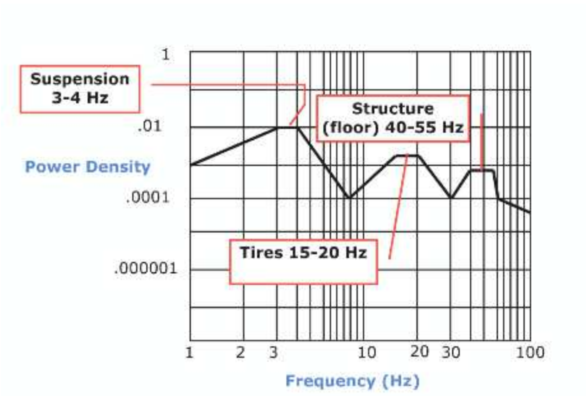

Figure 5. A typical PSD plot for heavy truck vibration

For a detailed and directed comparison the calculated PD levels of recommended ISTA 3A spectra and the observed PD levels in the layer were compared by splitting the entire spectrum to three frequency regions. This way the vibration intensity and the different response vibration can be comparable in those frequency bands where the real vehicle produces higher intensity or the recommended test spectrum has got peaks. The base of the splitting method can be seen in Fig. 6.

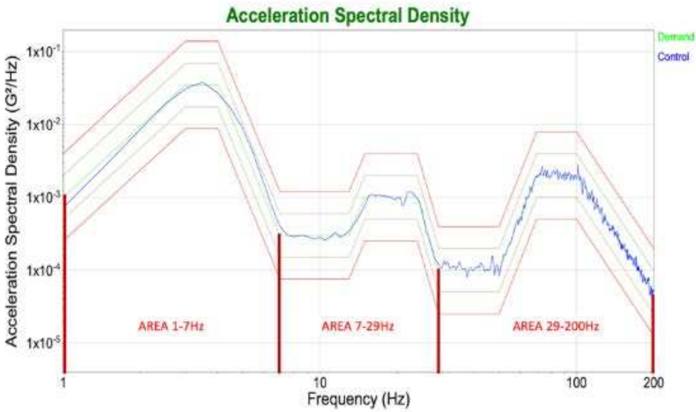

Figure 6. Frequency regions for comparison purposes

3. Results

3.1. Overall G_{rms} in the entire frequency bands

Fig. 7 shows the PSD plots for the recorded vibration on vibration table in the three layers. Fig. 8 contains the overall G_{rms} bar graphs of PSD for 1 – 200 Hz. Based on layers the highest values were in the 3rd level followed by 2nd, and the least in 1st level, respectively, of course increasing upward level by level. Below 50 Hz the vibration intensity was about 1 – 3 dB higher than the ISTA profile, over 50 Hz the reduction was between 8 – 26 dB.

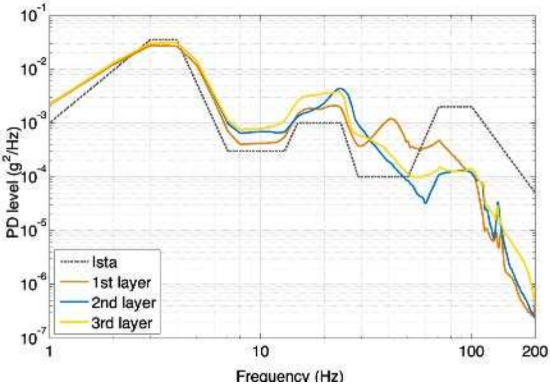

Figure 7. Recorded PSD plots for the three layers

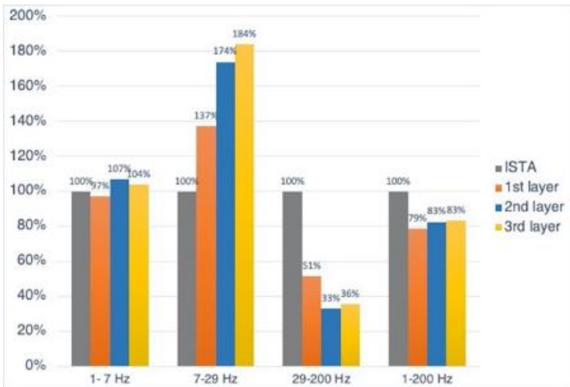

Figure 8. Overall G_{rms} values in the different frequency ranges

3.2. Comparison in varied frequency bands

Table 3 and 4 contains the numerical data for calculated Overall G_{rms} values and percentage comparison in the base of ISTA profile for the entire frequency band observed and for splitted frequency ranges. As it was former mentioned the reason of splitting these bands is to show a relative direct comparison to the standard ISTA 3A protocol.

Table 3. Numerical report for Overall G_{rms} in different frequency ranges

	1- 7 Hz	**7-29 Hz**	**29-200 Hz**	**1-200 Hz**
ISTA 3A Pick-up and Delivery	0.27915	0.11776	0.34597	0.45988
1st layer	0.27113	0.16145	0.17746	0.36204
2nd layer	0.29875	0.20497	0.11346	0.37966
3rd layer	0.29005	0.21652	0.12327	0.38237

Table 4. Percentage based comparison for Overall G_{rms} in different frequency range (ISTA = 100%)

	1- 7 Hz	**7-29 Hz**	**29-200 Hz**	**1-200 Hz**
ISTA 3A Pick-up and Delivery	100%	100%	100%	100%
1st layer	97%	137%	51%	79%
2nd layer	107%	174%	33%	83%
3rd layer	104%	184%	36%	83%

3.4. Limitations

Here has to be noted by the authors that the corrugated board that used for this study can influence to the results of measurements. Although the authors tried to fill the corrugated box perfectly with the aluminum frame to avoid the effect of damping mechanism by the box, the corrugated box may have slight damping effect. So, the readers have to consider that various corrugated board has different damping features to the results

Conclusion

- Results from the study show that it is obvious that between 7 – 29 Hz the G_{rms} levels show a high over-run for the layers upwards. It means almost double vibration intensity at the third layer. It can cause an over damage ratio in comparison to the standard circumstance where only a single parcel is under tested.
- In lower frequency range (1 – 7 Hz) the stack layers practically suffer in the same vibration intensity as the standard protocol perform.
- On the contrary, over 29 Hz, the G_{rms} value is lower upwards than ISTA test standard, which means an under-test in comparison to the standard requirement, if the upper layers are under investigated. This phenomenon can be attributed to the damping feature of corrugated samples used for this study.

- Obviously that the vibration response of stacked parcels cannot be same than a single parcel, but these parcels are often stacked in the industry practice. At the same time, it is definitely clear that the specification applied by the standard, namely only a single parcel is under tested, is not suitable for testing stacked parcels due to the not-uniformly vibration response over the entire spectrum, or a single parcel vibration test does not give properly feedback about the real vibration circumstances of industrial practice.

References

[1] E. Mazarenau. Global size of the courier, express and parcel (CEP) market 2009-2019. Statista.com [cited 11-03-2021]. URL `https://www.statista.com/statistics/723986/cep-market-total-revenue-worldwide/`

[2] P. Böröcz, B. Molnár, Measurement and Analysis of Vibration Levels in Stacked Small Package Shipments in Delivery Vans as a Function of Free Movement Space. *Applied Science* 10 (21) (2020) 7821. doi: `https://doi.org/10.3390/app10217821`

[3] R. K. Brandenburg, J. J. Lee, Fundamentals of Packaging Dynamics. L.A.B. Equipment, Inc.: Itasca, USA, 2001.

[4] P. Böröcz, S. P. Singh. Measurement and analysis of delivery van vibration levels to simulate package testing for parcel delivery in Hungary. *Packaging Technology and Science* 31 (5) (2018) pp. 1-11. doi: `https://doi.org/10.1002/pts.2327`

[5] H. Zhou, Z. W. Wang. Measurement and analysis of vibration levels for express logistics transportation in South China. *Packaging Technology and Science* 31(10) (2018) pp. 1-14. doi: `https://doi.org/10.1002/pts.2404`

[6] J. Stallings, J. Singh, SP. Singh. Measurement and Analysis of Vehicle Vibration for Parcel Delivery Vehicles in Single Parcel Shipments. *Journal of Applied Packaging Research* 4 (2010) pp. 75–82.

[7] V. Chonhenchob, S. P. Singh, J. J. Singh, J. Stallings, G. Grewal, Measurement and analysis of vehicle vibration for delivering packages in small-sized and medium-sized trucks and automobiles. *Packaging*

Technology and Science 25 (1) (2012) pp. 31-38.
doi: `https://doi.org/10.1002/pts.955`

[8] P. Böröcz, Vibration levels in vans as a function of payload and leaf spring sheet number. *Journal of Testing and Evaluation* 46 (1) (2017) pp. 236-243.
doi: `https://doi.org/10.1520/JTE20160538`

[9] P. Böröcz, Averaged vibration levels during courier parcel delivery service in small truck in Hungary. *FME Transaction* 46 (2) (2018) pp. 211–217.
doi: `https://doi.org/10.5937/fmet1802211B`

[10] M. A. Garcia-Romeu-Martinez, S. P. Singh, V. A. Cloquell-Ballester, Measurement and analysis of vibration levels for truck transport in Spain as a function of payload, suspension and speed. *Packaging Technology and Science* 21 (8) (2008) pp. 439-451.
doi: `https://doi.org/10.1002/pts.798`

[11] P. Böröcz, Vibration and acceleration levels of multimodal container shipping physical environment. *Packaging Technology and Science* 32 (6) (2019) pp. 269-277.
doi: `https://doi.org/10.1002/pts.2434`

[12] P. Böröcz, Vibration Levels of Stacked Automotive Engine Rack in Truck Shipments as a Function of Vehicle Speed and Road Condition. *Journal of Testing and Evaluation* 49 (1) (2021) pp. 613-628.
doi: `https://doi.org/10.1520/JTE20180782`

[13] ISTA Procedure 3A. Packaged-Products for Parcel Delivery System Shipments 70 kg (150 lb) or Less (Standard, Small, Flat or Elongated). East Lansing: International Safe Transit Association; 2006.

Acta
Technica
Jaurinensis

Vol. 14, No. 3, pp. 270-280, 2021
DOI: 10.14513/actatechjaur.00607

Study the effect of Heavy Oil Fuel Ash on the geotechnical properties of clay soil

R. Ousta[1], A. Tawalo[2,*]

[1]Tishreen University, Department of Geotechnical Engineering
AL-Thowra Street, GRF4+3W Latakia, Syria
[2]Széchenyi István University, Department of Structural and Geotechnical Engineering, Egyetem tér 1,H-9026 Győr, Hungary
*e-mail: aliibrahimtayalo@tishreen.edu.sy

Submitted: 21/03/2021; Accepted: 19/04/2021; Published online: 22/04/2021

Abstract: Power stations are widely spread in Arabic Syrian Republic, unlike most of power stations in the world that work by using coal as the operating fuel, most of Syrian power stations depend on the heavy fuel oil to generate electricity. Although there are a lot of studies about use of the fly ash produced from burning coal, the fly ash resulted by using heavy fuel oil as an operating material for the power stations had less attention. This paper aims to study the effect of this type of fly ash on the geotechnical properties of the clay soil and comparison it with the effect of fly ash resulted by power stations that use the coal. Two percentages of heavy oil fuel ash were mixed with the soil 5% and 10% of the dry soil weight with two curing periods 7 and 28 days. The results indicated that adding heavy oil fuel ash to the soil will decrease the cohesion in addition to increase the internal friction angle. There is not clear effect of the curing periods and the increase in the percentage of fly ash on the Atterberg limits.

Keywords: Fly ash, Clay soil, Geotechnical properties, Heavy oil fuel ash

1. Introduction

The Industrial Revolution made the things that we wouldn't expect to happen necessary things that we cannot imagine our life without them today. As is well known, every matter has advantages and disadvantages. The industrial revolution that was blessed by human at the beginning of the last century did not only bring benefit, but also the harm, as factory waste pollutes water, air and soil.

We can define soil pollution by saying: it is entrance of strange materials in the soil or an increase in the density of one of its natural components, which lead to a change in its chemical or physical properties or both, and these materials are called soil pollutants and may be pesticides, chemical fertilizers, acid rain or waste (industrial, household, radioactive, etc.) and others.

Power stations are widely spread in Syria and they are considered the main source of the electric power. Although most of countries use coal as the employed fuel of the power stations [1], most of Syrian power stations depend on the heavy fuel oil to generate the electric power.

Burning of coal and heavy fuel oil will produce fly and bottom ash. fly ash that caused by use coal in power stations is different from that caused by use heavy oil fuel.

Most of the research that studied the effect of fly ash on soils used the fly ash that caused by burning coal (Fig. 1). Erdal Cocka [2] studied the effect of fly ash produced from burning of coal on expansive soil and added it to the soil at percentages from 0% to 25% of the dry soil weight and two curing periods (7, 28) days, after that the mixtures were subjected to the free and oedometeric swell tests and their experimental results confirmed that the plastic index and the possibility of swell decreased with increase the percentage of fly ash and curing period. The optimum fly ash percentage for reducing swelling potential is 20% of dry soil weight.

Pandian et.al [3] studied two types of fly ash produced from burning coal, Raichur fly ash (Class F) and Neyveli Fly Ash (Class C) on the CBR properties of BC soil (Black Cotton Soil). The percentage of fly ash ranged from 0 to 100% of dry soil weight and the addition of fly ash to BC soil increased the CBR of the mixture (soil + ash) to the first optimum level. Further addition of fly ash more than the first optimum percentage caused a decrease in the CBR of the mixture by 60% and then the second optimum level.

Phanikumar and Sharma [4] conducted the same study on the effect of fly ash produced from burning coal on the geotechnical properties of the expansive soil by an experimental program. They studied the effect of fly ash on some parameters such as free swell, swell pressure, plastic index, and unconfined compressive strength. Fly ash was added at percentages 0, 5, 10, 15, 20 of the dry soil weight and they concluded.

- Increase percentage of fly ash reduced the plastic index and led to a decrease the free swell by 50% at 20% of fly ash.
- Increase percentage of fly ash also led to a decrease the optimum moisture content value (OMC) and an increase the maximum dry density (ρ_{max}).
- The undrained shear resistance (Su) increases with increase percentage of fly ash mixed with the expansive soil.

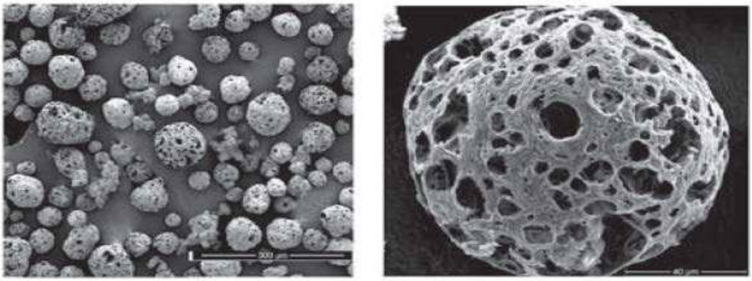

Figure 1. Carbon particle in heavy oil fuel ash [2]

Camilleri et al [7] used heavy oil fuel ash with Flowable Fill Concrete and with Hollow Masonry Units, and they concluded that the use of this type of ash with replacement percentages of the cement equal to 30% and 20%, respectively is recommended.

The aim of this paper is to study the effect of Heavy Oil Fuel Ash (fly ash caused by burning heavy fuel oil) on the geotechnical properties of clay soil, where the power stations in Arabic Syrian Republic produce large quantities of this type of fly ash. So, it is important to know the effect of it on the clay soils and the possibility to find useful utilization in the field of geotechnical engineering and soil stabilization like fly ash produced by burning coal.

2. Methods and materials

This research depends on the comparative experimental approach and carried out by following these phases.

(a) Study the geotechnical properties of the natural soil.

(b) Study the geotechnical properties of the mixtures (soil + HOFA "Heavy Oil Fuel Ash"): the soil was mixed with two different percentages of heavy oil fuel ash (5 and 10) % of the dry soil weight and the mixtures were tested for two curing periods (7 and 28) days.

(c) Compare and discuss the results.

2.1. The laboratory work

The following tests were carried out on the natural soil:

- specific gravity (ASTM D854-98),
- standard Proctor test (ASTM D 698-91),
- Unconfined Compressive Strength (ASTM D2166-98a),
- Direct Shear Test for Soils Under Consolidated Drained Conditions (ASTM D3080-98),
- Sieve Grain Size Analysis (ASTM D4318-98),
- Atterberg limits (ASTM D4318-98),
- free Swell (ASTM D4546-98).

For the mixture (soil + HOFA), the samples were formed with the same density of the natural soil and the following tests were carried out.

- Unconfined Compressive Strength (ASTM D2166-98a).
- Direct Shear Test for Soils Under Consolidated Drained Conditions (ASTM D3080-98).
- Atterberg limits (ASTM D4318-98).

Free swell (ASTM D4546-98). (it was carried out for the mixture after 7 days of curing) results of laboratory work were combined in Table 1.

Table 1. Geotechnical properties of the natural soil and the mixtures (soil + HOFA) for both curing periods.

Parameter	Soil	5% 7 days	5% 28 days	10% 7 days	10% 28 days
G_s	2.79				
$\rho_{max}[kg/m^3]$	14.8				
$\omega_{opt}[\%]$	29.4				
Percentage fines [%]	66.6				
$C_u[kPa]$	166	174	124	146	123
$C'[kPa]$	55	120	106	102	79
$\emptyset'[°]$	22	7.3	19.2	25.5	27.0
Liquid limit [%]	51.8	64.2	67.5	65.8	67.9
Plastic limit [%]	29.8	32.2	33.1	34.6	32.5
Plastic Index [%]	22.1	32.0	34.4	31.2	35.3
Free swell [%]	41.3	41.8		42.5	
$\rho_{max} = maximum\ density, \omega_{opt} = Optimum\ Water\ Content, C_u = undrained\ cohesion, C' = drained\ cohesion, \emptyset' = drained\ friction\ angel,$					

According to USCS (Unified Soil Classification System), the soil is classified as Sand Elastic Silt.

2.2. Mixture (soil + 5% HOFA)

The following statements can be drawn based on Table 1, for the mixture (soil + 5% HOFA).

- It can be observed a decrease in the value of the drained cohesion of the mixture (soil+5%HOFA) and an increase in the value of the internal friction angle by the time.
- For the undrained shear parameters (Cu), there is a decrease in the value of undrained cohesion by the time for the mixture (soil+5%HOFA).
- For the Atterberg limits, they maintain approximately the same values by the time.

2.3. Mixture (soil + 10% HOFA)

The following statements can be drawn based on Table 1, for the mixture (soil + 10% HOFA).

- Decrease the value of the drained cohesion and slight increase in the value of the internal friction angle by the time.
- For the undrained shear parameters (Cu), there is a decrease in the value of undrained cohesion by the time.
- For the Atterberg limits, they maintain approximately the same values by the time.

2.4. Comparison between the effect of two percentages 5% and 10%

The experimental results of mixtures (soil+5%HOFA) and (soil+10%HOFA) were compared for the both curing periods (7 and 28) days.

2.4.1. Curing period 7 days

From the date of Table 1 the following statements can be drawn.

- Decrease in the value of undrained cohesion (Cu) with an increase of the percentage of HOFA.
- Decrease in the value of the drained cohesion and an increase in the value of the internal friction angle with an increase of the percentage of HOFA.
- The liquid and plastic limits were almost the same when increasing the percentage of HOFA, resulting in approximately the same value for the plastic index.
- The free swell also increased slightly with an increase in the percentage of HOFA added to the soil.

2.4.2. Curing period 28 days

The authors summarize their statements based on Table 1.

- The value of undrained cohesion (Cu) is approximately same for the two mixtures.
- Decrease in the value of the drained cohesion and an increase in the value of the internal friction angle with an increase of the percentage of HOFA.
- The liquid and plastic limits were the same when increasing the percentage of HOFA, resulting in the same value for the plastic index.

2.5. Comparison between the mixture (soil+5%HOFA), mixture (soil+10%HOFA) and the natural soil

Since the samples of the mixture (soil+5% HOFA) and the mixture (soil+10% HOFA) were formed depending on the laboratory density and moisture (the same density and moisture for natural soil), while standard proctor was carried out to determine the density and optimum moisture for natural soil, thus the comparison can only for some of the studied parameters:

- Liquid limit (L_L).
- Plastic limit (P_L).
- Plastic index (P_I).
- Free swell.

Fig. 2 shows the change of Liquid Limit, Plastic Limit and Plasticity Index as the HOFA percentage increases, where we observe the followings:

- Increase the liquid limit for the mixture (soil+5%HOFA) compared with natural soil and it maintains approximately the same value for the mixture (soil+10%HOFA).
- The plastic limit increases slightly for the mixture (soil+5%HOFA) compared with natural soil and it maintains approximately the same value for the mixture (soil+10% HOFA).
- Increase the plasticity index at the percentage 5% of HOFA mixed with the soil, and this value being almost constant for the percentage 10%.

Fig. 3 shows the change of the free swell value with an increase the percentage of HOFA mixed with the soil. There are not large changes in the value of the free swell by increase of the HOFA.

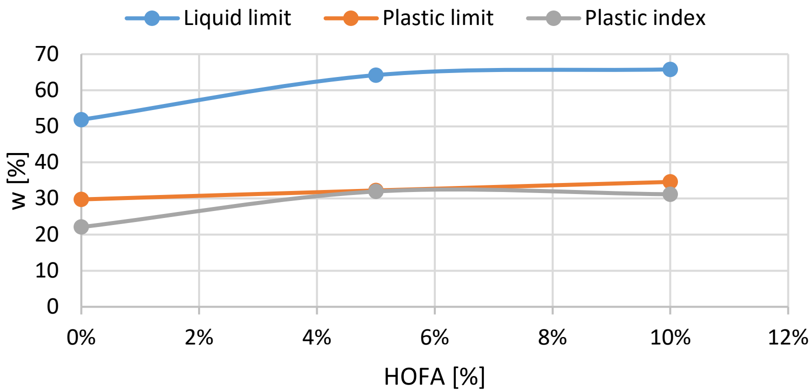

Figure 2. Change of Liquid Limit, Plastic Limit and Plasticity Index with an increase in the percentage of HOFA mixed with the soil

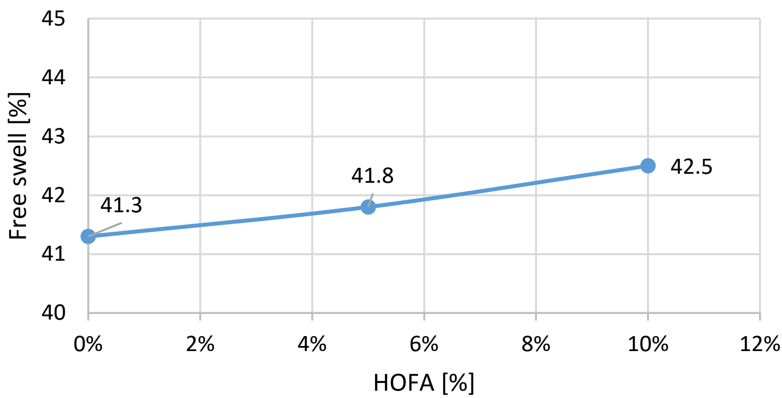

Figure 3. Change of the value of free swell with an increase in the percentage of HOFA mixed with the soil

3. Conclusions

This paper presented an experimental study of the effect of the fly ash that produced at power station of Banias city in Syria which operates by using heavy fuel oil on the geotechnical properties of clay soil. This paper was carried out by mix soil with two different percentages of Heavy Oil Fly Ash (5% and 10%) and by using two different curing periods (7 and 28) days. The main conclusions drawn may be summarized in the following:

- Unlike Fly Ash that caused by burning coal, HOFA chemically inert. Where lack of clear change when comparing the mixture (soil+5% HOFA) with mixture (soil+10% HOFA) for Atterberg Limits and Free Swell in addition to absence of clear effect of the curing period on the Atterberg Limits confirm that this type of ash chemically inert and tend to behave as a fill material.
- The increase in the values of the Atterberg Limits that appears at percentage of HOFA equal to 5% indicates that this type of ash is very voracious for water, and this is due to the very high specific surface area and the high level of carbon as well which had spongy shape and high porosity [1].
- The increase in the value of the friction angle ($\emptyset'$) with the increase in the percentage of HOFA mixed with the soil can be explained by the fact that the fuel ash granules fill the pores between the soil particles and this naturally leads to an increase in friction when the two percentages are compared (5%) and (10%).
- Unlike fly ash produced by burning coal, increase of percentage of HOFA caused decrease mixture cohesion. The decrease in cohesion ((Cu) and (C')) with an increase in the percentage of HOFA mixed with the soil can be explained by the low cohesion between the heavy oil fuel ash particles.
- The decrease in cohesion ((Cu) and (C')) by the time can be explained by the carbon particles absorbs the soil particles moisture.

Acknowledgement

The authors would like to express thanks to the faculty of civil engineering at Tishreen University, Latakia, Syria and especially for the department of geotechnical engineering. Furthermore, the authors are also grateful to the power station in Banias city for their collaboration with them to carry out this research.

References

[1] V. K. Lyubov, F. Z. Finker, Reducing the environmental impact of coal-fired thermal power station, *AIP Conference Proceedings* 2211, 040002 (2020) doi: https://doi.org/10.1063/5.0000816

[2] E. Cokca, Use of Class C Fly Ashes for the Stabilization – of an Expansive Soil, *Journal of Geotechnical and Geo-Environmental Engineering* 127 (7) (2001) pp. 568–573.
doi: https://doi.org/10.1061/(ASCE)1090-0241(2001)127:7(568)

[3] N. Pandian, K. Krishna, A. Sridharan. California Bearing Ratio Behavior of Soil/Fly Ash Mixtures, *Journal of Testing and Evaluation* 29 (2) (2002), pp. 220–226.
doi: https://doi.org/10.1520/JTE12249J

[4] P. R. Phani Kumar, R. S. Sharma, Effect of fly ash on Engineering properties of Expansive Soil, *Journal of Geotechnical and Geo-Environmental Engineering* 130 (7) (2004) pp. 764–767.
doi: https://doi.org/10.1061/(ASCE)1090-0241(2004)130:7(764)

[5] M. A. AL-Ghouti, Y. S. AL-Deg et al., Extraction and Separation of Vanadium and Nickel from Fly Ash Produced in Heavy Fuel Power Plants, *Chemical Engineering Journal* 173 (1) (2011) pp. 191–197.
doi: https://doi.org/10.1016/j.cej.2011.07.080

[6] Y. S. AL-Degs, A. Ghrir et al., Characterization and utilization of fly ash of heavy fuel oil generated in power stations, *Journal of Fuel Processing Technology* 123 (7) (2014) pp. 41–46.
doi: https://doi.org/10.1016/j.fuproc.2014.01.040

[7] J. Camilleri, M. Anastasi, A. Torpiano, The microstructure and physical properties of heavy oil fuel ash replaced Portland cement for use in flowable fill concrete and the production of concrete masonry units, *Journal of Construction and Building Materials* 38 (1) (2014) pp. 970–979.
doi: https://doi.org/10.1016/j.conbuildmat.2012.09.054

[8] M. Shmlls, D. Bozsaky, T. Horváth, Literature review on steel fibre, silica fume and fly ash: improving methods for recycled and multiple recycled

aggregate concretes, *Acta Technica Jaurinensis* 14 (1) (2021) pp. 60–79.
doi: `https://doi.org/10.14513/actatechjaur.00570`

[9] B. D. Nath, M. K. A. Molla, G. Sarkar, Study on Strength Behavior of Organic Soil Stabilized with Fly Ash, *International Scholarly Research Notices* 2017 (2017), Article ID 5786541, pp. 1–6.
doi: `https://doi.org/10.1155/2017/5786541`

[10] S. Mahvash, S. López-Querol, A. Bahadori-Jahromia, Effect of class F fly ash on fine sand compaction through soil stabilization, *Heliyon* 3 (3) (2017) pp. 1–27.
doi: `https://doi.org/10.1016/j.heliyon.2017.e00274`

Acta
Technica
Jaurinensis

Vol. 14, No. 3, pp. 281-299, 2021
DOI: 10.14513/actatechjaur.00608

A review of Turkey's high-speed rail experience

U. Sanili Aydin,[1,*] A.N. Uste[2]

[1]Manisa Celal Bayar University, Department of Political Science and International Relations, Manisa, 45140, Turkey
[2]Dokuz Eylul University, Department of Public Administration, Izmir, 35390, Turkey
***e-mail: ulaydin91@hotmail.com**

Submitted: 22/03/2021; Accepted: 25/04/2021; Published online: 07/05/2021

Abstract: The multidimensional characteristics of the HSR networks make debated the benefits of them. In this context, the aim of this study is to review of Turkey's HSR systems from spatial equity perspective within the framework of recent research and developments. The latest secondary data from the official statistics of the Ministries of Development; Environment and Urbanization; Industry and Technology of Turkey has been used for the purpose of the analysis. The research methods included: critical analysis of the source literature, analysis of secondary data (desk-research) and graphic methods (tables and maps), by means of which the results of the study have been presented. The main argument of study is that considering the current geographical location of the HSR network of the country, it creates challenges in terms of spatial equity and deepens the regional polarization. The existing HSR network has facilitated mobility, especially in terms of domestic tourism. However, the usage of the HSR by a limited part of population and restrictions applied due to the COVID-19 pandemic question the amount of returns of the HSR's costs, which are enough expensive investments in Turkey. On the other hand, increasing inequalities arising from the HSR infrastructures shaped on the basis of factors such as the geographical features of the country, general development level, population and demand density, are tried to be minimized by roadway and airway alternatives.

Keywords: COVID-19; economic development; high-speed rail; spatial equity; Turkey

1. Introduction

Technological innovations and globalization have increased the share of service sectors in countries' economies as well as their importance and efficiency. Although the process of globalization includes the relatively free movement of goods, services and capital, but not of labour [1], all these activities boost the free movement of people as much as possible. On the other hand, it would not be true to consider the increased human mobility only at the global level. As a part of the countries' development agenda, transportation projects facilitate the domestic mobility of people. The progress in transportation sector has been supported by the variety of access options making easier to travel more at the local and regional levels.

Railway is one of the first and most important elements of public transport, which is increasingly significant as a part of the transportation systems. The basic economic industries such as coal, iron and steel have been integrated among themselves by the railway. In this sense, the railway contributes to the formation of market relations at national and international scale by providing spatial integration. It is the engine of integration and economic development, making a great contribution to the economic, social and cultural development along the routes. However, except for developed economies, railway projects are enough expensive investments requiring costly maintenance afterwards. Therefore, they must be carefully planned [2].

As known an environmentally friendly mode in contemporary world in the light of the searches for alternative energy sources, railway allows to transport more passengers simultaneously at an affordable cost via wagons. In this sense the HSR networks are considered as the alternative projects to congested road traffics in 1960's. While countries like Japan, France are the pioneers of these projects, the HSR networks exist in several parts of the world today.

In its Council Directive 96/48/EC of 23 July 1996 on the interoperability of the trans-European high-speed rail system the Council of the European Union (EU) has defined the HSR as an infrastructure and rolling stock enabling at least 250 km/h on specially built lines and 200 km/h on upgraded high-speed lines [3]. HSR is still a grounded, guided and low grip transport system: it could be considered to be a railway subsystem [4]. However, the speed is the main factor distinguishing it from conventional railway networks. An easy access achieved by HSR has provided new opportunities for cities located on the route of the HSR lines and has often revitalized the significance of railway stations [5].

Since 2000s, Turkey has needed to revise its transportation policies in the light of global, international and regional developments. The start of membership negotiations in 2004 with the EU - the world's largest trading bloc - has been one of the most important driving forces in this process. Emerging new markets nearby in the post-Soviet areas and the softened relations of the West with Iran have created the need for more advanced transport networks in Turkey. Initiatives made in the field of freight transportation have also been reflected in domestic passenger transportation of Turkey. Traditionally, the country has a satisfying road network. A significant impetus has been achieved especially in domestic airline passenger transportation by widening local airport networks. By opening the intercontinental Marmaray and Baku-Tbilisi-Kars railway lines, a direct connection has been established with Georgia and Azerbaijan, and an important corridor has been established in the connection of the country to Asian and European transportation networks through the Black Sea region. Both lines are purposed for freight and passenger transportation. On the other hand, the most important development in the railway sector during this period is Turkey's investments in the HSR.

In the light of above mentioned, this paper aims to review the way that the country has reached in the HSR systems after 2000 as a part of Turkey's transportation policies from a spatial equity perspective, focusing on recent research and developments. The paper is conducted in six sections. Following the introduction part, the materials and methods used in this study have been explained in the second section. The literature has been reviewed in the third part of the paper. It has been aimed to draw a general framework of Turkey's railway transportation policies in globalization era in the fourth section. The same section involves an analysis of Turkey's experience on the HSR, reviewing policy documents, instruments for implementation, legal regulation documents, national development plans and similar documentations as well as surveys conducted previously. The research is supported by the official statistics. The findings of the study are included in the fifth section. The paper is concluded with final part.

2. Materials and methods

The article focuses on Turkey's HSR networks, which is a relatively new experience for this country in comparison with other modes of transport. The analyses included herein should be seen as a case study. The submitted findings are results of evaluations taking into the consideration the determinants of the HSR systems from spatial equity perspective. Research is conducted by Manisa Celal Bayar University in Manisa and Dokuz Eylul University in Izmir, Turkey.

The data were collected using various methods, including a review of the literature, public documents and statistics, interviews and official declarations of the HSR network authorities and results of surveys conducted by professional and public organizations on the usage, benefits and performance of the HSR network in Turkey.

The data obtained allowed to analyse the geographical orientation of the HSR network policies and numbers of the HSR users and their aim to prefer the HSR. The aim of the study was to provide a description of the HSR networks in Turkey in terms of equal benefit and inclusiveness.

The following hypotheses were formulated in the study preparation phase:

- Turkey's investments in the HSR systems are the results of multivectoral transport policies within the adaptation processes to the globalizing world.
- The development of the HSR network in the western region, which is more developed compared to the eastern region of the country, will increase the spatial inequality.

The research limitations included the availability of the detailed data about the socio-economic profiles of the HSR users.

3. Literature review

Investments made in the transport sector are generally carried out by the public sector, as they are included in public infrastructure expenditures and have a high multiplier effect [6]. Public spending on infrastructure is one of the contentious subjects of domestic policies due to the debates on its productivity and benefits. Aschauer's [7] argument about the significant benefits of transport infrastructure investment both for the economy and society has been responded counter-reactions in the literature. The disagreement arises regarding the multi-characteristic nature of transport infrastructure investment and appraisal methodologies of it in this sense [8].

But in spite of all disputes, as a model of development supported by several international and regional financial organizations, infrastructures have founded a basis of an industrial and information revolution in the transmission of goods, people, power, information and Internet over increasingly vast distances [9]. The distribution of a huge number of benefits providing by infrastructures has been far from equal that has been started to question by citizens [9].

Wider economic impacts of transport are enough well known issue, requiring benefit analysis of purposed infrastructure projects. Countries follow different paths in project assessments from macroeconomic, micro and meso economic effects such as agglomeration or competition benefits. The UK Department for Transport has preferred to develop the quantification method for the HSR project linking London to Birmingham, then Manchester and Leeds, which was the first major transport infrastructure project including wider economic impacts. However, countries like Chile or South Africa focuses on social mix and desegregation benefits of transport projects [10].

The growth-pole theory stresses the agglomeration benefits associating with the spatial concentration of population and activities, as well as the presence, quality and extent of the infrastructural systems [11]. Although long-distance transportation infrastructures connect territories, increase the possibilities of interconnections and exchanges [12], push economic development, they can also create the inequalities between regions.

Monzon et al. [13] has described equity as a distribution of a given effect, frequently associated with terms of ‘‘justice’’, ‘‘fairness’’ or ‘‘cohesion’’ in transport literature [14,15,16]. The level of equity analysis - international, national, regional or local – has direct effect on the results caused by the HSR and cities far from the HSR stations face with a risk of reallocation of economic activities as companies may prefer to move to regions closer to the transportation networks [15,13). Such preferences can increase easily the gap between regions and push polarization [13].

According to investigations of Church et al. [17], most of the studies on relationship between transportation and its impacts has mainly focused on two approaches: “category approach” and “spatial approach”. The first approach aims to examine the travel patterns, attitudes and needs of disadvantaged social groups concerned with the transport systems, like women, citizens without paid employment or older. However, the second approach is interested in spatial equity and problems caused by poor public transport access [17].

Thus, there are discussions in the literature regarding the contradiction between spatial equality and the transportation system. A spatial equity can be considered as a geographical location of an individual, group or region influenced by a transport infrastructure project [18].

Biggiero et al. [19] has defined the spatial equity or spatial accessibility “as a measure of the ease of travelling from an origin to a given destination via a given mode or set of transport modes”, emphasizing the cruciality of achievement of equity in the allocation of public resources. Although current investments in the HSR systems have made an easy access, but also have created equity issues. The benefits of new HSR lines are undeniable in terms of improvements in accessibility opportunities. Such infrastructure constructions can increase the attractiveness of the regions, fostering their locational values. However, the HSR systems networks can also create a spatial imbalance, increase development gaps between regions [19]. Polarizing the levels of development between territories, the region out of the routes of the HSR systems networks may stay in shadow of that one which is on the route of them. Considering the citizens’ equal rights of access to all services provided by the public authorities, the criticism about the HSR systems’ encouragement of inequality has a rational justification. Suggesting the new method – SUstainable

Mobility INequality Indicator (SUMINI) to appraise the transportation infrastructures as an alternative to Multi-Criteria Analysis (MCA) and Cost Benefit Analysis (CBA), Thomopoulos and Grant-Muller [8] have emphasized the role of new technological advances in more inclusive assessment of the wider impacts of them. Based upon a composite indicator and MCA, it is argued that as an easily accepted and complementary approach SUMINI is not in competition with traditional CBA. It could methodologically provide a new and important answer to the traditionally hard question of how to appraise equity and other wider impacts, such as accessibility, land use and socio-economic and environmental effects [8].

Defining spatial equity as an ambiguity, Buhangin [20] has evaluated it in both physical and socio-economic senses. While it can be the equitable development of land use from physical perspective, in the socio-economic terms it can be considered as an equitable flow of goods and services from one spatial arena to another. Buhangin [20] has accepted a spatial equity as a parameter for sustainable development especially in indigenous regions in both senses.

HSR is a type of transport by which the movement of people is mainly aimed as an integrated part of economic development goals, focusing on connectivity and cooperation between regions. As all types of transportation contain an interaction element in essence, the HSR projects have cultural and social aspects also. In this context, it can be considered that the HSR has the multidimensional characteristics. HSR policy, faces at the end a set of dilemmas that must be dealt with politically also [21]. Because the HSR system is an infrastructure construction and service operation with high cost that makes it a focus point of hot debates [22] alongside of spatial equity issues.

In the case study for Spain, Monzon et al. [13] has investigated the accessibility impacts of the HSR network construction on spatial equity. Determining a more polarised pattern in Spain, it has been found that a speed acceleration from 220 km/h to 300 km/h in a given route results in heavy negative effects on spatial equity between locations with and without the HSR service [13]. Several significant factors have been highlighted in the study that must be taken into consideration in the planning process. In order to achieve the maximum positive spatial equity results, following factors require to be considered at the planning period: "the level of accessibility of the city in the initial situation as regards the quality of its railway infrastructures; its geographical position in terms of proximity to major population centres; the existence of a HSR station; and the quality of the transport network from the cities to the nearest HSR station" [13].

The qualitative analysis of the equity impacts of the HSR network conducted by Biggiero et al. [19] has showed that in Italy the problem of economic/geographic exclusion perceived by travellers does exist.

In the case study of Yangtze River Delta (China), Wang and Duan [22] have argued that the HSR development may cause the new dimension in transport inequity and besides of the accessibility the affordability should be taken into consideration in future equity studies on the HSR development in China.

The spatial equity approach considers to act from a more strategic view, involving both the possible benefits and their spatial distribution. It's required an evolution of the consequences not only on the cities in the HSR corridors with a station, but also on other ones outside the route, regardless of whether or not they have a station [13].

4. Turkey's experience on high-speed rail

Following the Industrial Revolution in the Western Europe, railways have been constructed by using foreign capital as a result of the raw material supply of the colonial countries and their search for new markets for finished goods in the Ottoman Empire. With the declaration of the Republic, the railways have built and operated by the state, considering the economic and social benefits of the country. In this period, the construction of highways has been designed to connect railways and ports to the inner regions of the country. Another remarkable feature of this period is the construction of coherent lines. By providing loops, the coherent lines have shortened the distances, reducing the transportation costs [23].

However, after the 1950s, the importance given to the railway has decreased with the rapid development of highways, which had pushed the railway construction and transportation to the background (Table 1).

Table 1. Share of transport sector investments in total investments in development plans [24]

Five-year development plan by years	***Percentage of Transportation Sector in General Investments***	***Percentage of the Highway System in the Transportation Sector***	***Percentage of the Railway System in the Transportation Sector***
1963-1967	13.7	71.3	17.5
1968-1972	16.1	72.1	18.8
1973-1977	14.5	52.1	13.9
1979-1983	16.3	60.7	10.6
1985-1989	25.4	49.4	16.0
1990-1994	26.5	62.6	7.2
1996-2000	22.7	63.6	6.5

Since 2003, the allocation for railway investments has increased and the development of railways has been seen as one of the targets for transportation sector [23]. In 2009 Turkey has gained its first experience on the HSR with Ankara-Eskisehir line. In 2011, Ankara-Konya, in 2013 Eskishehir-Konya, in 2014 Ankara-Eskisehir-Istanbul and Konya-Istanbul train services have started, making possible the one-day travels between these regions. The total length of the completed HSR lines is 1,213 km.

Increasing importance of multi-modal transportation systems in globalization era in the context of environmental and climate change issues and membership negotiations with the EU have been the most significant motivators of this process. As one of the membership precondition within the negotiation chapters, the EU has proposed the restructuring of the railway sector of Turkey. In order to redefine the role of railway in the transportation sector, to produce efficient and compatible commercial-oriented services with the market conditions, TCDD Tasimacilik SJC has been established as subsidiary of TCDD Turkish Railways by the "Law on the Liberalisation of Railway Transportation in Turkey" in 2016.

In the light of these developments urban rail transportation systems have also provided significant advantages in parallel to increase of population in the cities of Turkey (Fig. 1).

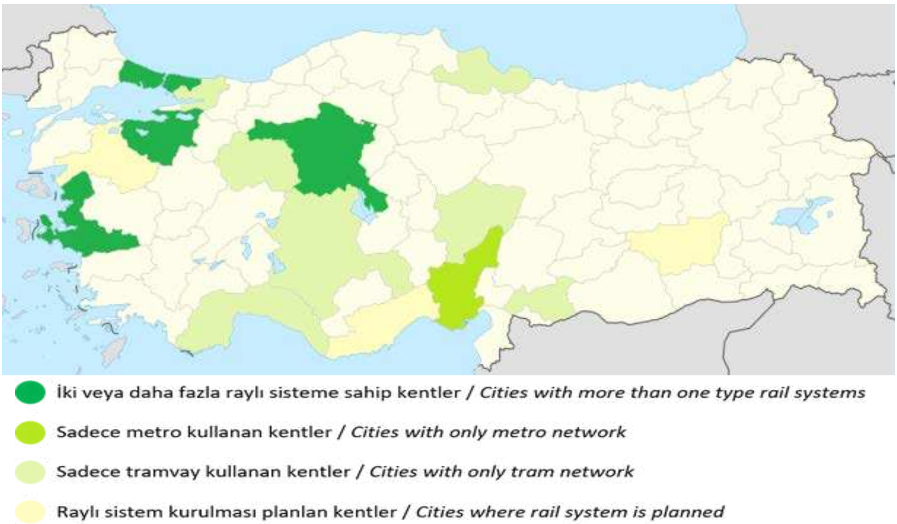

Figure 1. Map of urban rail systems in Turkey (2021) [25]

Metro, light rail system, tram, funicular and suburban system is used In twelve cities of Turkey. In spite of the restrictions during pandemic, the number of passengers reached 1.46 billion in 2020 with some improvements such as the newly opened lines, night services, and an integration of bus lines to the rail system. The total urban rail line length is 782 km [25].

In 2020 the length of the railway network (including both the conventional and high speed lines) summed up to 12,803 km in length (Table 2). While the share of the railway investments was 33 percent in 2013 in total investment for transportation and communication, this rate was increased to 47 percent in 2020. 29 billion US dollars has been invested in the railway sector between 2013-2020. It is estimated that railway network will be extended to 25,000 km in length by 2023 [26].

Table 2. Railway network by year (km) [26]

Years	2002	2005	2010	2015	2016	2017	2020
Length	10925	10973	11940	12532	12532	12608	12803

It has been planned to connect fifteen largest provinces of the country by the HSR. Primarily Ankara-Eskishehir, Ankara-Konya, Konya-Istanbul and Ankara-Istanbul HSR have been started to operate (Fig. 2) and Turkey has become the sixth country in Europe, eighth in the world in the HSR operation.

Figure 2. Map of Turkey's HSR network (2019)[29]

There are daily 44 train services in the winter season and 52 train services in the summer season. 53.2 million people have used the HSR as a travel mean between 2009-2019 in total [27]. 29.4 percent of the HSR users prefers it for business purposes and 12.7 percent of passengers uses the HSR to go to and from school. While women mostly use the HSR for visiting family members and friends (40.7 percent), men mostly use the HSR for business purposes (37 percent) [27].

Regulation on the rights of passengers traveling by rail has been published in 2019, involving the procedures and principles regarding the rights and obligations of passengers traveling by rail [28].

There is no connection between the HSR and conventional railway lines in Turkey. The HSR network is developing directly with the construction of the HSR infrastructure. However, there are studies in different regions of the country (south and north) for the utilization of various line connections as the HSR network by improving the conventional railway lines. There is no any HSR line implementation in Turkey by which both freight and passenger transportation is carried out together or as double line [30].

As it is shown in the map (Fig. 2), the current HSR network and the HSR lines have been planned to be completed in the near future is Ankara centered and connect the largest four cities of the country.

On the other hand, Ministry of Industry and Technology of Republic of Turkey General Directorate of Development Agencies has published a socio-economic development ranking research of provinces and regions - SEGE 2017 [31]. Totally fifty-two variables based on demography, employment, education, health, competitive and innovative capacity, finance, accessibility and life quality have been used in the conducting of research. According to the obtained index values, six levels of development of provinces have been determined in Turkey. The development levels that emerged as a result of the research are mapped (Fig. 3).

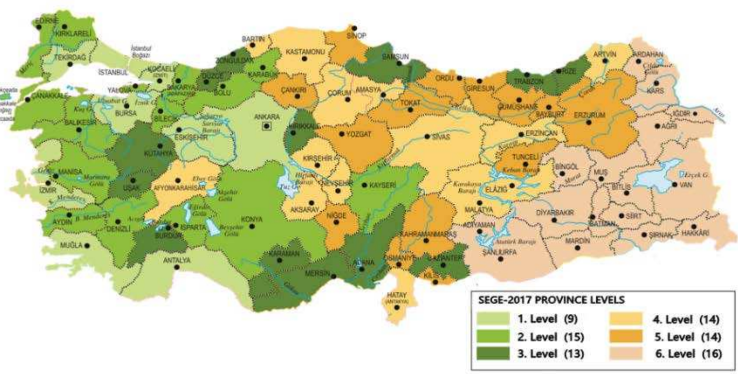

Figure 3. The map of development level of provinces of Turkey [31]

It must be noted that there are eighty-one provinces in total according to the administrative territorial division of Turkey. There are nine provinces in the first development level group, fifteen provinces in the second group, thirteen provinces in the third group, fourteen provinces in the fourth group, fourteen provinces in the fifth group and sixteen provinces in the sixth group [31].

SEGE - 2017 research provides a better understanding of spatial inequality, which is one of the basic hypotheses of our study, supporting it with visuals.

5. Findings

Comparing two maps (Figs. 2 and 3), it has been found that the first seven most developed provinces of the country are among the provinces that already have or will have the HSR connection in the near future. Four of the remained provinces with existing or potential HSR connection are among the provinces of the second development level group.

As it is illustrated in the map (Fig. 3), there is a great difference between country's western and eastern parts. The geographical characteristics distinguish these two regions. The eastern part of the country consists of more rugged terrain with high mountains (Fig. 4), which increases the cost of infrastructure and technically limits the ability to speed up and decelerate of the HSR systems. However, the western regions are relatively flat (Fig. 4).

Figure 4. Physical map of Turkey [32]

Secondly, the western regions of the country are located on the coastlines or close to them. However, eastern regions are lack of such opportunity. Turkey's geographical diversities are one of the primary factors shaping the socio-economic structural features between its regions.

The fact that the western and coastal parts of the country are more developed is the main starting point of a movement from the eastern regions to here.

Reducing the regional disparities and accelerating economic development has been determined as a priority in some HSR projects. Decreasing the traffic density has been determined as a secondary goal in such projects, aiming to transfer the economic and social dynamism of the developed regions to the developing regions with the HSR networks [33]. In terms of clear regional differences, inefficient resource allocation, current HSR infrastructures increase spatial inequalities rather than removing them. Considering that the HSR lines develop the intercity accessibility of peripheral cities along the HSR network based on the highway network and reduces the spatial inequalities, it must be focused on the peripheral areas in regional planning in order to maximize the benefits with limited investment [34]. Increasing the network density around cities with inferior accessibility and promoting multi-modes for accessing to HSR is also an effective way to improve regional development [34].

In order to achive the above mentioned concequences, the HSR networks must also cover underdeveloped regions. But considering the geographical conditions, population density, economic activities, or demand volume, such investments can be expensive and not rational.

On the other hand, the Turkish government has launched its transportation policies in parallel with country's tourism and trade policies after the 2000s. It has been succeeded to reduce the spatial inequalities between eastern and western regions as a result of opening new airports and increasing number of domestic flights. There are fifty-three airports (Fig. 5) in Turkey [35].

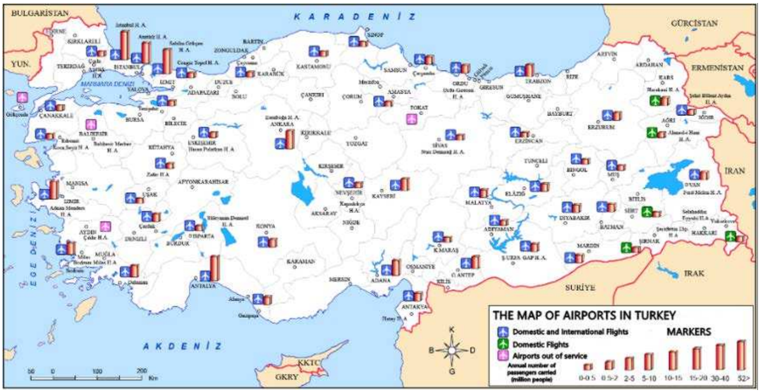

Figure 5. The map of airports in Turkey [35]

These developments have also revitalized existing airports located on the HSR network routes. In terms of temporal competition, scheduling strategies are important to improve network efficiency and optimize time slots for both air and the HSR travel [36] during planning and policy-making to achieve sustainable operations and the development of the passenger rail system [37].

The surveys conducted on the HSR systems operating in Turkey since 2009 have found that the existing network contributes mostly to domestic tourism sector. Considering the crucial role of transport for the increase of tourist flow [38], this has been an expected effect. Additionally, examining the profile of the passengers, findings have showed that the HSR lines are mostly used by students and preferred by those people who want to save time [39].

On the other hand, COVID-19 pandemic deeply affects each sector of economy as well as transportation sector. In this sense, the strict measures have been implemented against virus. Since pandemic has been declared, Turkey imposes curfew in several periods. Restriction on public transport, closing of touristic places decrease the usage of the HSR services in the country. Considering that the HSR infrastructures are the expensive infrastructures and have started to operate more recently in Turkey, this is a serious disadvantage in terms of cost recovery.

6. Conclusion

The HSR networks can be described as a product of technological solutions developed in the field of railways in order to meet the increasing demand for geographical mobility of the capital and labour. In fact, the experiences confirm that the regions which are accessible by the HSR systems, become more attractive for capital to invest, while the regions where the HSR does not reach, are spatially polarized. Therefore, unequal investment in the HSR systems causes an increase in unequal development between regions.

More than 420,000 passengers are carrying by the HSR on a typical weekday in Japan. An extensive HSR networks include several cross-border international links between several European countries. The HSR projects have been rapidly developed in China in last 15 years, supported by huge governmental funding. While expensiveness of the HSR systems has been questioned in developing countries, whereas it is costly for workers to pay for faster travel, they are favoured due to the energy savings, transportation benefits and environmental considerations.

Turkey has achieved an important step in the transport sector after the 2000s. Due to its geographical position and the role of bridge between continents, Turkey is a significant part of several regional and international transportation projects in the globalization age.

The geographical conditions of the country also play a deterministic role in shaping the domestic transportation policies. The main goal of the domestic part of transport policy has been focused on the elimination of the development disparities between the western and eastern regions of the country in these years.

In this context, Turkey has started to operate the HSR in 2009. The existing HSR network is generally located in the western parts of the country, which are geographically more suitable for such infrastructures and where a large number of the population lives. This situation has deepening the spatial inequalities between the developed western and underdeveloped eastern part of Turkey. These inequalities arising from transport opportunities have been tried to be removed by the airline mode.

On the other hand, the share of rail passenger transport has fallen to 1.3 percent in 2018, which has been accounted 42 percent in the 1950s, mainly due to the new opened highways and airports in both parts of the country. In addition to infrastructure investments, it is inevitable for the country to realize reforms involving participation of private companies and liberalization in passenger transportation in order to increase the share of the passenger transportation by the HSR.

The HSR systems are known as environmental and economical transport mode, but expensive investments. The restrictions, lockdowns and a need to protect social distance due to the COVID-19 have added a new dimension to both urban and public transport policies [40]. Therefore, the HSR infrastructure investments in Turkey must be addressed so as to ensure the financial efficiency and spatial equity, considering the factors such as increasing natural disasters, health threats, climate change and environmental issues in recent years.

References

[1] S.J. Burki, Rising Powers and Global Governance, 1st Edition, *Palgrave Macmillan*, New York, 2017.

[2] B. Eller, Sz. Fischer, Tutorial on the emergence of local substructure failures in the railway track structure and their renewal with existing and new methodologies. *Acta Technica Jaurinensis* 14 (1) (2021) pp. 80–103. doi: *https://doi.org/10.14513/actatechjaur.00565*

[3] The Council Directive 96/48/EC. *Official Journal* L 235 17/09/1996 pp. 6–24. [cited 2021-04-24]. URL *https://eur-lex.europa.eu/legal-content/EN/TXT/?uri=CELEXpercent 3A31996L004*

[4] UIC. The Definition of High Speed Rail. "UIC eNews" Nr 596 dated 26 April 2018 [cited 2021-04-24]. URL *https://www.uic.org/com/enews/nr/596-high-speed/article/the-definition-of-high-speed-rail?page=thickbox_enews*

[5] M. Garmendia, C. Ribalaygua, J.M. Urena, High speed rail: Implication for cities. *Cities* 29 (2012) pp. 526–531. doi: *https://doi.org/10.1016/j.cities.2012.06.005*

[6] M. Demir, E. Sever, The effect of public infrastructure expenditures on economic growth: the case of Turkey (1980-2007) (Kamu altyapi harcamalarinin ekonomik buyume uzerindeki etkisi: Turkiye uzerine bir inceleme (1980-2007)). *Marmara Universitesi I.I.B.F. Dergisi* XXV (2) (2008) pp. 99–118 (in Turkish).

[7] D.A. Aschauer, Is public expenditure productive? *Journal of Monetary Economics* 23 (2) (1989) pp. 177–200. doi: *https://doi.org/10.1016/0304-3932(89)90047-0*

[8] N. Thomopoulos, S. Grant-Muller, Incorporating equity as part of the wider impacts in transport infrastructure assessment: An application of the SUMINI

approach. *Transportation* 40 (2013) pp. 315–345.
doi: `https://doi.org/10.1007/s11116-012-9418-5`

[9] D. Durrant, Infrastructure, equity and urban planning: A just process for the allocation of benefits and burdens, In: J. Bishop (Ed.), Building sustainable cities of the future. green energy and technology, 1st Edition, *Springer*, Cham, 2017, pp. 141–162.
doi: `https://doi.org/10.1007/978-3-319-54458-8_8`

[10] C. Cheze, R. Negre, Wider economic impacts of high-speed rail: Example of agglomeration benefits assessment on Bretagne Pays de Loire high speed rail project, *Transportation Research Procedia* 25 (2017) pp. 5307–5324.

[11] M.D. Thomas, Growth pole theory, technological change, and regional economic growth, *Papers In Regional Science* 34 (1) (1975) pp. 2–25.
doi: `https://doi.org/10.1007/BF01941308`

[12] G. Mazzeo, Impact of high speed trains on the hierarchy of European cities, *Jahrbuch für Regionalwissenschaft* 32 (2012) pp. 159–173.
doi: `https://doi.org/10.1007percent 2Fs10037-012-0066-1`

[13] A. Monzon, E. Ortega, E. Lopez, Efficiency and spatial equity impacts of high-speed rail extensions in urban areas, *Cities* 30 (2013) pp. 18–30.
doi: `https://doi.org/10.1016/j.cities.2011.11.002`

[14] J. Bröcker, A. Korzhenevych, C. Schürmann, Assessing spatial equity and efficiency impacts of transport infrastructure projects, *Transportation Research Part B* (44) 2010 pp. 795–811.
doi: `https://doi.org/10.1016/j.trb.2009.12.008`

[15] E. Lopez, J. Gutierrez, G. Gomez, Measuring regional cohesion effects of large-scale transport infrastructure investments: An accessibility approach, *European Planning Studies* 16 (2) 2008 pp. 277–301.
doi: `https://doi.org/10.1080/09654310701814629`

[16] D. Peters, Cohesion, policentricity, missing links and bottlenecks: Conflicting spatial storylines for Pan-European transport investments, *European Planning Studies* 11 (3) (2003) pp. 317–339.
doi: `https://doi.org/10.1080/09654310320000708 11`

[17] A. Church, M. Frost, K. Sullivan, Transport and social exclusion in London, *Transport Policy* 7 (2000) pp. 195–205.
doi: `https://doi.org/10.1016/S0967-070X(00)00024-X`

[18] N. Thomopoulos, S. Grant-Muller, M.R. Tight, Incorporating equity considerations in transport infrastructure evaluation: Current practice and a proposed methodology, *Evaluation and Program Planning* 32 (1998) pp. 351–359.
doi: `https://doi.org/10.1016/j.evalprogplan.2009.06.013`

[19] L. Biggiero, F. Pagliara et al., Spatial equity and high-speed rail systems, *International Journal on Transport Development and Integration* 1 (2) (2017) pp. 194–202.
doi: `https://doi.org/10.2495/TDI-V1-N2-194-202`

[20] J. Buhangin, Spatial equity: A parameter for sustainable development in indigenous regions, In: S.S. Zubir, C.A. Brebbia (Eds.), Sustainable City VIII, *WIT Press*, Southampton, 2013, pp. 1343–1350.
doi: `https://doi.org/10.2495/SC131142`

[21] A. Audikana, Is planning still political? The politicization of high-speed rail in Spain (1986–2016), *Political Geography* 84 (2021) 102269.
doi: `https://doi.org/10.1016/j.polgeo.2020.102269`

[22] L. Wang, X. Duan, High-speed rail network development and winner and loser cities in megaregions: The case study of Yangtze River delta, China, *Cities* 83 (2018) pp. 71–82.
doi: `https://doi.org/10.1016/j.cities.2018.06.010`

[23] H. Gulnar, Financing high-speed train investment by revenue sharing certificates (2016) [cited 2021-04-24].
URL `https://sbb.gov.tr/wp-content/uploads/2018/11/HalilG%c3%bclnar.pdf`

[24] F. Akin, F. Sultanoglu, 150th year of railways from 1856 to 2006 (1856'dan 2006'ya demiryollarinin 150 yili). 1st Edition, *Gurup Matbaacılık A.S.*, Ankara, 2006 (in Turkish).

[25] Rail Turkey. Urban rail systems (2021) [cited 2021-04-24].
URL `https://railturkey.org/travel/trains/hst`

[26] Ministry of Environment and Urbanisation of Republic of Turkey, Environmental indicator, Highway-railway network intensity (2021) [cited 2021-04-24].
URL *https://cevreselgostergeler.csb.gov.tr/en/highway---railway-network-intensity-i-86034*

[27] TCDD Tasimacilik A.S. Genel Mudurlugu, Annual report 2019 (2019 faaliyet raporu) (2020) (in Turkish) [cited 2021-04-24].
URL *https://www.tcddtasimacilik.gov.tr/uploads/images/Strateji/TCDD-Tasimacilik-2019-Faaliyet-Raporu.pdf*

[28] Official Gazette of Republic of Turkey, Regulation on the rights of passengers traveling by rail (T.C. Resmi Gazete, Demiryolu ile seyahat eden yolcularin haklarina dair yonetmelik) (8 March 2019) (in Turkish) [cited 2021-04-24].
URL *https://www.resmigazete.gov.tr/eskiler/2019/03/20190308-6.htm*

[29] Rail Turkey. High speed trains (2021) [cited 2021-04-24].
URL *https://railturkey.org/travel/trains/hst*

[30] M.F. Altan, M.C. Kiziltas, A review on the context of comparison of passenger and freight transport and high speed railways, *Dicle University Journal of Engineering* 11 (1) (2020) pp. 319–328.

[31] Ministry of Industry and Technology of Republic of Turkey General Directorate of Development Agencies. A Socio-economic development ranking research of provinces and regions SEGE-2017, *Ministry of Industry and Technology of Republic of Turkey General Directorate of Development Agencies*, Ankara, 2017.

[32] Physical map of Turkey (2021) [cited 2021-04-24].
URL *https://tr.pinterest.com/pin/742038476076089349*

[33] M. Inan, M. Demir, Rail transportation and effects of high speed railway investments in Turkey: Eskisehir - Konya example, *Firat University Journal of International Social Sciences* 27 (1) (2017) pp. 99–120.
doi: *https://doi.org/10.18069/firatsbed.346415*

[34] H. Luo, S, Zhao, Impacts of high-speed rail on the inequality of intercity accessibility: A case study of Liaoning Province, China, *Journal of Transport Geography* 90 (2021) pp. 1–16.
doi: `https://doi.org/10.1016/j.jtrangeo.2020.102920`

[35] Milliyet, The map of airports in Turkey: Which provinces have airports? The cities with airports in Turkey (Türkiye havalimanları haritası: Hangi illerde havaalanı vardır? Türkiye'de havalimanı olan sehirler), 4 November 2020 (in Turkish) [cited 2021-04-24].
URL `https://www.milliyet.com.tr/egitim/haritalar/turkiye-havalimanlari-haritasi-hangi-illerde-havaalani-vardir-turkiyede-havalimani-olan-sehirler-6311212`

[36] J. Wang, J. Huang, Y. Jing, Competition between high-speed trains and air travel in China: From a spatial to spatiotemporal perspective, *Transportation Research Part A* 133 (2020) pp. 62–78.
doi: `https://doi.org/10.1016/j.tra.2019.12.030`

[37] X. Ren, Z. Chen et al. Impact of high-speed rail on social equity in China: Evidence from a mode choice survey, *Transportation Research Part A* 138 (2020) pp. 422–441.
doi: `https://doi.org/10.1016/j.tra.2020.05.018`

[38] F. Pagliara, F. Mauriello, Y. Ping, Analyzing the impact of high-speed rail on tourism with parametric and non-parametric methods: The case study of China. *Sustainability* 13 (2021) pp. 1–10.
doi: `https://doi.org/10.3390/su13063416`

[39] M. Afsar, Z. Erdogan et al. A Study of the effects of high speed train on Eskisehir (Yuksek hizli trenin Eskisehir'e etkileri arastirmasi). Eskisehir Ticaret Odasi Yayinlari, Eskisehir, (2015) (in Turkish).

[40] P. Coppola, F.D. Fabiis, Impacts of interpersonal distancing on-board trains during the COVID-19 emergency, *European Transport Research Review* 13 (13) (2021) pp. 1–12.
doi: `https://doi.org/10.1186/s12544-021-00474-6`

Acta
Technica
Jaurinensis

Vol. 14, No. 3, pp. 300-314, 2021
DOI: 10.14513/actatechjaur.00587

Advantages and limitations of using foamed bitumen

A. Saleh[1], L. Gáspár[1,2,*]

[1]Széchenyi István University, Department of Transport Infrastructure and Water Resources Engineering
Egyetem tér 1., H-9026 Győr, Hungary
[2]KTI Institute for Transport Sciences Non-Profit Ltd.
Than Károly u. 3-5, H-1119 Budapest, Hungary
*e-mail: gaspar@kti.hu

Submitted: 19/01/2021; Accepted: 25/02/2021; Published online: 16/03/2021

Abstract: Foamed asphalt refers to a bituminous mixture of road-building aggregates and foamed bitumen, produced by a cold mix process. There are a lot of related issue that has not been sufficiently investigated so far. It is worthwhile to overview the main theoretical and practical results in the field in several countries including those of the authors of the paper. It is clear that the foamed asphalt is usually characterized by high quality and reasonable cost, can be used in cold road pavement rehabilitation, in addition to it the technique is environ-mentally friendly preserving natural resources. Using foamed bitumen reduces the emissions of carbon dioxide and gases resulting from combustion, especially when it is used as a cold rehabilitation binder and mixed with re-claimed asphalt pavement materials.

Keywords: foamed bitumen; warm mix asphalt; reclaimed asphalt pavement

1. Introduction

The use of foamed bitumen in road infrastructure projects starts in the mid-1950s [1]. First it was applied for soil and base stabilization using hot liquid bitumen foamed by steam [2]. In 1968, the foaming process was modified by Mobil Oil Australia [3]. In this process, known as mechanical foaming, the hot liquid bitumen was mixed by a controlled flow of cold water (rather than steam) in an expansion chamber, and was carried through a nozzle onto the aggregate mass [4]. The foamed bitumen has been used in the stabilization of a variety of materials including RAP (Reclaimed Asphalt Pavement material) as a part of cold recycling, and can be applied as pavement and base material for low and heavily trafficked roads [5]. In order to improve the coating ability and workability of foamed bitumen, it was mixed with aggregates pre-heated to different temperatures [6]. Later, recent foaming technologies developed to be included the incorporation of zeolites, i.e. metal additives having some 18–20wt% of water in their internal structure [7].

2. Bitumen foaming techniques

Foamed bitumen can be produced by applying appropriate shares of air, bitumen and water. It has much lower viscosity (being in its liquid state) than the same bitumen before foaming process, and its volume is expanded up to (20) times its original volume; in such a way it becomes suitable for mixing with cold (even damp) aggregates [8]. So, bitumen foaming is a comprehensive concept that a small amount of cold water (1-4% by weight) is introduced into very hot (160-200 °C) asphalt at a certain pressure. Then the hot bitumen – in direct contact with water – expands scattering the binder into air that spreads the bitumen 5-20 times its initial size, see in Fig. 1 [9].

Optimal amount of water needed for asphalt foaming spans between 2 and 4 wt% with regards to the asphalt mass, in case of insufficient amount of water the foaming is ineffective, whereas with the excessive water there is a significant risk of adhesion failure between asphalt and aggregate [10].

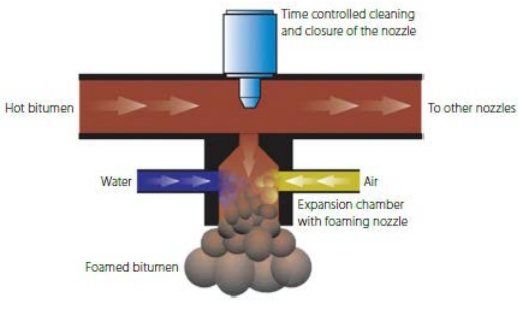

Figure 1. Schematic process of bitumen foaming

The following parameters of foamed bitumen are widespread [8]:

- Expansion Ratio (ER): ratio of the maximum volume of foam related to the original volume of bitumen (Fig. 2).

- Half Life (HL): the time measured in seconds for foam asphalt to descend from its maximum volume upon expansion to half the volume of expansion, see in Fig. 2 [11].
- Foam Index (FI): an area of the decay curve within specific limits providing an integrated measure of expansion and stability of foam [14]; it characterizes the "foamability" of a bitumen for a given foamant water application rate (Fig. 3) [6].
- Collapse rate of semi-stable bubbles (k-value): analysing images of the surface of foamed bitumen by taking periodically photos as it collapses over time and the bubble size distribution for a typical foamed bitumen using 1wt% water [12].

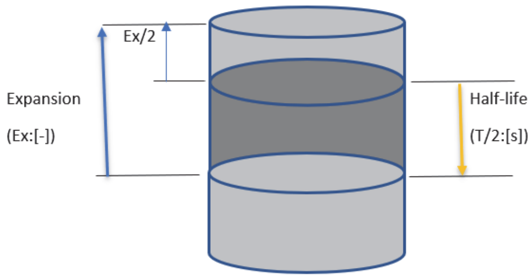

Figure 2. Main parameters for foamed bitumen

3. Production methods of foamed bitumen

Foamed bitumen can be produced by the injection of water and air into hot bitumen at 150-180 °C [13]. The reaction between water and hot bitumen leads to heat exchange between water and bitumen. Consequently, water is converted into steam that is pushed into the bitumen chain under pressure forming many vapour-containing bitumen bubbles containing [14].

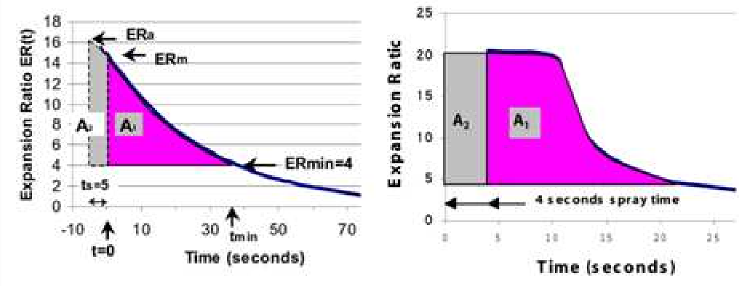

Figure 3. Foam Index calculation for Asymptotic and Non-Asymptotic Decay [14]

There are various techniques with different levels of water contents by bitumen weight 1-3%, bitumen temperatures 140-200 ºC and air pressures of 100-1000 kPa. In the foaming process, the water vapour is coated within a binder in the form of many small to large sized water bubbles [5]. For example, in case of Wirtgen WLB 10 S foaming plant, foaming is done by adding 3 wt% water to hot bitumen at 160°C at a compressed air of 500 kPa [11].

Another widely used technique is the addition of zeolite to bitumen at a rate of 5% by the total asphalt binder [15]. Zeolites allow for asphalt foaming due to the incremental release of water stored in their internal structure. Discharge of zeolite water from the crystalline structure is a long-term process. Therefore, it is feasible to improve warm mix asphalt (WMA) workability during production, construction and compaction [10].

4. Mechanical structure of foamed bitumen formation

In a research paper [16] the mechanical process of foamed bitumen creation was introduced indirectly, when it was aimed to assess the dispersion of aqueous nanoparticles. The occurrence of clumps after the dispersion of these particles was confirmed indicating that the formation of foamed asphalt is not only that water turns into vapour, since bitumen consists of a group of oils, and the contact between water and hot oil leads to oil dispersion. Then the oil particles contact surrounding water vapour, since the asphalt is hydrophobic, thus air bubbles are created. After foaming bitumen gradually bonds aggregate grains (Fig. 4). The foam dissipates very quickly and hence vigorous mixing is required to distribute adequately the bitumen throughout the material. During the mixing process, foamed bitumen layers encapsulate fine particles that form a slurry that effectively binds the mixture together [5]. Foamed bitumen usually contains 0.5% additive 97% bitumen and 2.5% water.

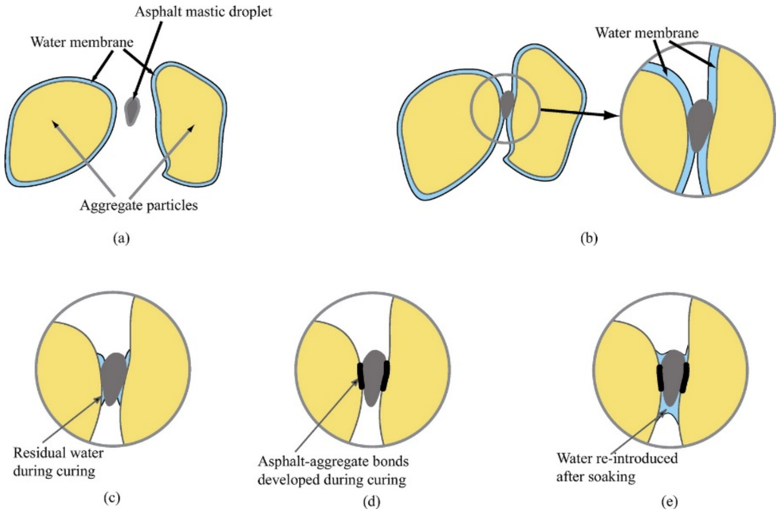

Figure 4. Coating phases of foamed bitumen [16]

5. Benefits of foamed bitumen and foamed asphalt with addition of RAP

5.1. Technological benefits from using reclaimed asphalt pavement material (RAP) and/or foamed bitumen

RAP (Fig. 5) is less variable than aggregate, and the "old" bitumen in it, is considered often as an active component during the mixing [17]. The materials slowly unite under the influence of the dynamic loads applied from the traffic loads, and the effective scraped materials act as a bond with 30% of the volume of crushed stone [18]. Foamed asphalt can be stockpiled with no binder runoff or leaching. Since foamed asphalt remains workable for much extended periods the usual time constraints for achieving compaction, shaping and finishing the layer are avoided. Foamed asphalt layers can be built also in rather poor weather, without jeopardizing the good quality of the asphalt layer.

Figure 5. RAP material storage [18]

5.2. Temperature

Foamed bituminous mixtures can be produced also in low temperature. Recycled foamed asphalt mixtures have small shrinkage stress at lower temperatures and thus less premature damage from pavement cracks [19]. Wirtgen group demonstrated the possibility of mixing at low temperatures; the results obtained are demonstrated in Table 1 [11].

Table 1. Temperature limits for binder types [11]

Binder type	***Foamed bitumen***	***Emulsion***	***Road bitumen***
Mixing temperature (°C)	>10	>5	140-160
Aggregate temperature (°C)	15	10	140-200

5.3. Environmental benefits

Using reclaimed asphalt material (RAP) coming from "old" pavement makes it possible to reduce the volume of new "virgin" material that is available in limited quantity [11]. The overall energy consumed by recycling is less than that of any other rehabilitation method [20]. Foam treatment can be used with a wider range of aggregate types than other of cold mix processes [22]. When using foamed bitumen, energy conservation can be attained since this technique makes it necessary to heat the binder and not the aggregate fractions, which can be used in cold and damp without drying. The poisonous evaporation of volatiles does not occur this time unlike hot asphalt mixtures.

Harmonious, high quality mixing of RAP with water and added agents can be achieved using modern recyclers; controlled pumping systems can ensure the accurate addition of fluids, see Fig. 6 [22]. When using foamed bitumen as asphalt binder, higher shear strength and less moisture susceptibility of aggregate can be attained. Another of its advantages is increased resistance to fatigue and flexibility while its strength approaches that of cemented mixtures.

5.4. Structural issue

Modern recycling machines have the ability of producing rather homogeneous, durable and thick asphalt layers [23].

5.5. Minimized disturbance

The disturbance of the underlying pavement layers is rather small because recycling is typically a single-pass operation and the wheels of the machine run without contacting lower layers when running on top of the reclaimed material [4].

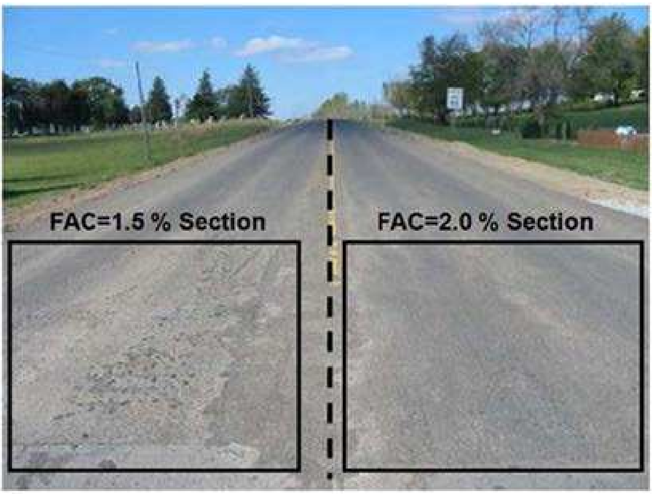

Figure 6. Homogenizing foamed bituminous mixture increasing the rate of water [22]

5.6. Reduction of construction time

In the case of cold recycling in place, the mixing and the paving are carried out in the same process reducing construction time and costs. Besides, traffic disruption for shorter periods results in additional benefits for road users [21].

5.7. Safety

It is an advantageous fact from traffic safety point of view that recycling machine works within a single traffic lane (Fig. 7), and the road can be used immediately after the completion of rehabilitation [11]. Saving in time comes from the fact that foamed asphalt can be compacted immediately and can carry traffic almost immediately after compaction is completed.

5.8. Cost

Time and movement reduction and saving material resources results in decreased cost. Not only its construction costs are not as much as the typical cold asphalts have but also the transportation costs coming from its limited bitumen and water needs [25].

Figure 7. Use of a single lane

6. Limitations of the usage of the technologies

The design procedure of foamed bituminous mixtures (FMA) including foaming, mixing, compression, curing and tests are rather uniform [25]. Since its production requires fairly high (some 180 °C) temperature, there is a risk of burning of binder [24].

Asphalt mixtures with foamed bitumen are not suitable for all pavement types, e.g. for wearing course repair and light asphalt pavement, it cannot be used [17].

The use of foamed bituminous asphalt mixtures is not really wide-spread in the world. The reasons of this situation include the limited number of related international literature, not too high strength, increased sensitivity to moisture and rutting. Recently there have been a lot of research and investigation to solve the difficulties mentioned by the use of crushed asphalt aggregate [26]. It was shown that several of these negative phenomena could be considerably reduced by utilizing RAP aggregates.

7. Some foamed asphalt mixture design methods

The most popular methods of designing foamed asphalt mixtures which are:

1. South African design method (Foam Index, aggregate gradation, resilient modulus, shear parameter, permanent deformation under repeated loading) [27].
2. Queensland design method (pavement design software CIRCLY, maximum design modulus for foamed bitumen layer, bitumen content, strength of post cracked phase, Poisson's Ratio, indirect tensile strength) [28].

English design method (use of the gyratory compaction method, optimized mixing water content and compaction effort, consideration also Reclaimed Asphalt Pavement material, optimised the foamed bitumen content, indirect tensile stiffness modulus, indirect tensile strength) [29] [30].

8. Foaming bitumen research in Syria

In Syria, a bitumen foaming apparatus (Fig. 8) was made for research purposes. The device consists of an asphalt chamber, a water tank, and an air compressor, in addition to an electrical network to measure temperatures and control external and internal heating. After adjusting the measuring instruments, the valves are opened and the materials enter the expansion chamber where the foaming process takes place.

Figure 8. Foaming bitumen device

The laboratory test series performed covered the investigation of foamed bituminous mixtures with four binder types (foamed bitumen with 1.5…2.0…2.5…3.0 wt% water content using base bitumen 65 penetration) and five aggregate variants with 0…25…50…75…100 wt% RAP. The optimum water content of asphalt mixture was determined using Expansion Rate and Half Life parameters, see point 2 (Figure 9).

Figure 10 shows the Marshall-stability results of 20 foamed bitumen asphalt mixture variants. Foamed bitumen was produced using a moisture content of 2.3m% (see Figure 10) at 190 °C binder temperature. The foamed bitumen bound asphalt mixture variants were created by 1.5, 2.0, 2.5 and 3.0 wt% binder contents. Each of these 4 mixture variants was produced using the following RAP contents:

- Type (A) – 100% new aggregate.
- Type (B) – 75% new aggregate + 25% RAP.
- Type (C) – 50% new aggregate + 50% RAP.
- Type (D) – 25% new aggregate + 75% RAP.
- Type (E) – 100% RAP.

Significant differences can be seen between the Marshall-stability values in Figure 10 coming – among others – from the different residual binder share in RAP materials.

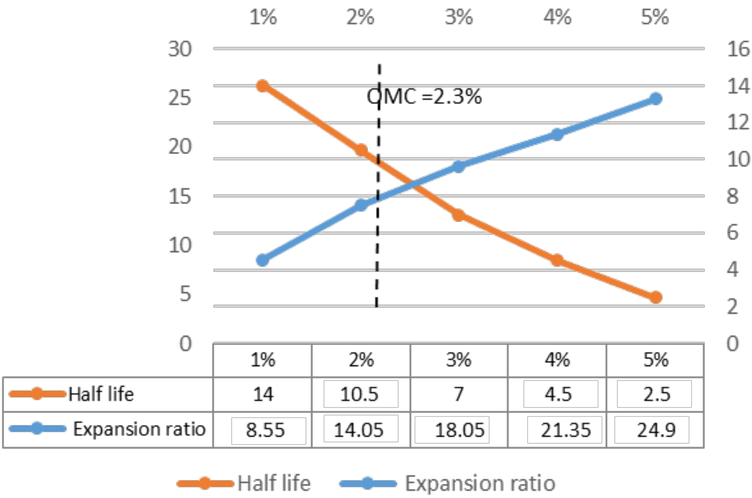

Figure 9. Calculation of the optimum water content (OMC) of foamed bitumen at 170 °C

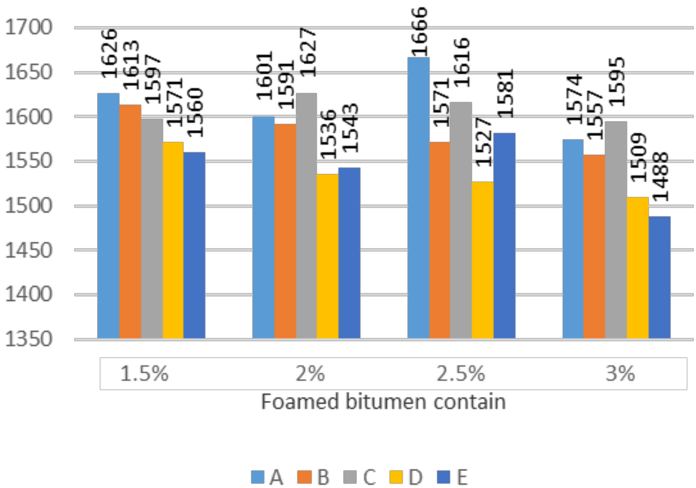

Figure 10. Marshall-stability results (kg)

The results presented in Fig. 9 and 10 will be utilized as inputs for the future PhD thesis of one of the paper authors.

9. Concluding remarks

Foamed bitumen is produced by adding small amounts of water to hot bitumen. When injected into the hot bitumen the water evaporates abruptly, causing foaming of the bitumen in the saturated steam; the bitumen expands by 20 to 30 times its original volume. Foaming of the bitumen results in a number of improvements: more durable coating con be reached also in case of cold and wet aggregate fractions; less viscous binder can be produced in the foaming process; this type of binder has a rather low temperature typically not exceeding 60 ºC. Cold-treated material produced with foamed bitumen can be stored for very long time. The use of foamed bitumen can be even more environmental friendly when also reclaimed asphalt pavement material is utilized.

The increasing use of asphalt mixtures with foamed bitumen binder can be considered as a successful solution of road industry for energy efficient, environment-friendly and cost-effective construction techniques. This kind of asphalt is a cold bituminous mixture of various aggregate types and foamed bitumen. The technology of foamed bitumen process is more than 70 years old and used in a lot of countries all over the world, there are still many related topics that has not been sufficiently tested so far. That is why it is worthwhile to overview the main theoretical and practical results in the field in several countries including those of the authors of the paper. It is clear that the foamed asphalt is usually characterized by high quality and reasonable cost, can be used in cold road pavement rehabilitation, in addition to it the technique is environmentally friendly preserving natural resources. Using foamed bitumen reduces the emissions of carbon dioxide and gases resulting from combustion, especially when it is used as a cold rehabilitation binder and mixed with reclaimed asphalt pavement materials.

Since the road construction and maintenance techniques are relatively new, no global reference mix methods are existing. That is why there are still a lot of related unsolved research areas.

References

[1] B. Bairgi. A. Rafiqul, Characterization of foaming attributes to binder tribology and rheology to better understand the mechanistic behavior of foamed asphalt, *International Journal of Pavement Research and Technology* 1 (10) (2020). doi: `https://doi.org/10.1007/s42947-020-0283-x`

[2] L. Csanyi, Foamed asphalt in bituminous paving mixtures. *Highway Research Board Bulletin* 160 (1957) pp. 108-122.

[3] Mobil Oil Australia, *Foamed bitumen: A new development*. Technical Bulletin (1971).

[4] D. Sánchez, Effect of foaming technique and mixing temperature on the rheological characteristics of fine RAP-foamed bitumen mixtures. *Road Materials and Pavement Design*, (21) (8) (2020) pp. 2143-2159.

[5] S. Pitawala, A. Sounthararajah, J. Grenfell, Experimental characterisation of fatigue damage in foamed bitumen stabilised materials using dissipated energy approach. *Construction and Building Materials* (216), (0) (2019) pp. 1-10.

[6] D.E. Newcomb, E. Arambula et al., Properties of Foamed Asphalt for Warm Mix Asphalt Applications. *NCHRP Report* 807 Transportation Research Board, (2015) 126 p.

[7] M. Corrigan, *Warm mix asphalt technologies and research*. Federal Highway Administration- FHWA. (2008).
URL `https://www.fhwa.dot.gov/pavement/asphalt/wma.cfm`

[8] S. Khosravifar, D. Goulias, Ch.W. Schwartz, Laboratory Evaluation of Foamed Asphalt Stabilized Base Materials, *Geotechnical Special Publications*, GeoCongress 2012 (2012)
doi: `https://doi.org/10.1061/9780784412121.164`

[9] D. Palha, P. Fonseca et al., Recycled asphalt mixtures with foamed bitumen: an alternative to build ecofriendly road pavements. *AECEF2015* Proceedings, 8th Symposium, Universidade Porto – FEUP, 5/6 November 2015, (2015) 6 p.

[10] A. Saleh, البحث بإمكانية تصميم الخلائط الإسفلتية باستخدام الإسفلت الرغو, *Tishreen University Journal,* Engineering Sciences Series, (41), (2019) 3 p.

[11] A. Woszuk, A. Zofka et al., Effect of zeolite properties on asphalt foaming, *Construction and Building Materials* 139, (2017) pp. 247-255.

[12] Wirtgen, *Wirtgen Cold Recycling Technology*. Windhagen, 1st Ed. (2012) 22 p.

[13] B.K. Bairgi, R.A. Tarefder, A Synthesis of Asphalt Foaming Parameters and Their Association in Foamed Binder and Mixture Characteristics, ASCE Proceedings, *T&DI Pavement Conference*, PA, USA, (2017) pp. 256-267.

[14] S. Kumrawat, D. Vinay, Foamed Bitumen, *International research journal of engineering and technology* 5, (2018) pp. 401-404.

[15] R. Bowering, C. Martin, Foamed bitumen production & application of mixes evaluation & performance of pavements. Proceedings of the *Association of Asphalt Paving Technologists (AAPT*) 45, (1976). 453–477.

[16] PQ Corporation. *Production, testing and compaction details*. Advera WMA Warm mix asphalt, (2012) 33 p.

[17] Z. Zhang, C. Cong et al.,. Application research on the performances of pavement structure with foamed asphalt cold recycling mixture. *Construction and Building Materials* 169, (2018) pp. 396-402.

[18] K. Kuna, K. Airey, N. Thom, Mix design considerations of foamed bitumen mixtures with reclaimed asphalt pavement material, *International Journal of Pavement Engineering* 18 (10), (2017) pp. 902-915.

[19] R. David, H. Allen, *Foamed Asphalt Overview of Mix Design and Construction.* American Engineering Testing (2013).

[20] L. Gao, F. Ni et al., High-temperature performance of multilayer pavement with cold in-place recycling mixtures. *Road Material and Pavement* (15), (8), (2014) pp. 804–819.

[21] A. Sharma, Energy savings and reduction of CO_2 emission using $Ca(OH)_2$. Incorporated zeolite as an additive for warm and hot mix asphalt production. *Energy* (2016).
doi: `https://doi.org/10.1016/j.energy. .03.085`

[22] C. Almeida, A. Benta, Economic and environmental impact study of warm mix asphalt compared to hot mix asphalt, *Journal of Cleaner Productions* (112), (4), (2016) pp. 2308–2317.
doi: `https://doi.org/10.1016/j.jclepro.2015.10.077`

[23] A. Stimilli, G. Ferrotti, et al. Performance evaluation of cold recycled mixture containing high percentage of reclaimed asphalt. *Road Materials and Pavement,* 14, (2013) pp. 149–161.

[24] A. Loizos, In-situ characterization of foamed bitumen treated layer mixes for heavy-duty pavements. *International Journal of Pavement Engineering,* 8, (2007) pp. 123–135.

[25] CSIR, *Foamed Asphalt Mixes– Mix Design and Procedure*. South Africa: Contract Report, CR-98/077, (1998).

[26] URL `https://asphalt.csir.co.za/foamasph/index.htm`

[27] C. W. Schwartz, S. Khosravifar, *Design and Evaluation of Foamed Asphalt Base Materials.* Technical Report MD-13-SP909B4E, University of Maryland, College Park, MD, (2013) 86 p.

[28] K.J.Jenkins, A.A.A. Molenaar, et al., Development in the uses of foamed bitumen in road pavements. *HERON*, (45), (3), 167-176. ISSN 0046-7316. (2000).

[29] L.R. Laraogitharan, K. Somasundarasavaran, J.M. Ramaniyam, Rehabilitation works in Queensland using foamed bituminous stabilisation*, International Journal of Geomate*, (8), (2), (2005) pp. 1308-1315.

[30] C. Weston, A study into the mechanical properties of foamed bituminous stabilised materials. *Dissertation,* Peninsula Technikon. (2001).

Acta
Technica
Jaurinensis

Vol. 14, No. 3, pp. 315-338, 2021
DOI: 10.14513/actatechjaur.00610

Review of materials used for ballast reinforcement

M. Ahmad*

Széchenyi István University, Structural and Geotechnical Engineering Department, Egyetem tér 1, 9026 Győr, Hungary
***e-mail: ahmad.majd@hallgato.sze.hu**

Submitted: 13/04/2021; Accepted: 29/04/2021; Published online: 14/05/2021

Abstract: This mini review summarizes the most recent research in ballast reinforcement. Several materials are being used for the purpose of improving the ballast layer in railways, including geosynthetics, rubber sheets and binding agents. Such methods of reinforcement have proven to be beneficial for increasing the strength, stiffness, and resilience of the ballast layer in addition to reducing settlement, breakage, degradation, and maintenance cost and frequency. Latest studies try to find the best types, placement, and combination of geosynthetics to achieve the highest strength and resistance, in addition to obtaining the optimum percentage of binding agents and methods of applying them in order to discover the most effective binder that achieves the most improvement to the mechanical properties of the layer for a reasonable price. An overview of the recent tests conducted to study the reinforced ballast layer and their results is presented in this paper, as well as an overall evaluation of the implementation of these reinforcement methods in railways.

Keywords: ballast reinforcement; geosynthetics, polyurethane, binding agents

1. Introduction

The ballast layer plays an important role as a foundation of the railway tracks. It is vital to ensure the quality of the ballast in order to transmit the loads applied on the superstructure to the substructure safely while maintaining adequate longitudinal and cross-direction stability to the railway track. Granular materials with high strength and inner friction are used for this layer to allow fast seepage of precipitation and low permanent deformations. Many problems may develop in the ballast due to the static and cyclic loading conditions imposed by the trains, including large settlements which cause speed restrictions and compromise the passengers' comfort. Ballast fouling is also a common issue, when the finer material mixes with the fresh ballast, altering the particle size distribution, settlements, and permeability characteristics of the ballast. This phenomenon might be due to the crushing of the top granular material or when finer particles infiltrate the ballast from underlaying layers. Excessive deformations can also be caused by substructure failures which lead to very costly maintenance procedures [1].

Poorly constructed ballast will lead to excessive deformations and differential settlements in the railway track, causing concerns about the safety of the passengers. Quick and usually costly measures should be taken regularly in that case to maintain the good functional quality of the railway and to ensure not to exceed the serviceability limit state. In order to reduce the maintenance costs and frequency, several methods were introduced to reinforce the ballast layer with the aim of increasing the shear strength, stiffness, lateral resistance, and resilient modulus and decrease deformation, degradation and breakage of the ballast.

The most common methods used for ballast reinforcement are geosynthetics (e.g., geogrid, geonet and geotextile), Polyurethane, rubber energy absorbing drainage sheets, and binding agents such as bitumen, organosilane and lignosulphonate. A variety of field and laboratory tests are conducted recently to assess the performance of these improvement methods. The most used tests include direct shear test, plate load test, drop hammer impact test, repeated load triaxial tests, single tie push test and track panel displacement test. An overview of the recent research conducted to evaluate the efficiency of the improvement methods of ballast is presented in this paper, and an overall comparison between the methods is introduced.

2. Ballast reinforcement methods

2.1. Geosynthetics

Geosynthetic is defined as "a planar product manufactured from a polymeric material that is used with soil, rock, or other geotechnical-related material as an integral part of a civil engineering project, structure, or system" [2]. It has several application depending on its type and shape including reinforcement, filtration, and separation. 3 main types of geosynthetics are used for ballast improvement:

- Geotextiles consist of synthetic flexible and porous fabrics characterized by a relatively high percentage open area (6-30%), mainly used in the ballast for separation to reduce the amount of fouling leading to a reduction in settlement and maintenance cost.

- Geonets are created by a continuous extrusion of parallel sets of polymeric ribs at acute angle to one another, mainly used for their in-plane drainage capabilities and usually used along with another type of geosynthetics for reinforcement and drainage improvement.
- Geogrids are plastics formed into a very open, grid-like configuration, the openings between the adjacent longitudinal and transverse ribs are large enough to allow for soil communication. they function almost exclusively as reinforcement materials due to its high strength, high modulus, and low creep. The usage of geogrids to stabilize the ballast layer has proven to be effective by increasing its shear strength, lateral resistance and vertical stiffness and decreasing breakage, deformation, and degradation.

2.2. Polyurethane

Polyurethane is made by chemical reaction of isocyanate compound with hydroxy compound. It can be found in different forms, including rigid foams, flexible foams, chemical-resistant coatings, and elastomers. The two most common polyurethane used for ballast improvement are XiTRACK and Elastan, which are unfoamed material, performing stiff bonding. XiTRACK has a much lower gel-time (10 secons) than Elastan (30-60 minutes) and reaches 90% of its strength in a shorter time (one hour) than Elastan (72 hours).

The two components of the polyurethane are mixed in situ through mixing equipment and poured, sprayed, or injected in the track. When it flows through the voids of the ballast particles, a gel-like material is created around the particles, generating a strong ballast-polyurethane matrix that is hard to break even at temperatures up to 230^{o}. The voids of the ballast are partially filled with the polyurethane; therefore, it maintains both permeability and the ballast track's capacity to support train loads.

A new more economical type of polyurethane was introduced in Korea called ERSBallast, it has properties that are similar to XiTRACK. However, it uses a different method when applied to the ballast layer, where it is designed to be injected based on the pressure distribution applied by train and transmitted to the ballast, reducing the amount needed by injecting only to regions where train loads are directly applied [3]. Recent research shows improvement in the ballast's shear strength, stiffness and friction when treated with polyurethane.

2.3. Binding agents

The use of different types of binding agents in the ballast layer was found useful to increase its strength and improve drainage in addition to reducing permanent deformations and maintenance cost and frequency. For example, bituminous emulsion can be applied by spraying onto the ballast layer along the track to form what is called Bitumen Stabilised Ballast (BSB). Furthermore, a nanoscale agent called Organosilane which is not affected by change of temperature and ultraviolet radiation, showed positive results for improving the ballast because its components help forming an impervious nanolayer of alkyl siloxanes on the particles' surface.

Lignosulfonate can also be applied to the ballast (Lignosulfonate Stabilised Ballast LSB). It is an organic water-soluble material gained in papermaking industries. The recent research related to the use of lignosulfonate to improve the properties of coarse crushed rocks similar to the material used for ballast has shown promising results.

2.4. Rubber mats

Rubber mats were first used in railway to decrease noise and vibration. Subsequently they were used between the rail foundation and the ballast layer for better load distribution leading to a reduction in permanent deformations and improving stability. T.N. Ngo et al. [4] studied the influence of rubber energy absorbing drainage sheets (READS) in decreasing breakage, degradation, and deformation of the ballast layer by placing recycled rubber mats underneath the ballast layer and conducting large-scale impact tests. It can also be used in combination with different types of geosynthetics, especially geogrids.

3. Field and laboratory tests for ballast evaluation

3.1. Single tie push test (STPT)

This test is used to measure the lateral resistance of the railway track, where a hydraulic jack is connected to the outer surface of the rail where the lateral forces are applied, and a linear variable displacement transducer (LVDT) is installed on the outer surface of the other rail to measure the outer displacement (Fig. 1). The test can be conducted in the field on real constructed railway tracks, or smaller models can be created in the laboratory to simulate the same conditions of the field on a smaller scale with a vertically loaded or unloaded tie.

3.2. Direct shear test

This test is used to find the shear strength of the specimen, by applying a predetermined normal stress followed by a shearing deformation with a constant rate while measuring the lateral displacement and the shearing force in the meantime. The test is described in (ASTM D3080). For ballast testing, a large-scale direct shear test machine that consists of two square boxes is used, with adequate dimensions to marginalize the impact of boundary conditions on the outcomes. The ballast is placed in the boxes in layers, and the geogrid is positioned on the interface of upper and lower boxes in case of testing the effect of geogrid on the shear resistance, or the ballast can be treated with the tested binding agent before placement to evaluate its shear strength. The friction angle can be calculated from the relationship between normal stress and shear stress at failure which is used to evaluate the shear strength of the specimen. Furthermore, breakage of the ballast due to shearing can be measured by retrieving the specimen from the shear box after the test and sieving it to assess the changes in ballast gradation. Marsal's Breakage index (Bg) is usually used which is the total sum of the positive values of ΔW_k in percentage, where positive ΔW_k is the reduction in percentage retained in each sieve.

3.3. Process simulation test

Large scale process simulation tests (PST) are used to simulate a track segment consisting of a sleeper beneath the rails that contribute to transmitting the applied loads to the ballast. In this test, the transverse and longitudinal movement of the track are simulated by the in and out movement of the walls of the PST apparatus. Five movable plates are placed in the middle of the shorter side walls to measure the lateral movement of the ballast along its depth. A set of five servo-controlled actuators are installed on each side of the walls to apply the lateral loads, and a vertical dynamic actuator is installed to apply a vertical pressure with a frequency up to 50Hz. The deformations are measured, and the resilient modulus is calculated for different frequencies.

3.4. Plate load test

This test is performed on the ballast material to find its stiffness and vertical load-settlement curve, where ballast materials are compacted in several layers in a big chamber placed under a steel solid frame to withstand the reaction loads, which is fastened firmly to a robust huge base or foundation. The vertical stress is applied in phases through a hydraulic jack. Two important strain moduli are calculated as an assessment of the mechanical properties of the aggregates forming the ballast layer. E_{V1} is a short-term property obtained from the first cycle of loading, which is related to the in-situ density of the ballast. and E_{V2} is calculated from the second cycle, and it is more concerned with the mid to long-term characteristics.

3.5. Los Angeles abrasion test (LAA)

LAA test defined in (AASHTO T 96) or (ASTM C 131) is used to test durability and strength properties of ballast, by measuring the mass loss rate (LAA loss %). The sample is placed in a rotating steel drum with a speed of 31~33 r/min along with steel balls. “After being subjected to the rotating drum, the weight of aggregate that is retained on a No. 12 (1.70 mm) sieve is subtracted from the original weight to obtain a percentage of the total aggregate weight that has broken down and passed through the No. 12 sieve. Therefore, an L.A. abrasion loss value of 40 indicates that 40% of the original sample passed through the No. 12 sieve” (AASHTO T 96).

3.6. Triaxial test

Normal and large scale triaxial tests are conducted to measure the stiffness and deformation resistance of the aggregates. The specimen is subjected to a uniform confining stress through pressurised water, in addition to a vertical static or dynamic stress (deviatoric stress) by using a hydraulic jack, with a maximum stress that adequately simulates the train loads. The resilience modulus is then calculated which is the ratio between the variation in the dynamic vertical stress and vertical strain.

3.7. Drop hammer impact test

Drop weight impact tests are conducted to assess the capability of the reinforcement material to mitigate dynamic impact loads and reduce the degradation of the ballast. The device consists of a hammer allowed to free fall using rollers which are guided through low-friction runners on vertical steel columns fixed onto a reinforced concrete floor. The thickness of the ballast layer and the capping are determined to simulate the conditions in the field. The acceleration is measured through an accelerometer installed at the top surface of the sample, and the impact loads during the tests can be recorded by a dynamic load cell attached to the hammer, and the deformations are recorded by using a highspeed camera.

The vertical displacement, lateral deformations and ballast breakage are measured to evaluate the performance of the ballast and the reinforcement method under the dynamic impact loads.

A different and more up to date and unique laboratory test to measure ballast breakage was also introduced by Juhász and Fischer [5].

4. Results

The placement of the geogrid layer plays an important role for achieving a maximum effectiveness. F. Horvát et al. [6] conducted multi-level shear box tests on granular aggregate that is used as a railway ballast layer to study the inner shear resistance with and without compaction, and the effect of reinforcement with 2 types of geogrid combined in some cases with geotextile (geocomposite). The inner shear resistance was increased after the reinforcement. However, it was found that the maximum shear strength was not at the geogrid-ballast interface, but 0-10 cm above the interface. Furthermore, geogrid with glued geotextile decreased the inner shear resistance because it obstructs the interlocking between the aggregates and the geocomposite.

M. Esmaeili et al. [7] studied the effect of geogrid reinforcement on ballasted track's lateral resistance by conducting field and laboratory STPT to evaluate its performance with different number of geogrid layers in the ballast. In the lab, they used a 4x1 m geogrid sheets on different levels of a (30,40 and 50 cm) thick ballast and under the central of 5 concrete ties (type B70), which was chosen for receiving the loads. The test was conducted on a vertically unloaded tie, and the jack applies a rate of 0.5 mm lateral displacement on the outer surface of the rail until it reaches 2mm. Their laboratory tests showed an increase in the lateral resistance of 31 % for one layer of geogrid in a 30 cm thick ballast. This improvement diminished with the increase in the thickness of the ballast to 15% for a thickness of 40 cm and to 13% for 50 cm. A further improvement was noticed when using two layers of geogrid, as the lateral resistance grew by 42% for a 30 cm thick ballast when compared to non-reinforced ballast. Similar behavior was noticed as before when increasing the thickness of the ballast layer, and the effect of the geogrid declined with the installation distance from the sleeper as can be seen in Fig. 2.

In the field, a part of a preconstructed railway track was removed to install two layers of geogrid in a 30 cm thick ballast supporting B70 concrete ties and two UIC60 rails. A robust wall was used to support the hydraulic jack. The filed findings showed very good compatibility with the laboratory results with a maximum of only 0.39 KN difference in lateral force (5.6% of the total force), and similarly, a 42% increase in lateral resistance was achieved with 2 layers of geogrid and 34% for a single layer.

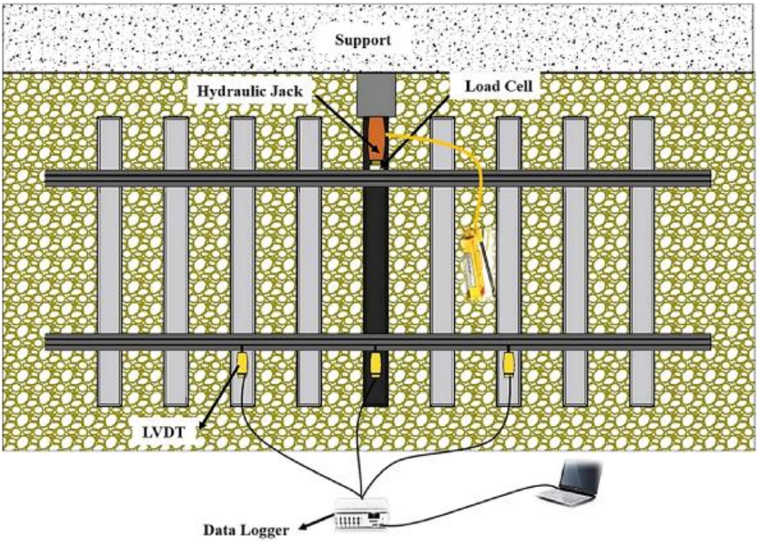

Figure 1. Illustration of the STPT test [7]

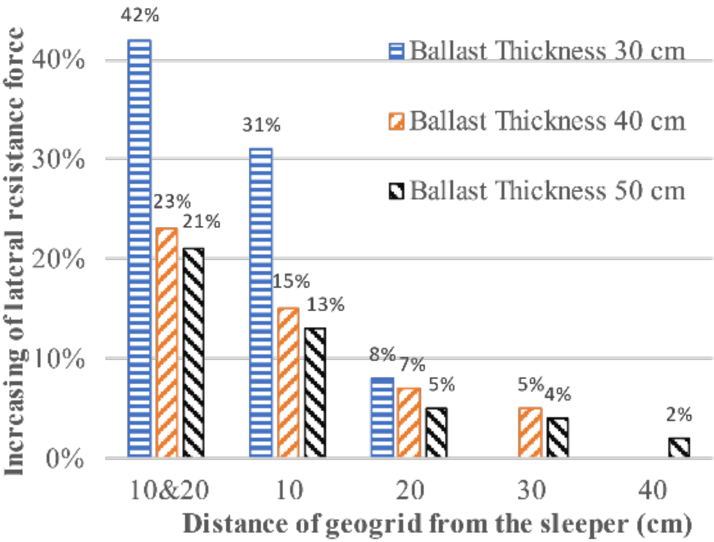

Figure 2. the increase in lateral resistance in STPT [7]

Sweta and Hussaini [8] performed large scale direct shear tests on fresh granite to study the influence of different types of geogrid on the shear strength of the ballast-subballast interface. The used apparatus consists of two 450x450 mm square boxes with a depth of 300 mm, the lower box is fixed, and the upper box moves laterally to apply the shear forces. The subballast was compacted and placed in two layers in the lower box and the ballast was placed by the same means of compaction in the upper box after the geogrid was placed at the interface of the two layers. Loads were applied in magnitudes and rates that represent the real field conditions for a typical track with low confinement. The tests show a significant increase in the friction angle after reinforcement. However, this increase depends on the vertical stress and the shearing rate. The angle of friction could be increased to a maximum of 67.96^{O} when using PP (blaxial) geogrid (G1) with square aperture shape, and ultimate tensile strength of 30 KN/m, compared to 63.42^{O} for unreinforced interface. They also found that the change in the angle of friction is given by a logarithmic equation which is a function of the rate of shear (S_r) and the vertical stress(σ_n):

$$\delta = -a_1 \ln(\sigma_n) + a_2, \tag{1}$$

$$\delta = -b_1 \ln(S_r) + b_2, \tag{2}$$

The equations show that apparent friction angle of ballast-geogrid-subballast interface (δ) declines with the increasing vertical stress and rate of shear stress, as the interface efficiency factor α which is the ratio tan (δ)/tan $(\emptyset)$ drops from 1.22 to 1.15 as S_r rises from 2.5 to 10.0 mm/min.

The ballast was retrieved from the shear box after each test and sieved in order to study the breakage of the ballast during shearing. According to their observation, "the breakage of ballast (B_g) increases with the increase in σ_n and S_r for both unreinforced and reinforced conditions" [8]. However, using the previously mentioned type of geogrid at the ballast-subballast interface reduced the breakage from 3.88 to 3.10%.

In a later study, Sweta and Hussaini [9] used the same type of ballast and geogrid as their previous study to conduct process simulation tests (PST), this time to study the effect of geogrid on deformation response and resilient modulus of railroad ballast under cyclic loading. The apparatus box is 950x650 mm with a depth of 730 mm, the loads are transferred from the rail to one sleeper of 950x250 mm, and the walls move in a way that simulates the real field conditions as can be seen in Fig. 3. The strains were measured in the transverse direction to find the lateral spreading of the ballast. The subballast was compacted in the box in two layers of 75 mm and a geogrid layer of reinforcement was installed, then the ballast was compacted in three layers of 127 mm to achieve the field density. The test specimen was loaded up to 250,000 cycles and at loading frequencies between 10 and 40 Hz. Their results show a significant reduction in lateral displacement at the level of the geogrid (G1) of 59% for a loading frequency of 10 Hz. This enhancement was reduced to 49% for a frequency of 20 Hz. On the other hand, the vertical displacement was decreased by 43% and 35% for frequencies of 10 and 20 Hz, respectively. Nevertheless, the reduction in lateral and vertical deformation decreases substantially with the increase in vertical distance from the ballast-geogrid-subballast interface until it diminishes entirely at a certain distance (close to the sleeper). Moreover, the resilient modulus given by:

$$M_r = \frac{\sigma_{cyc}}{\epsilon_r}, \tag{3}$$

Where "σ_{cyc} is the cyclic deviator stress, ϵ_r is the recoverable axial strain during cyclic triaxial unloading" [9]. It was noticed that reinforcing with geogrid improves the resilient modulus of the ballast considerably, as it has increased by 25.8% and 21.4% for frequencies of 10 and 20 Hz respectively due to the increase in the effective confining pressure of the ballast. Fig. 4 shows the benefit of using the geogrid in improving the resilient modulus and the breakage of the ballast and the effect of the increasing frequency.

Figure 3. Illustration of the PST test [9]

Ballast contamination is a common problem that causes a change in the properties of this layer. J. Sadeghi et al. [10] addressed the issue of ballast contamination with sand and studied the effect of ballast layer reinforcement with geogrid to improve the mechanical properties of this layer. large-scale direct shear tests were done on dolomite limestone aggregates that comprise the ballast layer with several degrees of sand contamination. The degree of contamination as a percentage was defined as the ratio of the dry weight of contaminant particles with size less than 9.5 mm to the total dry weight of the sample. For the large-scale direct shear tests, the ballast was poured and compacted in two layers for each of the two boxes, and the sand was spread on each of the layers with different percentages to simulate the contamination conditions in real railway tracks. Three different types of geogrid with square aperture (24, 34 and 46 cm width) were placed on distances of 10 cm and 20 cm from the bottom. Their results shown in Fig. 5 indicate that the angle of friction decreases with the increasing contamination percentage regardless of the reinforcement. The angle of friction could be improved by up to 13% for clean ballast when using 34×34 geogrid installed 10 cm above the bottom of the ballast. The same type of geogrid with the same placement caused an enhancement in the ballast's shear strength by 25% as a result of the particle-grid interlocking. However, this enhancement declines considerably when the contamination level with sand increases due to the friction and contact loss between the aggregate particles, and the slip and slide of the particles on the geogrid.

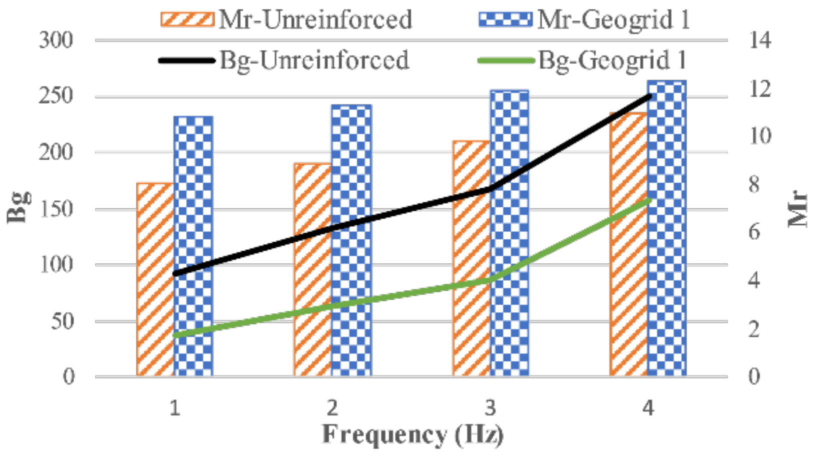

Figure 4. The effect of frequency and reinforcement on the resilient modulus (M_r) and breakage (B_g) of the ballast [9]

Javad Sadeghi et al. [10] also examined the same conditions as before by using the plate load test to find the vertical load-settlement curve of reinforced sand contaminated ballast. The test was conducted in a (120 × 120 cm2) chamber with a depth of 100 cm. The ballast was compacted in 3 layers of 10 cm each and two cycles of loading were applied. It was observed that the vertical settlement increased with the increasing percentage of contamination. However, the inclusion of the 34x34 geogrids 10 cm from the bottom caused a 30% decrease in the settlement. Fig. 6 shows how the strain modulus for the second cycle (EV2) decreases with the increase in contamination. Furthermore, the increase in stiffness is noticed for different types of geogrids and their distances from the bottom. It can be also seen that when the contamination level exceeds 24% it is highly less effective to use geogrid and in that case cleaning of the ballast is necessary.

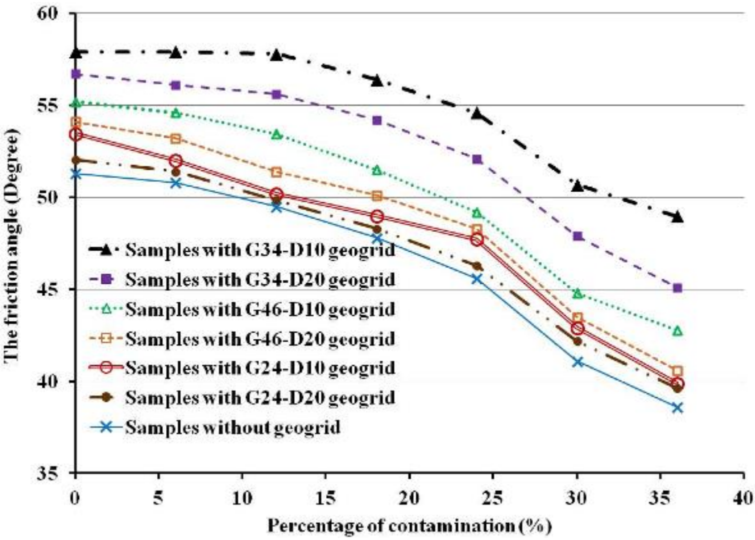

Figure 5. Change in friction angle of ballast samples with the increasing degree of contamination [10]

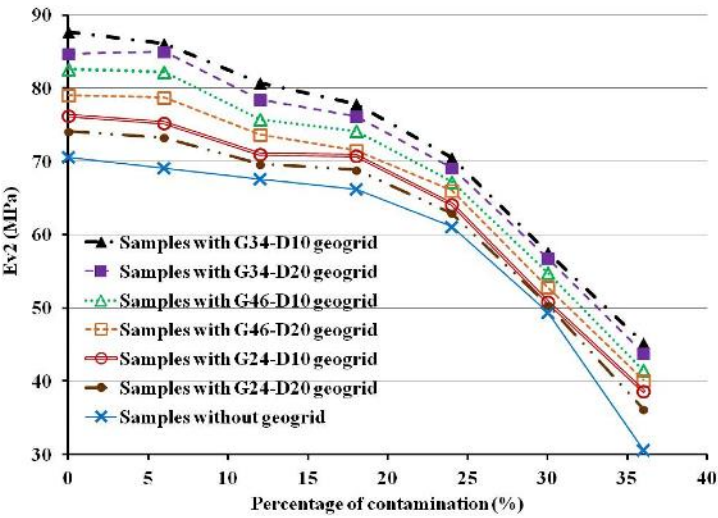

Figure 6. Change in the strain modulus of ballast samples with the increasing percentage of sand contamination in the second cycle of loading [10]

Raghvendra Pratap Singh et al. [11] explored the effect of woven geotextile on the stability of the track by placing them at the ballast-subgrade interface and analyzing the degradation and fouling of the ballast. For this purpose, 173 ballast samples were collected from different locations of the single-track section (DN), and double-track section (UP) between Bhusawal and Akola in the state of Maharashtra, India, where about 20 trains pass per day of 20.5 tons for UP track (coal loaded trains), and 5.8 tons for the DN track (empty trains). The collected samples (with and without geotextile) were tested in the laboratory to assess ballast fouling, degradation and change in Los Angeles abrasion loss.

The fouling index is calculated from the particle size distribution curve as follows:

$$\mathrm{FI} = \mathrm{P}_{4.75} + \mathrm{P}_{0.075}, \tag{4}$$

For the UP track, including the woven geotextile decreased the ballast fouling by 74% and 64% for parts of the track with 239 million load cycles (MGT) and 327 MGT respectively. However, fouling was reduced by about 28% for the down track after the passage of 434 MGT traffic (11 years). Furthermore, installing woven geotextile decreased the breakage index (Bg) by 17% on both tracks. They also found that for tracks reinforced with geotextile at the ballast-subgrade interface, "the deep screening cycles could be increased by 5 years on DN track and by 200 MGT traffic on UP track" [11].

The optimum content of additives that strengthens the ballast layer is an intruiging topic for multiple researchers. S. H. Lee et al. [3] conducted large-scale triaxial tests to examine the properties of ballast mixed with polyurethane with different mixing ratios. Ballast only samples were compacted in a 300 mm diameter and 620 mm height steel mold and confined before applying the axial loading since it cannot be self-supported. On the other hand, for the polyurethane-mixed ballast samples, the polyurethane was poured on previously compacted ballast in an acrylic cylinder and was left to cure. The tests were conducted on specimens with (70, 140, and 210 kg/m^3) polyurethane contents in unicaxial conditions, which is more similar to the field conditions. The polyurethane-mixed ballast showed two linear regions seperated with two drops in the stress-strain curve with a lower stiffness for the first line which is more governed by the ballast than the polyurethane. The two regions were fitted with a function for each of the polyurethane contents. It was found that the deformation moduli which is the slope of the stress-strain line (stiffness) increased linearly with the increasing polyurethane content as shown in Fig. 7.

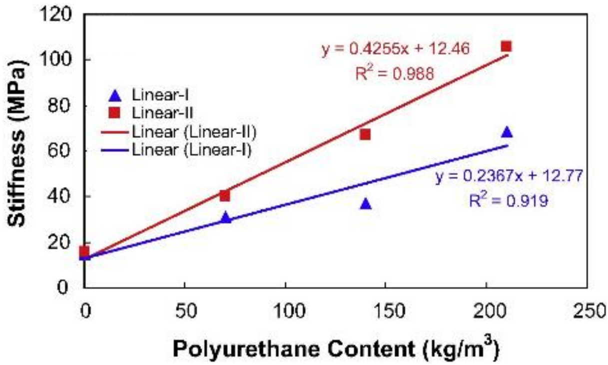

Figure 7. Ballast stiffness vs polyurethane contents under confining stress of 30 kPa [3]

The strength of the mixture was measured, which is here the maximum stress on a stress-strain curve. It was observed that the strength increased linearly with the increasing polyurethane content as shown in Fig. 8.

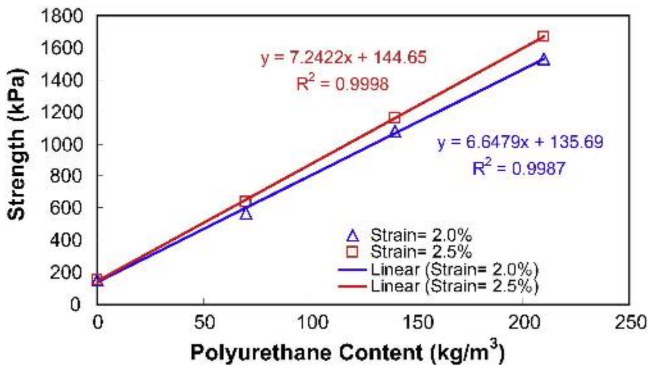

Figure 8. Uniaxial strength of polyurethane-mixed ballast under confining stress of 30 kPa [3]

Gundavaram and Hussaini [12] investigated the effect of adding Elastan-polyurethane stabilizer on the shear strength and breakage of the ballast, then it was compared to the geogrid reinforced ballast by using large-direct shear tests with two 450x450 mm boxes of a 300 mm depth. The unstabilized ballast was compacted in 3 layers of 100 mm, and in case of geogrid reinforcement, the layer of geogrid was placed at the interface of the two boxes (the shear plan). However, for Elastan-polyurethane stabilized ballast, the aggregates with 3% of the additive by weight of ballast were mixed previously in a concrete mixer for 5 minutes and then compacted with the same method as before and left to cure for 1, 3 and 7 days before the test starts. Most of the strength was obtained after 3 days of curing, therefore, all the tests were conducted after that period. The results showed an increase in the secant shear stiffness (shear stress/shear strain) from 5.4 MPa for unreinforced ballast to 5.7 MPa for geogrid reinforced ballast while it reached a max of 10.3 MPa for Elastan-stabilized ballast for a normal stress of 60 KPa and shear rate of 3 mm/min. Furthermore, for the same normal stress and shear rate, a substantial enhancement was reached in the terms of the angle of friction, from 65° to 75° after stabilization. Fig. 9 shows the decrease of the angle of friction with the increasing normal stress for the three cases, which can be given as a logarithmic relationship.

Values of stabilization efficiency factor S_{ef} (given by the shear strength of stabilized ballast divided by the shear strength of unstabilized ballast) illustrated in Fig. 10 proved the advantage of using Elastan-stabilized ballast with S_{ef} between 1.6–1.75. Additionally, in case of Elastan-stabilized ballast, the particles could not be separated to conduct a particle size distribution test, therefore no breakage of ballast was inspected.

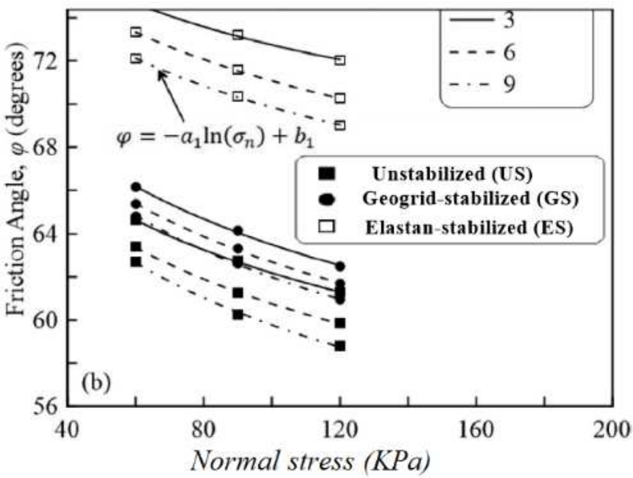

Figure 9. Change of friction angle with normal stress for unstabilized, geogrid-stabilized and Elastan-stabilized ballast [12]

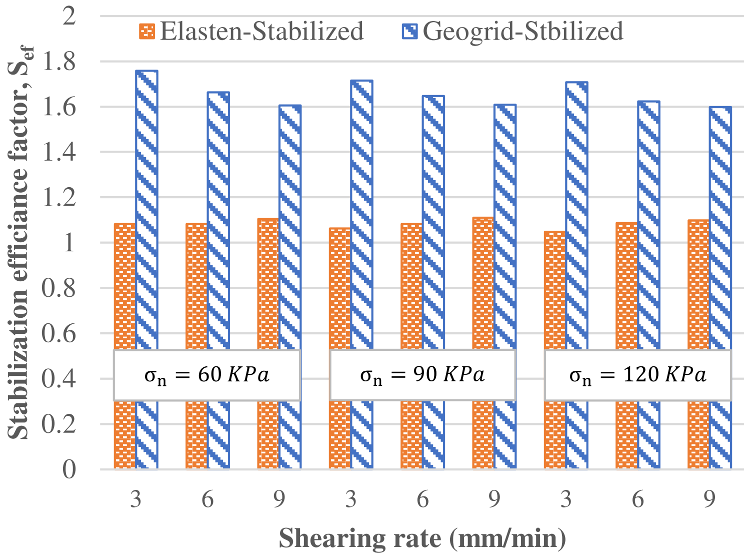

Figure 10.Comparison of stabilization efficiency factor for Elastan and geogrid-stabilized ballast for different normal stresses and shear rates [12]

The effect of using rubber energy absorbing drainage sheets (READS) beneath the ballast layer to reduce its deformation and degradation (breakage) when subjected to impact loads was examined by T.N. Ngo et al. [4] by conducting large-scale drop hammer impact tests. The tested layers were formed to simulate track conditions as follows: 350 mm ballast layer placed on a 100 mm subballast layer separated by the recycled (READ) layer and all resting on a 50 mm subgrade. 16 tests were performed with soft and concrete subgrade, with and without the rubber mats and with various drop heights which leads to a variation in dynamic stress. After the impact, the ballast layer attains a maximum displacement and then rebounds to its permanent settlement. For a drop height of 150 mm the maximum and permanent deformations of the ballast without reinforcement reached 84.76 mm and 74.2. However, adding the rubber mat at the ballast-subballast interface helped diminishing these values to 77.05 mm and 64.5 mm, respectively. The breakage of the ballast was also measured after the test, and the highest breakage occurred at the top of the specimen where the impact stress is the highest and it decreases as we go deeper. The percentage reduction of ballast breakage (R_b) given by:

$$\mathrm{R}_b = \frac{\mathrm{BBI}_{NoReads} - \mathrm{BBI}_{withreads}}{\mathrm{BII}_{NoReads}} \cdot 100, \tag{5}$$

Where BBI is the breakage index defined in [4] as "A/(A+B), where A is shift in the PSD curve after the load application, and B is potential breakage or the area between the arbitrary boundary of maximum breakage and the final PSD curve". For stiff subgrade, the drop in breakage reached 28%, on the other hand, R_b was between 10-17% for soft subgrade. Moreover, a reduction in lateral deformation was obtained after the inclusion of the rubber mats as shown in Fig. 11.

Similar drop hammer tests were conducted by B. Indraratna et al. [13] to study the degradation of ballast reinforced with three different types of biaxial geogrid (various tensile strengths) at different locations under impact loads, in addition to studying the effect of adding under-ballast mat (UBM) or under-sleeper pad (USP) which are 10 mm thick recycled rubber mats. A variety of tests were performed with two types of subballast, and with either a 150 mm capping layer of aggregates or a concrete layer of the same thickness. The same process then as the previous test was followed with the inclusion of the rubber mats at the ballast-capping interface in some cases and on top of the ballast layer in other cases. The geogrid was placed at the ballast-capping interface, 10 cm, or 20 cm above.

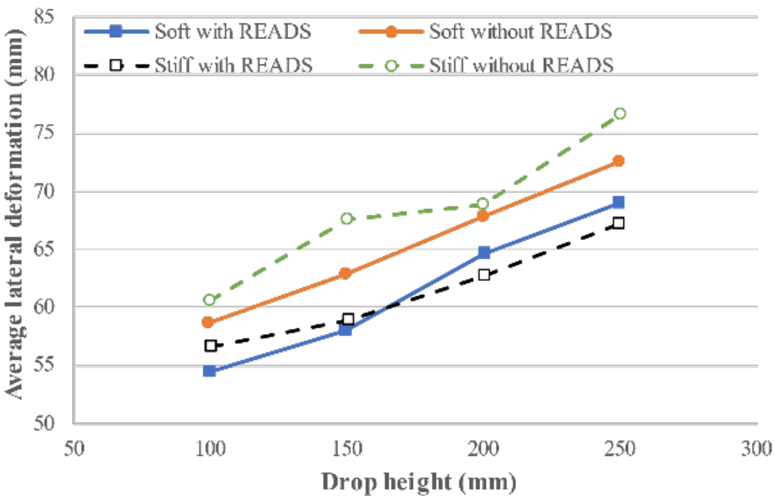

Figure 11.Effect of READS and subgrade type on the final lateral deformation of the ballast [4]

The highest reduction in axial and lateral deformation was achieved when placing the geogrid layer 10 cm above the ballast-capping interface (up to 18.2% for axial strain and 21.9% for lateral strain). Moreover, the inclusion of geogrid diminished the breakage of the ballast by 13.3% in average of the 3 tests where the geogrid was placed in different places, and the highest decrease was noticed when placing the geogrid 10 cm above the geogrid as (BBI) decreased from 0.1503 to 0.1298.

The tests also proved that the best combination to enhance the ballast's deformation resistance is to place the geogrid 10 cm above the ballast-subballast interface and the shock mats at the bottom of the ballast layer, as the axial and lateral strains were reduced by 17.2% and 26.1% respectively. On the other hand, when it comes to breakage, the USP placed above the ballast layer reduced breakage by almost 35% showing a better performance than UBM which showed only a slight improvement. Fig. 12 shows the improvement in deformation resistance when increasing the tensile strength of the geogrid, where the peak tensile strength of GGR1, GGR2, GGR3 is 24.8, 41.7 and 55.3 kN/m respectively.

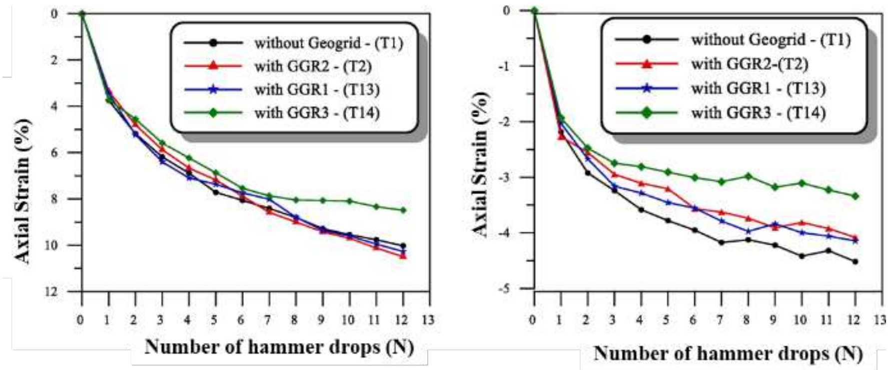

Figure 12. Effect of different geogrids on the performance of ballast under impact loads [13]

D.M. Barbieri et al. [14] tested the benefit of several additives on the mechanical properties and stability of the ballast layer using repeated load triaxial tests. Bitumen Stabilized Ballast (BSB) contained 3% of bitumen by weight and were mixed in a steel bowl. On the other hand, Polyurethane Stabilised Ballast (PSB), Lignosulfonate Stabilised Ballast (LSB), and Organosilane Stabilised Ballast (OSB) contained 1.5%, 0.65% and 1.5% of polyurethane, lignosulfonate and organosilane binders by weight, respectively, by adding the binder and mixing in plastic bags, then each specimen was compacted and cured for a certain time as shown in Table 1.

Table 1. Summary of the tested samples by D.M. Barbieri et al [14]

Additive	***Code***	***Additive content (weight %)***	***Curing***		***Bulk density (t/m^3)***	***Price estimate (EUR/kg)***
			Time (day)	Temperature (c^o)		
Untreated	UGM	-			1.68	-
Bitumen 70/100	BSB1	3.0	2	22	1.73	0.4
Bitumen 160/220	BSB2	3.0	2	22	1.73	0.4
organosilane	OSB	1.5	7	22	1.73	9
lignosulfonate	LSB	0.7	2+5	50+22	1.7	0.6
polyurethane	PSB	1.5	2	22	1.69	4.5

The diameter of the specimens was 150 mm with heights varying between 176-188 mm. Five sequences of different confining stresses and increasing intensities of sinusoidal dynamic vertical stresses up to 600 KPa with 6 loading steps were applied to the specimen. the resilient modulus for a certain sequence here was given by:

$$\mathrm{M}_R = \frac{\Delta\sigma_d^{dyn}}{\varepsilon_a^{el}} \tag{6}$$

Where, $\Delta\sigma_d^{dyn}$ is the dynamic deviatoric stress and ε_a^{el} is the axial resilient strain.

Fig. 13 shows the calculated resilient moduli plotted based on Hicks & Monismith equation given by:

$$\mathrm{M}_R = \mathrm{K}_{1.HM}\sigma_a\left(\frac{\theta}{\sigma_a}\right)^{\mathrm{K}_{2.HM}} \tag{7}$$

where "σ_a is a reference pressure (100 kPa) and $\mathrm{K}_{1.HM}$, $\mathrm{K}_{2.HM}$ are regression parameters" [14], and $\theta = \sigma_1 + \sigma_2 + \sigma_3$. The resilient modulus was significantly increased for all the additives except for polyurethane. As an example, the values of the resilient moduli for UGM, OSB, BSB2, BSB1, and LSB are 460 MPa, 756 MPa 1612 MPa, 1935 MPa, and 2335 MPa, respectively for $\theta = 200$ kPa. This shows that the lignosulfonate was the most effective. Furthermore, the vertical displacements were compared for the five loading sequences. The comparison indicated a considerable decrease in the permanent deformations after using the additives especially for PSB and LSB. The values of permeant vertical deformations for the first sequence and for a vertical stress to confining stress ratio of 5 were 5.55, 1.40, 2.90, 4.10, 0.65, 0.50 for UGM, BSB1, BSB2, OSB, LSB and PSB, respectively.

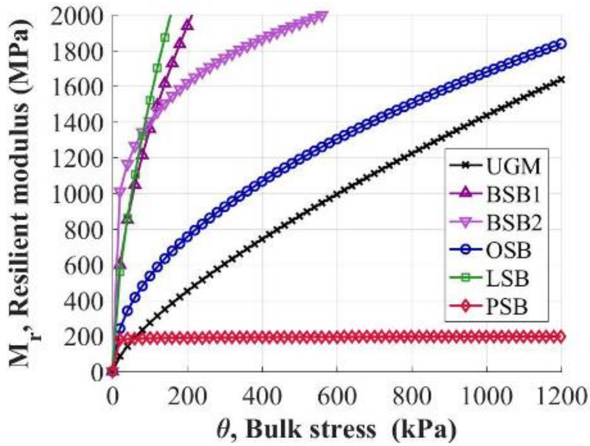

Figure 13. Resilient moduli vs Bulk stress of tested samples according to Hicks & Monismith model [14]

G. Jing et al. [15] presented three new methods of bonding to strengthen ballast with the use polyurethane, for the purpose of investigating the lateral resistance of the ballast, they conducted single sleeper pull-out test (SSPT) to assess the lateral resistance of the strengthened ballast layer. In these new methods only 4 regions of the ballast are reinforced which are considered the most vulnerable regions, two regions close to the center of the sleeper and the other two are at the sleeper ends as can be seen in Fig. 14. In method (E), the parts of the shoulder ballast close to the two sleeper ends should be bonded. On the other hand, in method (C) it is required for the crib ballast near the sleeper center to be bonded. For the last method (B), both the ballast near the sleeper end and center shall be bonded. G. Jing et al. [15] also studied two bonding depths of 200 mm and 300 mm.

For the test, the ballast layer was compacted in 4 layers to a thickness of 350 mm with a width of 3600 mm for a 12 m long track. Type IIIc pre-stressed concrete sleepers were used on the top of the ballast. A spraying mechanism was employed to apply the polyurethane to the top surface of the ballast. A lateral force was applied to the sleepers and the lateral resistance and deformations are measured. The test results show a substantial improvement in the lateral resistance after reinforcement for the three bonding methods, and the improvement is higher for a bonding depth of 300 mm. A comparison between the enhancement that the different methods provide at a sleeper displacement of 2 mm are shown in Fig. 15, where the numbers above the bars indicate the difference between the bonding method and tests with no binders.

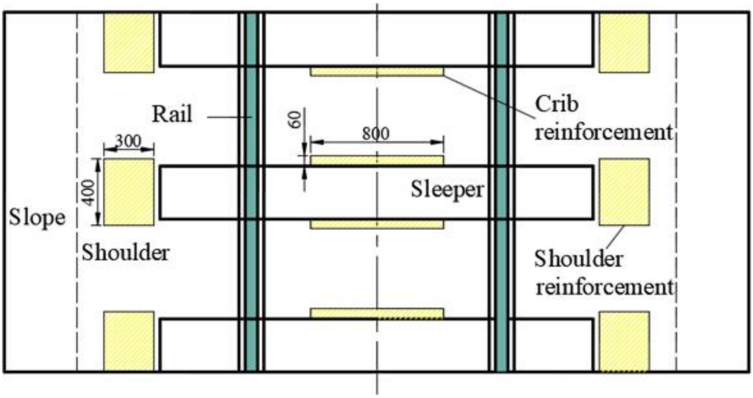

Figure 14. Sketch of the new bonding schemes for strengthening the ballast layer using polyurethane (the target regions are in yellow) [15]

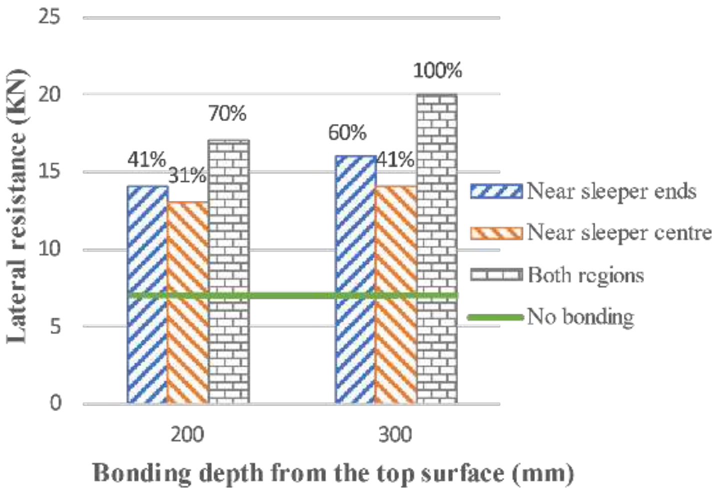

Figure 15. Lateral resistance forces of ballast at d=2 mm in various tests and their differences [15]

5. Conclusions

The review presented in this paper indicates substantial benefits of reinforcing the ballast layer to decrease the permanent deformations and improve the railway stability in addition to decreasing the cost and frequency of maintenance work. This enhancement is attributed to the geogrid-ballast interlocking which increases the shear strength and the effective confining pressure of the ballast which detains and restricts the displacement and rotation of the ballast. As a result, it is more beneficial to install the geogrid in the ballast layer (about 10 cm above the bottom) rather than underneath it, in order to gain more contact between the two elements.

Studies have proven that using square shaped geogrid caused a better improvement in the ballast layer shear strength than using triangle shaped geogrid, due to the higher effective aperture of such type of geogrid which is more compatible with the particle size distribution of the aggregates that comprise the ballast, and it was also found that geogrid with higher tensile strength can further improve the deformation resistance as well as adding another layer of geogrid. However, it was found that a better performance can be achieved with the use of some types of binders to stabilize the ballast because of the strong bonding between all the ballast particles of different sizes due to the additives' coating, rather than a few particles of specific size gets interlocked in the geogrid apertures. Nevertheless, a disadvantage accompanies this feature by making the maintenance a more difficult and complicated process in addition to the extended construction cost and time, while it is easier to perform the maintenance work of the railway in case of geogrid reinforced ballast. Such factors should be taken into consideration depending on the country's resources and circumstances before choosing the reinforcement method. Furthermore, bitumen, lignosulfonate and polyurethane are the best binders with a slight advantage for lignosulfonate considering the price difference. It can be also mentioned that more viscous binders attain a major increase in stiffness.

The new scheme of additives distribution reduces the height of the ballast shoulder and the dosage of the polyurethane considerably as the percentages of the areas occupied by the reinforced ballast in the three new methods of bonding are only 18.1%, 7.2%, and 25.3% of the total area, respectively. Thus, the new methods of bonding are more cost effective in both the dosage of polyurethane material, and the ballast, considering the high cost of the polyurethane that could reach 150.000 Euros per kilometer, which limits its application in ballast reinforcement.

In case of impact dynamic loading, it was observed to be very beneficial to use rubber mats at the ballast-subballast interface along with the usage of a geogrid layer to attenuate the loads and absorb the energy resulted from such types of loads, leading to a decrease in the vertical and lateral displacement.

References

[1] B. Eller, S. Fischer, Tutorial on the emergence of local substructure failures in the railway track structure and their renewal with existing and new

methodologies. *Acta Technica Jaurinensis* 14 (1) (2021) pp. 80–103, 2021.
doi: `https://doi.org/10.14513/actatechjaur.00565`

[2] R.M. Koerner, Designing with Geosynthetics, 6th Edition, Vol. 1, *Xlibris*, USA, 2012.

[3] S.H. Lee, S.J. Lee et al., An experimental study on the characteristics of polyurethane-mixed coarse aggregates by large-scale triaxial test. *Construction and Building Materials* 145 (2017) pp. 117–125.
doi: `https://doi.org/10.1016/j.conbuildmat.2017.03.107`

[4] N.T. Ngo, B. Indraratna, C. Rujikiatkamjorn, Improved performance of ballasted tracks under impact loading by recycled rubber mats. *Transportation Geotechnics* 20 (2019) 100239.
doi: `https://doi.org/10.1016/j.trgeo.2019.04.002`

[5] E. Juhász, S. Fischer, Railroad Ballast Particle Breakage with Unique Laboratory Test Method. *Acta Technica Jaurinensis* 12 (1) (2019) pp. 26–54.
doi: `https://doi.org/10.14513/actatechjaur.v12.n1.489`

[6] F. Horvát, S. Fischer, Z. Major, Evaluation of railway track geometry stabilisation effect of geogrid layers under ballast on the basis of laboratory multi-level shear box tests. *Acta Technica Jauriensis* 6 (2) (2013) pp. 21–44.

[7] M. Esmaeili, J.A. Zakeri, Laboratory and field investigation of the effect of geogrid-reinforced ballast on railway track lateral resistance. *Geotextiles and Geomembranes* 45 (2017) pp. 23–33.
doi: `https://doi.org/10.1016/j.geotexmem.2016.11.003`

[8] K. Sweta. S.K.K. Hussaini, Behavior evaluation of geogrid-reinforced ballast-subballast interface under shear condition. *Geotextiles and Geomembranes* 47 (1) (2019) pp. 23–31.
doi: `https://doi.org/10.1016/j.geotexmem.2018.09.002`

[9] K. Sweta. S.K.K. Hussaini, Effect of geogrid on deformation response and resilient modulus of railroad ballast under cyclic loading. *Construction and Building Materials* 264 (2020), 120690.
doi: `https://doi.org/10.1016/j.conbuildmat.2020.120690`

[10] J. Sadeghi, A.R.T. Kian et al., Effectiveness of geogrid reinforcement in improvement of mechanical behavior of sand-contaminated ballast. *Geotextiles and Geomembranes* 48 (6) (2020) pp. 768–779. doi: `https://doi.org/10.1016/j.geotexmem.2020.05.007`

[11] R.P. Singh, S. Nimbalkard et al., Field assessment of railway ballast degradation and mitigation using geotextile. *Geotextiles and Geomembranes* 48 (3) (2020) pp. 275–283. doi: `https://doi.org/10.1016/j.geotexmem.2019.11.013`

[12] D. Gundavaram, S.K.K. Hussaini, Performance evaluation of polyurethane-stabilized railroad ballast under direct shear conditions. *Construction and Building Materials* 255 (2020) 119304. doi: `https://doi.org/10.1016/j.conbuildmat.2020.119304`

[13] B. Indraratna, N.T. Ngo et al., Laboratory examination of ballast deformation and degradation under impact loads with synthetic inclusions. *Transportation Geotechnics* 25 (2020) 100406. doi: `https://doi.org/10.1016/j.trgeo.2020.100406`

[14] D.M. Barbieri, M. Tangerås et al., Railway ballast stabilising agents: Comparison of mechanical properties. *Construction and Building Materials* 252 (2020) 119041. doi: `https://doi.org/10.1016/j.conbuildmat.2020.119041`

[15] G. Jing, X. Zhang, W. Jia, Lateral resistance of polyurethane-reinforced ballast with the application of new bonding schemes: Laboratory tests and discrete element simulations. *Construction and Building Materials* 221 (2019) pp. 627–636. doi: `https://doi.org/10.1016/j.conbuildmat.2019.06.114`

[16] Standard Test Method for Direct Shear Test of Soils under, ASTM D3080 (2003).

[17] Standard Test Method for Resistance to Degradation of Small-Size Coarse Aggregate by Abrasion and Impact in the Los Angeles Machine, ASTM C131 / C131M-20 (2020).

Acta
Technica
Jaurinensis

Vol. 14, No. 3, pp. 339-363, 2021
DOI: 10.14513/actatechjaur.00612

Special reinforcement solutions of railway permanent ways' soil substructures

M. Habashneh[1,*]

[1]Széchenyi István University, Department of Structural Engineering
Egyetem tér 1, 9026 Győr, Hungary
***e-mail: habashneh.muayad@hallgato.sze.hu**

Submitted: 26/04/2021; Accepted: 16/052021; Published online: 21/05/2021

Abstract: This mini review aims to summarize relevant international publications. Thus, based on this, giving a comprehensive review about the reinforcement solutions of permanent ways' soil substructure. Generally, the core weakness of soil is its inadequacy to resist tensile stresses. The main target of strengthening the soil is to enhance the engineering characteristics of the soil to build up specific parameters such as shear strength, compressibility, density, and hydraulic conductivity. In addition, special reinforcement techniques of railway permanent ways' soil substructures will be considered in this paper due to the increasing demand of improving railways and rehabilitation process. The main findings of this study that there are a lot of special reinforcement techniques which can be considered as effective solution for soil stabilization such as geosynthetic reinforcement.

Keywords: permanent ways; soil reinforcement; substructures; subgrade

1. Introduction

It is known that soils possess a low tensile strength. So, civil engineers have attempted to address this challenge for quite a long time. To increase the tensile and shear strengths of soil, various methods of reinforcing have been utilized in different sorts of earth designs, for example, retaining walls, earth dams, slopes, etc. Various reinforced earth rehearses have been used throughout the world [1][2].

The substructure of railway track incorporates the ballast, subballast, and subgrade layers that handle the track superstructure of rails and ties. Substructure of tracks affect the stability and performance as well as vehicle dynamics of track superstructure. The fundamental role of the track substructure is to support the applied loads uniformly and without perpetual deformation that might influence the geometry of track. The resulted loads of the railway elements and its transfer way are represented in Fig. 1.

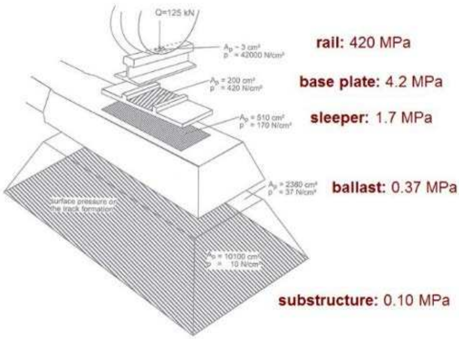

Figure 1. Load distribution in superstructure [3]

The performance of the track substructure is depending on the performance and properties of each layer. The track superstructure transfers the load which comes from the wheel from the highest point of the rail, through the ties and into the foundation. The ballast should offer resilient support for the tie. In any case, the development of the tie under singular wheel loads will be resulted in permanent differential settlement. Thus, the rigid support would be resulted in the failure of other track segments. Ballast of open-graded hard rock gives the vital strength. However, when the voids filled with fouling material and moisture, the flexibility is decreased along with the inter-particle contact stress, which leads to relative movement of the ballast particles and settlement of the tie [4][5].

In case of unfavourable conditions, different kinds of subgrade problems could be developed which in turns could lead to failure or iterative maintenance of railway track. The significant causes that might engaged in the development of subgrade problems could be classified mainly into load factor, soil factor, and environmental factor.

- Load factor

It is the external factor which might lead to subgrade problem. There are different types of loads which are involved in this context: self-weights of material and repeated dynamic loads. The first one could be the main concern that may cause consolidation settlement or massive shear failure and the second type is defined as the repeated traffic loading which has two features characterize it, the magnitude of the individual wheel load and the number of repetitions [6][7][8].

- Soil factor

The impact of soil type on the subgrade is firmly identified with its moisture content and its sensibility to the effects of moisture change. Many soils have no problem if it goes as subgrade depending on its ability of keeping low sufficient moisture content. A significant reason behind why subgrade problems which are regularly connected with fine-grained soils is that this type of soils is generally vulnerable to diminishing in stiffness and strength with increasing water content and do not drain well. In contrast, the performance properties of coarse-grained soils are lesser extent affected by the presence of water, because such soils can drain well so that they typically have low moisture contents.

- Environmental factor

The term environmental factor includes soil moisture and soil temperature. The presence of water in the subgrade can lessen the strength and stiffness of subgrade soils drastically. Additionally, soil temperature is considered as main concern when it causes patterns of freezing and thawing [9][10].

In this study, a comprehensive review of various scientific journal papers about soil substructures special reinforcement techniques. Also, different case studies of railway rehabilitation are considered in this study.

The layout of the rest of this study is coordinated as follows: Section 2 gives an outline of the soil reinforcement. An overview of various methods of soil reinforcement is presented in Section 3. Section 4 illustrate the factors that affecting the soil reinforcement. Reviewing of literature of different scientific papers related to soil reinforcement and railway substructures as well as some case studies which are related to the topic are showed in Section 5. Conclusion, remarks, and future perspective are given in Section 6. Finally, the summary is introduced in Section 7.

2. Soil reinforcement

Generally, soils can be considered as four fundamental sort blends: gravel, sand, clay, and silt. The soil usually has the characteristics of low tensile strength and is exceptionally subject to natural conditions. Thus, the concept of soil reinforcement had been coming out which can be defined as a technique to improve the engineering characteristics of soil, such as shear strength, compressibility, and density. In other word, soil reinforcement can be specified as a method for improving the mechanical properties of the soil like shear, compression, hydraulic conductivity, and density. Therefore, the crucial purposes of reinforcing soil mass could be concluded as improving its stability, bearing capacity, and reducing settlements and deformation. Soil reinforcement can be done by stone columns, root piles or micro-piles, soil nailing and reinforced earth. In other words, soil reinforcement is a technique used to stabilize soil. Essentially, reinforced earth is a composite material comprising of substituting layers of compacted inlay and man-made building up material. The use of reinforcement materials in the soil is resolved as an interaction for improving the characteristics of soil [11][12].

In the following sections, different methods of soil stabilization and reinforcement will be discussed from several aspects such as the benefits of these techniques, general mechanism for applying such methods of reinforcement and its effect on different kinds of soils.

3. Methods of soil reinforcement

During the previous forty years, innovative techniques to improve soil have been reached out to handle soil problems. Several techniques were used for reinforcing the soils to decrease the deformation of soils which undergo applied load. These techniques are viewed as the most practical approaches to improve the conditions of undesirable sites compared to the traditional construction methods. For instance, rope fibers, metal strips, tire shreds, metal bars and geotextiles.

As it was referenced, reinforcement of soil is a technique where characteristic or incorporated added materials are utilized to improve the properties of soils. Various reinforcement techniques are available for stabilizing soils. However, based on reinforcing performance, Fig. 2 presents different methods of soil reinforcement.

3.1. Thermal stabilization

Soil thermal stabilization has gotten more habitually usage in expanding the bearing limit of foundations of a structure. Researchers and specialists have created and introduced a few techniques of thermal stabilization previously by allow roasting soil segments through boreholes of different depths and diameters [13]. Because of heat treatment of soils, its strength increases fundamentally; this increase relies on the monolithic phase of the heated soil.

3.2. Mechanical stabilization

In general, diverse particle sizes are added to existing soil for purposes of changing the uniformity degree and grading size. This process raises friction angle magnitude and cohesion. Considering that such method is used prior to a construction phase to avoid the issues that might occur if we perform it during construction.

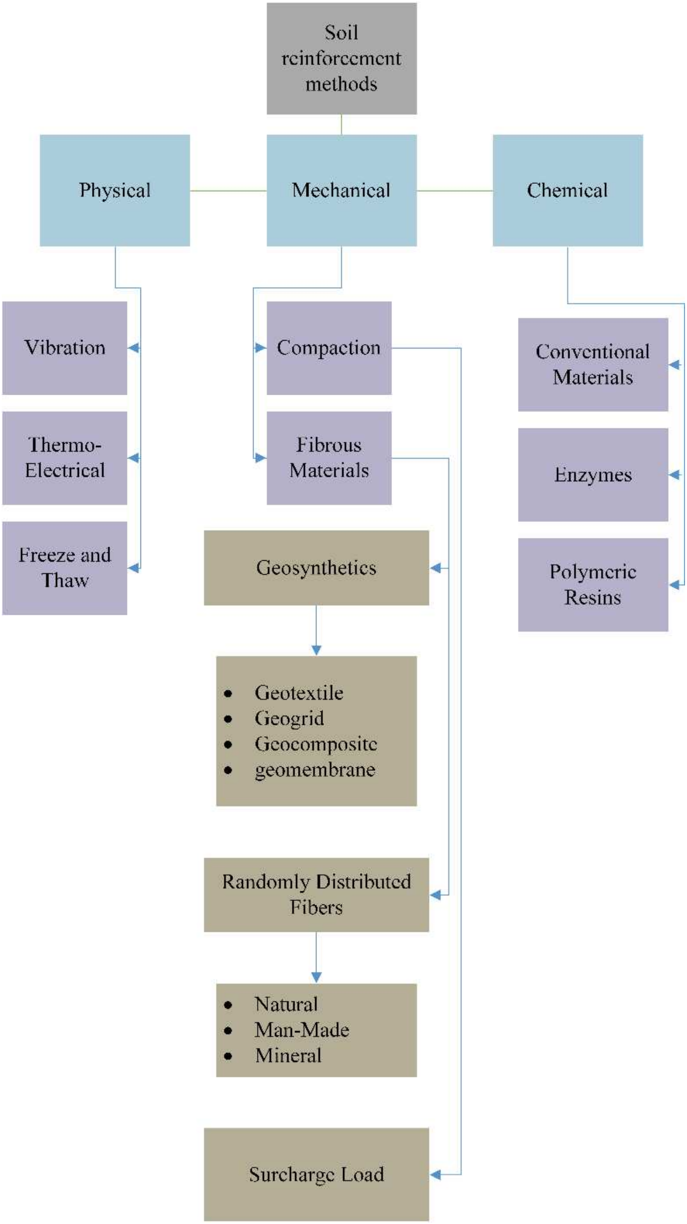

Figure 2. Different techniques of soil reinforcement

3.3. Chemical soil reinforcement

Chemical soil reinforcement has been used broadly applied in last decades in different fields such as foundations and hydraulic constructions. This method of soil reinforcement showed that this technique is truly dependable and in various cases it can be considered as the only method which can be used to strengthen weak soils. Also, it has been utilized to save significant designs and remarkable noteworthy landmarks.

3.4. Geosynthetic reinforcement

These days, geosynthetics are widely used in geotechnical engineering. Numerous construction projects in the world have not utilized of geosynthetic reinforcement which as a result, these projects have not succeeded. Fig. 3 represents one of geosynthetics reinforcement applications which includes replacing the poor soil with better granular fill combined with the geosynthetics reinforcement.

Figure 3. Geosynthetic membrane [14]

3.4.1. Geotextile

Geotextile is one type of geosynthetic. These are materials which comprise of synthetic fibers rather normal ones. Geotextiles, a centre member of geosynthetic family, are broadly utilized to improve soil in civil engineering applications. Geotextiles are not a solitary product; they are manufactured by both synthetic and natural fibers with various aspects and its fundamental objective is separation of aggregate.

3.4.2. Geogrid

Geogrid is generally produced from polymer materials, which might be woven or sewn from yarns, heat-welded from pieces of material, or delivered by punching a standard opening in sheets of material, at that point extended into a lattice. triaxial geogrids reinforcement example is represented in Fig. 4.

Figure 4. Geotextile reinforcement [15]

3.4.3. Geocell

Geocell confinement system is cell structure that gave regulation of compacted fill soils. It reduces the settlement by reducing the soil lateral movement. Besides, it is a useful method for increasing the bearing capacity of the soil. Geocells utilized in many engineering applications such as canals, retaining walls, trenches, embankments, and railways with different preparation conditions of reinforced geocell which are shown in Fig. 5.

Figure 5. Different geocell reinforcement [16]

4. Factors affecting soil reinforcement

There are some factors which could be considered as crucial factors that affecting the reinforced soil such as the distribution of the reinforcement, the state of the soil and soil density. In this section, these influencing factors will be discussed to see its impact on the performance and behaviour of reinforced soils.

4.1. Distribution of reinforcement

- Location

In general, the failure of structures occurs when the applied stresses are greater than the stresses capacity of the structure. Stresses are falling into two categories of which are normal and shear stresses. As a simple definition of these two stresses, we can say that the stress which is perpendicular to a plane is referred as normal stress, while if it parallel to a plane it defined as shear stress and they are anticipated to characterize the strain field. Accordingly, the place of reinforcement is in the tensile region where most deformation occur.

- *Orientation*

The vertical spacing between the reinforcement is playing a major role of peak reinforcement load. However, tiny, or huge spacing could result in an aberration from this direct relationship.

4.2. State of soil

- *Density*

Unique soil states would have various impacts on soil reinforcement, also shifted soils densities directly affect relationships between stress and strain in soil reinforcement.

- *Overburden*

Overburden pressure has direct effects on the friction angle between soil particles and its reinforcement. In fact, the friction coefficient reduces as overburden pressure rises; thus, the shearing stress peak angle of a granular particles soil also decreases with the increasing in normal stress.

- *State of Stress*

In case of reinforced structure, the stress states are dissimilar with growing height. The void ratio diminishes as the height of the soil rises because of increasing in normal stress.

- *Degree of Saturation*

An issue which is related to saturated soil is generally fine-grained material and cohesive soils which are sometimes poor in seepage have a powerful stress transforming that might not be prompt. Therefore, to stabilize the soil, there would be an impermanent decrease in shear strength which diminishes the construction rate.

5. Literature review and case studies

5.1. Literature review

5.1.1. Fibrous material reinforcement

The work depicted in the study of Rowe and Soderman [17] can be considered as a crucial work for amended design procedures of the geotextile reinforced dikes. A technique for assessing the stability of reinforced embankments was discussed in this paper. This methodology kept up the straightforwardness of regular limit equilibrium methods while consolidating the impact of soil-geotextile interaction regarding allowable compatible strain of geotextile. It was showed that this allowable strain might be derived from a design chart and relies on several factors such as geometry and height of embankment, depth of the deposit, and the bed stiffness. The methodology was validated through finite element results which compared with the results of analysis for one benchmark problem. Geosynthetic materials were used extensively in embankments to increase stability. Geosynthetic reinforcement as can be seen in Fig. 6 can be used widely in embankments for purposes of increasing stability.

A study of the resistance to pull-out of geogrid reinforcement had been done by Khalid et al. [19]. Sample's preparation and testing equipment are presented for geosynthetic reinforcements in granular soils. Standard testing equipment was consisting of pull-out boxes which has designed and constructed according to GERL/LTRC-LSU. The study obtained that there were considerable differences in direct shear or pull-out tests used in experimental models of soil-geosynthetic interaction mechanism and performance evaluation of geosynthetics properties. Based on their study, we can sum up the results of their work as:

- the peak pull-out load decreases by the effect of side frictions of the walls, sleeve length and increased thickness of soil.
- In general, the peak pull-out load increases by increasing of densities and confinement which resulted in increasing of passive resistance.

Figure 6. Reinforcement method of embankment [18]

A geosynthetic wall case has been studied by Allen and Bathurst [20] to find the loads in reinforced soil by estimation of strain then convert these data to load through reinforcement material stiffness. The paper summed up these assessed loads, depicted general patterns in the information, and compared those reinforcement loads to apply to wall case histories. It was discovered that reinforcement loads got from strain estimations are, all in all, lower than would be anticipated dependent on current limit equilibrium design techniques that utilization traditional earth pressure theory. This methodology would assist with lessening design traditionalism and would be steady with the way of thinking of forestalling failure of a significant part of the reinforced soil. When the soil has been failed, the wall has been failed also. Uncertainties in the estimation esteems were assessed in the figuring of the loads assessed from estimated strains in contrast with anticipated loads utilizing current design methodologies.

By considering that assessment, it was resolved that the contrasts among estimated and anticipated qualities were huge, both regarding consistency of the expectation and the propensity of the current design methods to considerably overestimate reinforcement loads, justifying re-assessment of the current methods utilized for predicting of reinforcement loads in walls. The authors had also suggested that it would be imperative to evaluate the impacts of toe restriction and facing stiffness on reinforcement loads, just as the impacts of reinforcement stiffness to gauge the reinforcement loads even more precisely of geosynthetic walls as well as their distribution. Hejazi et al. [21] presented a study which aimed to make a review about soil reinforcement by using various kinds of fibers. In addition, a discussion about models used for short composite fibers had been considered.

Natural and synthetic fibers that had been yet utilized to reinforce soil were examined. The importance of using fibers as a soil reinforcement technique was discussed. From the study, it could be noticed that there are several factors that helps in increasing strength and stiffness of soils which could be summed as sand characteristics, test condition and fiber characteristics. Several tests had been performed to approve that shear strength increase when the soil is mixed with discrete fibers. Fiber incorporations likewise hinder the compaction cycle, causing a decrease in the most extreme dry density of reinforced samples with expanding fiber content. It is reported that the mechanism of load transformation still not well understood in case of clayey soils, thus further research required to get better understanding of fibers effect on such kinds of soils. The authors mentioned three significant executive issues engaged with composite soil production which were: clustering and balling of fibers, lack of scientific standards and adhesion between soil and fibers. The technical advantages of soil reinforcement by fibers that were mentioned are: rising hydraulic conductivity, decreasing thermal conductivity, preventing tensile cracks from occurrence, and decreasing the total weight of structure materials. Fig. 7 shows the impact of Polypropylene fiber inclusions which can be observed while implementing triaxial tests.

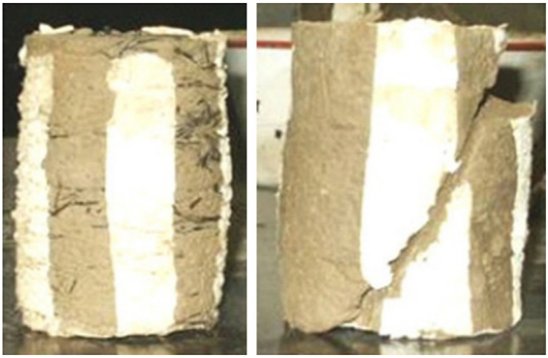

Figure 7. Specimen deformation shape for unreinforced specimen – left and reinforced specimen – right [21]

For purposes of investigating the impact of freeze–thaw on the strength characteristics of geotextile reinforced soil by performing Unconsolidated Undrained (UU) triaxial compressive tests. Ghazavi and Mahya [22] worked on clayey soil with geotextile reinforcement layer which was compacted and tested in the laboratory by applying freeze–thaw cycles. It was found that for unreinforced soil, the triaxial compressive strength decreased as the number of cycles increased. On the other hand, for the reinforced soil samples, exhibited better strength and performance. Additionally, the impact of freeze–thaw cycles on the variations of resilient modulus and cohesion of the soil can be reduced by reinforcement.

A glance at flow rehearses, late advances, momentum research regions, and recommend future headings for the utilization of geosynthetics as reinforcement materials in asphalt frameworks was presented by Perkins et al. [23]. The importance of using geosynthetics as reinforcement of subgrade and their applications fields and purposes was discussed widely in their study. The work which presented in this study would prompt precise design techniques, yet simultaneous with the author's advancement on these turns of events. In addition, geosynthetics ought to be seen as another asphalt material used to impact things such as cracking and rutting.

A methodology was introduced in the study which was done by Leshchinsky and Ralph [24] for stability design and analysis of geosynthetic soil reinforcement. The methodology included external analysis and internal analysis as well. The internal stability analysis depends on variational restricting equilibrium and fulfils all requirements of equilibrium. Two tensile resistance of reinforcement inclination were examined. The orthogonal to radius which defines the geosynthetic sheet and the horizontal which implying the as installed position. The results of both analysis (internal and external) were introduced in a form of design charts that can be used to determine tensile resistance and the profile of reinforcing sheets.

The study which had been done by Brian and Benjamin [25] came out because of upgrades in geosynthetic properties and manufacture methods. The utilization of geosynthetic in soil is expanding and improving. In fact, coastal structures of geosynthetic have accomplished progressed stage regarding applications and proficiency. However, others still actually need specifications and design details based on scientific basis. Subsequently proceeded with test works for better understanding of these geosynthetic coastal structures such as its modes of failure, hydraulic performance, and its stability. Based on this information, this paper came out to review the applications of geosynthetics in soil stabilization, its historical developments, and the techniques of coastal areas protection by introducing significant empirical research data as well as showing the difficulties in the using of geosynthetics in the field of soil stabilization. Laboratory creep test set-up of geosynthetics is shown in Fig. 8.

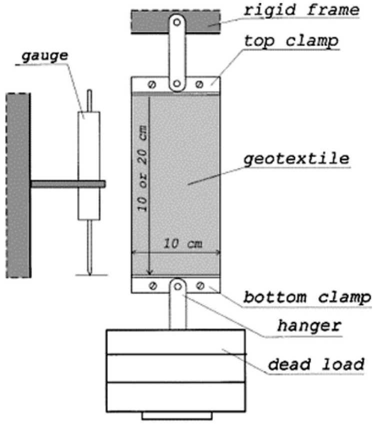

Figure 8. Typical creep set-up of geosynthetics [25]

Venkateswarlu and Hegde [16] presented in their study an investigation of isolation efficiency of geocell reinforced bed which is filled with various materials by several block resonance tests. For testing and experimental purposes, a novel polymeric alloy was used. Different infill cases were considered for testing such as: geocell reinforced sand, geocell reinforced slag, geocell reinforced aggregate, geocell reinforced silty sand, and unreinforced infill. Because of geocell, screening effectiveness of foundation bed has been improved regardless of type of infill material. The greatest isolation proficiency was noted within aggregate presence, among the other infill materials. From the logical investigation, a huge improvement in damping proportion of the foundation bed was seen in the sight of geocell reinforcement also. Field vibration test preparation is shown in Fig. 9.

Using fibers for reinforcing soils considered as ease, proficient and low-cost technique especially in case of recycled fibers usage. Thus, Valipour et al. [26] investigated the impact of using recycled fibers on improving the engineering characteristics of clay soils. The method of this study involved a progression of direct shear tests, unconfined compression and compaction were performed on correctly arranged composite clay soils. In general, 5 mm length of fibers showed better enhancement of clay soils. The results of laboratory tests indicated that the sample ductility increased while the fibers content increased. Thus, higher strength until reaches the optimum content of fibers. Besides, the inclusion of fiber was powerful in increasing cohesion. An example of fibers is shown in Fig. 10 which represents glass fibers.

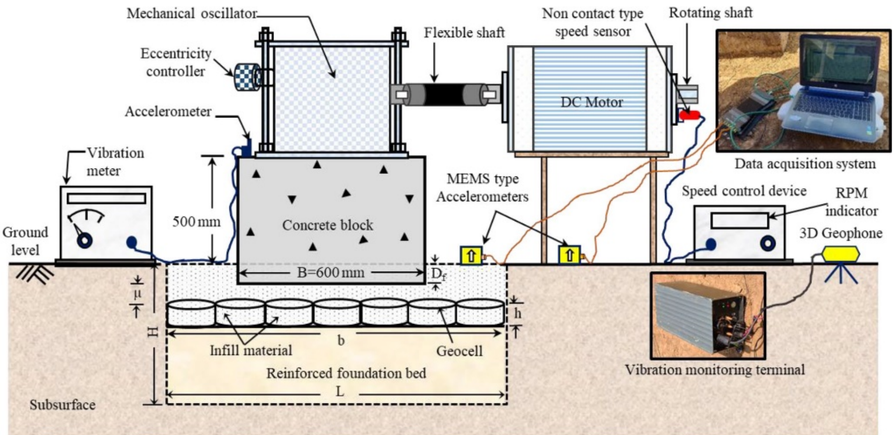

Figure 9. Test setup [16]

Figure 10. Recycled glass fibers [26]

In Alsirawan [27] study, a review of geosynthetic-reinforced pile-supported (GRPS) embankments had presented. The goal of this study was directing an outline of GRPS embankments. Thus, this paper presented a survey about the main boundaries influencing the conduct of geosynthetic-reinforced pile-supported (GRPS) embankments. By considering the design techniques that gauge load efficiency and tensile forces in the geosynthetic layers. In addition, it aimed to cope the problems which resulted because of soft foundations soils such as instability of sliding, excessive settlement and decrease in bearing capacity. Results featured the significance of utilizing GRPS embankments, yet in addition uncover the irregularities between design techniques. At long last, general decisions about the plans and development of GRPS frameworks were introduced. Typical GRPS embankment is shown in Figure 11 which contains piles and platform of load transferring.

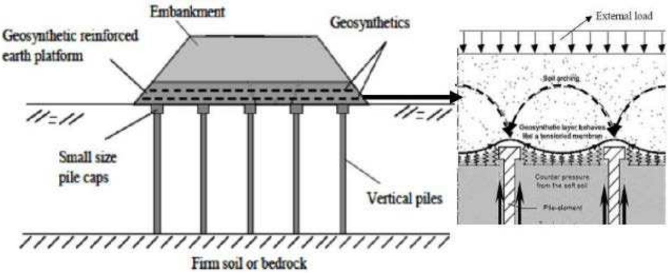

Figure 11. Geosynthetic-reinforced pile-supported embankment [27]

5.1.2. Stabilization and reinforcement of soil

In the article which had done by Salençon and Pecker [28], an extended theoretical framework of yield design theory. In case of shallow foundations assessment, the seismic bearing capacity could be evaluated by implementing yield design theory. That idea which was dependent on in-situ soil reinforcement, was simple to execute, economic and fundamentally improved the seismic bearing capacity for the foundations. The theory validated through series of numerical studies. Much more significant was the way that this foundation concept authorizes philosophy of design capacity in foundation engineering. It looked thusly extremely encouraging for expanding the safety of structures.

A comprehensive review about low-cost soil stabilization methods had done by Ramaji [29] where different methods of expansive soil reinforcement discussed including rewetting, control of compaction and moisture, thermal methods, and chemical stabilization. Each of these techniques might have the disservices of being inadequate and costly. In view of writing, Portland concrete, lime, fly debris and scrap tire were ease and successful to soil reinforcement. According to the study, it was reported that every year a ton of waste rubber are created and consumed an extraordinary space. Thus, it was important to discover an answer for take care of this issue. One of the arrangements is utilization of various size waste rubber in reinforcement of soil.

Shukla et al. [30] made an overview of the essential concepts of reinforcement of soils. Two major groups had classified the reinforced soil which were: randomly distributed fibers and systematically reinforced soil. This study stated that even if the reinforcing technique differs from one type to another, the fundamental concept still the same for all kinds of soils. In other words, the friction/adhesion of soil-reinforcement was basic for all reinforcement. The authors suggested that performing more triaxial tests of large specimens is crucial to show reinforced soil behavior.

Another review had done by Gowthaman et al. [31] which showed the characteristic of plant fibers as situated dispersed fiber- reinforced soil and arbitrarily conveyed fiber- reinforced soil were widely talked about and accentuated the motivation of fiber- reinforced soil dependent on the arising pattern. Review likewise endeavours to investigate the significance of biochemical structure of natural fibers on performance in subsoil reinforced circumstances. The treatment techniques which improved the lifetime and behavior of fibers, were likewise introduced. While illustrating the flow capability of fiber reinforcement technology. Finally, some key research gaps had been featured at their significance. Also, the review clearly showed that there was an impressive research gap because of the absence of large-scale examinations on fiber-soil reinforcing technique, as large portion of the investigations performed up to that day were small-scale laboratory studies.

5.1.3. Stabilization and reinforcement of soil

Eller and Fischer [15] presented a comprehensive review about railway substructures. The authors' point was to sum up the aftereffects of significant international publications and, in view of these, to give a thorough survey about the advanced ballasted tracks' foundation. The approach which was implemented in this article was doing a summary of the foundation and its protection layers. Besides, the geosynthetic cementitious composite materials were talked about. The main discoveries of the proposed work were that the encounters of the geosynthetics and other protection layers capacities showed that a potential utilizing of geosynthetic cementitious composite mat beneath the ballast could be a decent solution for reestablishing short segments of the railway tracks. After examined the related research, the benefits, and weaknesses of GCCM layers in the railway foundation can be adequately characterized. In addition, factual deterioration interaction can be resolved. Finally, the authors mentioned according to the encounters which was attracted the article that the failures of local track could be solved by using concrete canvas or GCCM.

A cost efficiently techniques to solve the local substructures problems had considered in the study of Eller et. al. [3]. The factors which might cause failures of local substructures were viewed. In addition, the protection layers of railway were viewed as well which are competent for railway structures. By summarizing the material properties and previous experiences, the authors reported that the usually used techniques do not provide cost productively improving solution for substructure issues. However, they researched the implicit qualification of the referenced new advances such as the injection technologies and cementitious geosynthetic mats which can be cost efficiently solutions of the mentioned issues. Some failures of local substructures that lead to track's distortion are presented in Fig. 12.

Figure 12. Local substructure failure [32]

A brief literature review according to the fracture of the railway ballast particles was introduced by Juhász and Fischer [32]. Providing better understanding of the international achievements was the goal of this work. With the assistance of the prepared articles with the principal subject of discrete element modelling (DEM). Rock materials can be examined from a different viewpoint. The components can be analysed in laboratory conditions absolutely from the quarry, or by acquiring previously fragmented particles came from railway tracks. Furthermore, DEM models can be made by utilizing PC programming. This article handled just a small fragment of the literature. Although each DEM theme was interesting, they all elaborate assessment of debasement of particles here and there. This review paid attention to model structure, including particle calibration and construction.

5.2. Case studies

5.2.1. Rehabilitation of railways

Fortunato et al. [33] presented a few aftereffects of exploratory work completed on a deactivated rail stretch, utilized as an experimental site. This examination was acted to evaluate the practicality of some structural solutions, utilizing reinforcement layers worked with unbound granular materials (UGM) and concrete bound granular mixtures (CBGM). Since that diverse structural solutions can be set up for recovery purposes, with respect to the current track conditions. Among different perspectives, the plan of these structural solutions relies upon the hydrogeological conditions that happen along the line, on the attributes of the foundation soils and on the current ballast layer. The non-destructive in situ tests had been considered as helpful tools for the assessment of the current railway and take into consideration the reinforcement condition and its development in time. The qualities of the materials got with in situ testing showed that lab triaxial tests can give appropriate resilient modulus values. The measured deflections of tests are presented in Fig. 13.

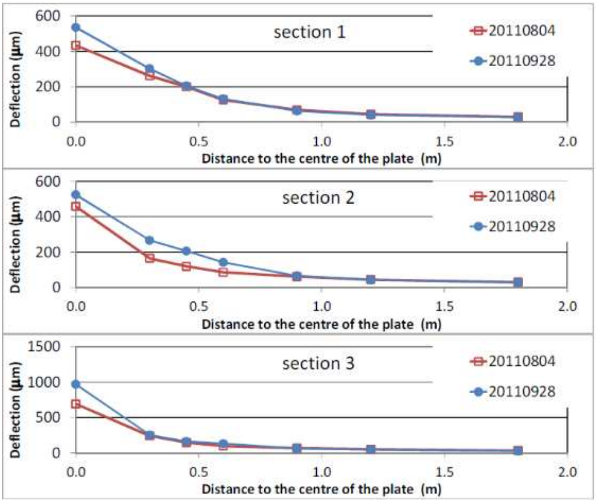

Figure 13. Results of tests [33]

It tends to be reasoned that it is feasible to reinforce the rail track foundation with a moderately dainty layer of aggregate blended in with aggregate. In any case, it ought to be focused on that lone the evaluation of versatile behavior of the materials was finished with these investigations. It was important to gauge the drawn-out exhibition of every one of the arrangements tried. Execution assessment ought to think about the perpetual deformity. Because of CBGM, it is important to assess the chance of cracking and corruption of the layer and the expansion of the permeability, which is lacking to the foundation behavior. Fig. 14 represents test device of ground penetrating radar which contains pairs of air-coupled antennas.

Figure 14. Test equipment of Ground penetrating radar [33]

The research subject of the breakage test for the railway ballast particles with remarkable lab test outcomes was showed by Juhász and Fischer [34]. Since most of railway lines on the planet have purported customary superstructure (ballasted tracks). The authors reported that in the previous few years there were a great deal of railway restoration projects in Hungary, just as abroad. Also, according to their suggestion, we can notice that these days cannot be considered typical that there was enough railway ballast in satisfactory quality, due to the changes and limitations in the connected guidelines in Hungary since 2010.

The principal objective of that study was to have the option to simulate the stress-strain impact of ballast particles in genuine and target path in research facility conditions just as in discrete element modelling. The methodology which was mentioned in the study can be considered as more practical for testing ballast samples than standardized abrasion tests. Different derelictions identified with computation of time spans between ballast screenings have been considered, such as: in the entire ballast cross area tantamount measure of breakage was not figured as the one that was estimated in referred laboratory tests, contaminating impacts on ballast (for example dust and breakage), and the impact of track geometry.

5.2.2. Rail track substructure improvement

Indraratna et al. [35] outlined the benefits of the proposed DEM and FEM models regarding catching the right stress-strain and degradation reaction of ballast with specific accentuation on particle breakage and fouling, just as uses of geosynthetic. Numerical modelling could mimic these perspectives subject to different sorts of loading and boundary conditions for a scope of material properties. So, in this work, the stress strain and degradation reaction of ballast was examined through discrete element (DEM) and limited component (FEM) techniques. In DEM, sporadically moulded ballast aggregates were reproduced by amassing together circles in fitting sizes and positions.

In FEM, a composite multilayer track framework was mimicked and an elastic-plastic model with a non-affiliated flow rule was utilized to catch ballast debasement. These DEM and FEM reproductions showed a decent concurrence with enormous scope lab tests. two distinct instances of subgrades had a match between the FE predictions and the laboratory data which resulted from experimental tests. The discoveries of these numerical examinations at the miniature and full scale, took into consideration a superior comprehension of urgent perspectives, for example, the mechanism of ballast-geogrid interface and long-term distortion and corruption.

In their study, Chawla et al. [36] performed static and cyclic tests on railroad track models. Tests were performed with two distinct thicknesses of subballast layers. Geogrid or geotextile or both were used to reinforce the tracks at appropriate interfaces. The results of tests on supported track models were introduced to assess the impacts of the sort of geosynthetic reinforcements, subballast thicknesses and kinds of subgrades on relocations of and incited vertical weights on each track layer.

Due to low permeability and high plasticity of the clay, it was noticed that mud-pumping was not critical in case of tracks which laid on clayey soil subgrade. For such tracks, the provision of a geogrid alone at the ballast-subballast interface was more effective in reducing the tie displacements, ballast and subballast strains, and subgrade displacements when compared to the provision of a geotextile alone at the subballast-subgrade interface.

6. Conclusion

The current review endeavours to draw out the comprehension of soil reinforcing methods to have better understanding of numerous techniques which are highly important for considerable stabilization. Thus, the aim of this paper was to review the literature of special reinforcement solutions of railway permanent ways' soil substructures. According to various experimental tests such as triaxial and direct shear tests, the shear strength of the soil is increased when the fibers is added to the soil. The significant factors that might lead to the failures of substructures such as excessive water in the subgrade and existence of fine-grained soils were viewed in this paper also.

Based on the review, the following remarks could be obtained:

- There are various reinforcement methods can be considered as effective techniques for enhancing engineering properties of soils.

- Potential utilizing of geosynthetic cementitious mat beneath the ballast could be a decent solution for re-establishing short segments of the railway tracks.
- Subgrade problem might occur because of several factors such as load, environment, and soil factors.
- According to the literature, various methods can be considered as effective techniques for railways strengthening.
- Special reinforcement solutions such as geosynthetic and fibrous reinforcement methods approved that it can be used as crucial methods for support the foundations of the railway tracks.

7. Summary

To sum up, this paper aimed to make detailed review of the previously published scientific journal papers. In general, most of papers that listed in this study approved that strength and stiffness of soils was improved by introducing reinforcement. In other words, as mentioned previously, soils are weak in tension generally, thus the using of different soil reinforcement techniques approved that the load efficiency of the soil increases in case of reinforcement presence.

Many of substructure failures which are related to railway tracks have been considered and cost efficiently solutions have been studied through this literature. Finally, different laboratory and in-situ tests have been considered to show the effects of each reinforcement method.

8. Research gap and future scope

Based on this review, key research gaps have been mentioned. In addition, valued suggestions and recommendations have been given for the future development and promotion of various soil reinforcement techniques. Understanding the behavior of different soil reinforcement techniques at different subsoil conditions is highly essential for reliable improvement of soil properties. Further studies will allow more practical and accurate analysis and consequently spreading reinforced soil techniques.

Up to date, challenges about cost, maintenance availability, drainage and construction restrict the application of the special reinforcement solutions of railway permanent ways' soil substructures. However, some of those problems are settled, further researches are still needed to improve the ballasted track.

References

[1] S. Kazemian, B. B. K. Huat et al. A review of stabilization of soft soils by injection of chemical grouting, *Australian Journal of Basic and Applied Sciences* 4 (12) (2010) pp. 5862–5868.

[2] H. I. Ling, D. Leshchinsky, F. Tatsuoka, eds. Reinforced soil engineering: advances in research and practice. *CRC Press*, 2003.

[3] B. Eller, S. Fischer. Tutorial on the emergence of local substructure failures in the railway track structure and their renewal with existing and new methodologies, *Acta Technica Jaurinensis* 14 (1) (2021) pp. 80–103. doi: `https://doi.org/10.14513/actatechjaur.00565`

[4] W. E. Ebersohn, E. T. Selig. Evaluation of Substructure Using Field Tests. Report No. LA-009, *Association of American Railroads*, Washington, DC, (1996).

[5] E. T. Selig, J. M. Waters. Track geotechnology and substructure management. *Thomas Telford*, 1994. doi: `https://doi.org/10.1680/tgasm.20139.fm`

[6] D. Li. Railway track granular layer thickness design based on subgrade performance under repeated loading. Ph.D. thesis. University of Massachusetts Amherst (1994).

[7] D. Li, E. T. Selig. Wheel/track dynamic interaction: track substructure perspective, *Vehicle System Dynamics* 24 (1) (1995) pp. 183–196. doi: `https://doi.org/10.1080/00423119508969624M`

[8] G. P. Raymond, Z. Cai. Dynamic track support loading from heavier and faster train sets. *Transportation Research Record* 1381 (1993).

[9] T. Dahlberg. Some railroad settlement models – a critical review, *Proceedings of the Institution of Mechanical Engineers, Part F: Journal of Rail and Rapid Transit* 215 (4) (2001) pp. 289–300. doi: `https://doi.org/10.1243/0954409011531585`

[10] D. Li, E. T. Selig. Method for railroad track foundation design. I: Development. *Journal of geotechnical and geoenvironmental engineering* 124 (4) (1998), pp. 316–322.

doi: `https://doi.org/10.1061/(ASCE)1090-0241(1998)124:4(316).`

[11] R. L. Michalowski, A. Zhao. Failure of fiber-reinforced granular soils. *Journal of geotechnical engineering* 122 (3) (1996) pp. 226–234.
doi: `https://doi.org/10.1061/(ASCE)0733-9410(1996)122:3(226)`

[12] A. Sawicki. Plastic limit behavior of reinforced earth, *Journal of geotechnical engineering* 109 (7) (1983) pp. 1000–1005.
doi: `https://doi.org/10.1061/(ASCE)0733-9410(1983)109:7(1000)`

[13] S. Wang et al. Volume change behaviour and microstructure of stabilized loess under cyclic freeze–thaw conditions, *Canadian Journal of Civil Engineering* 43 (10) (2016) pp. 865–874.
doi: `https://doi.org/10.1139/cjce-2016-0052`

[14] V. Toufigh. Experimental and Analytical Studies of Geo-Composite Applications in Soil Reinforcement. *Ph.D. thesis*, The University of Arizona (2012).
URL `http://hdl.handle.net/10150/255167`

[15] B. Eller, S. Fischer. Review of the Modern Ballasted Railway Tracks' Substructure and Further Investigations, *Science and Transport Progress. Bulletin of Dnipropetrovsk National University of Railway Transport* 6 (84) (2019) pp. 72–85.
doi: `https://doi.org/10.15802/stp2019/195831`

[16] H. Venkateswarlu, A. Hegde. Effect of infill materials on vibration isolation efficacy of geocell-reinforced soil beds, *Canadian Geotechnical Journal* 57 (9) (2020) pp. 1304–1319.
doi: `https://doi.org/10.1139/cgj-2019-0135`

[17] R. K. Rowe, K. L. Soderman. An approximate method for estimating the stability of geotextile-reinforced embankments, *Canadian Geotechnical Journal* 22 (3) (1985) pp. 392–398.
doi: `https://doi.org/10.1139/t85-050`

[18] D. T. Bergado, C. Teerawattanasuk. *2D and 3D numerical simulations of reinforced embankments on soft ground*, Geotextiles and Geomembranes 26

(1) (2008) pp. 39–55.
doi: *https://doi.org/10.1016/j.geotexmem.2007.03.003*

[19] K. Farrag, Y. B. Acar, I. Juran. Pull-out resistance of geogrid reinforcements, *Geotextiles and Geomembranes* 12 (2) (1993) pp. 133–159.
doi: *https://doi.org/10.1016/0266-1144(93)90003-7*

[20] T. M. Allen, R. J. Bathurst. Soil reinforcement loads in geosynthetic walls at working stress conditions, *Geosynthetics International* 9 (5-6) (2002) pp. 525–566.
doi: *https://doi.org/10.1680/gein.9.0227.*

[21] S. M. Hejazi, M. Sayyed et al. A simple review of soil reinforcement by using natural and synthetic fiber, *Construction and building materials* 30 (2012) pp. 100–116.
doi: *https://doi.org/10.1016/j.conbuildmat.2011.11.045*

[22] Ghazavi, Mahmoud, and Mahya Roustaei. "Freeze–thaw performance of clayey soil reinforced with geotextile layer." Cold Regions Science and Technology 89 (2013): 22-29.
doi: *https://doi.org/10.1016/j.coldregions.2013.01.002*

[23] Perkins, S. W., J. J. Bowders et al. Geosynthetic reinforcement for pavement systems: US perspectives, *International Perspectives on Soil Reinforcement Applications* (2005) pp. 1–13.
doi: https://doi.org/10.1061/40788(167)2

[24] F. Vahedifard, S. Shahrokhabadi, D. Leshchinsky. Geosynthetic reinforced soil structures, *Journal of Geotechnical Engineering* 115 (10) (1989) pp. 1459–1478.
doi: *https://doi.org/10.1016/j.geotexmem.2016.01.004*

[25] B. O. Oyegbile, B. A. Oyegbile. Applications of geosynthetic membranes in soil stabilization and coastal defence structures, *International Journal of Sustainable Built Environment* 6 (2) (2017) pp. 636–662.
doi: *https://doi.org/10.1016/j.ijsbe.2017.04.001*

[26] M. Valipour, Mehdi, P. T. Shourijeh, A. Mohammadinia. Application of recycled tire polymer fibers and glass fibers for clay reinforcement,

Transportation Geotechnics 27 (2021) p. 100474.
doi: `https://doi.org/10.1016/j.trgeo.2020.100474`

[27] R. Alsirawan. Review of Geosynthetic-Reinforced Pile-Supported (GRPS) embankments-parametric study and design methods, *Acta Technica Jaurinensis* 14 (1) (2021) pp. 36–59.
doi: `https://doi.org/10.14513/actatechjaur.00566`

[28] A. Pecker, J. Salenc. Ground reinforcement in seismic areas. *Proceedings of the XI Panamerican Conference on Soil Mechanics and Geotechnical Engineering*. Iguac¸u, Brazil; 1999.

[29] A. E. Ramaji. A review on the soil stabilization using low-cost methods, *Journal of Applied Sciences Research* 8 (4) (2012), pp. 2193-2196.

[30] S. Shukla, N. Sivakugan, B. Das. Fundamental concepts of soil reinforcement – an overview, *International Journal of Geotechnical Engineering* 3 (3) (2009) pp. 329–342.
doi: `https://doi.org/10.3328/IJGE.2009.03.03.329-342`

[31] S. Gowthaman, K. Nakashima, S. Kawasaki. A state-of-the-art review on soil reinforcement technology using natural plant fiber materials: Past findings, present trends and future directions, Materials 11 (4) (2018) p. 553.
doi: `https://doi.org/10.3390/ma11040553`

[32] E. Juhász, S. Fischer. Tutorial on the fragmentation of the railway ballast particles and calibration methods in discrete element modelling, *Acta Technica Jaurinensis* 14 (1) (2021) pp. 104–122.
doi: `https://doi.org/10.14513/actatechjaur.00569`

[33] E. Fortunato, S. Fontul et al. Case study on the rehabilitation of old railway lines: experimental field works, *Proceedings of the international conferences on the bearing capacity of roads, railways and airfields*. 2013.

[34] E. Juhász, S. Fischer. Railroad ballast particle breakage with unique laboratory test method, *Acta Technica Jaurinensis* 12 (1) (2019) pp. 26–54.
doi: `https://doi.org/10.14513/actatechjaur.v12.n1.489`

[35] B. Indraratna, S. S. Nimbalkar et al. Performance improvement of rail track substructure using artificial inclusions – Experimental and numerical studies,

Transportation Geotechnics 8 (2016) pp. 69–85.
doi: *https://doi.org/10.1016/j.trgeo.2016.04.001*

[36] C. Sowmiya, J. T. Shahu. "Reinforcement and mud-pumping benefits of geosynthetics in railway tracks: model tests." *Geotextiles and Geomembranes* 44.3 (2016): 366-380.
doi: https://doi.org/10.1016/j.geotexmem.2016.01.005